

**ASSESSMENT OF SURFACE RUNOFF AND SOIL EROSION  
IN DZUMAH WATERSHED OF UPPER DHANSIRI,  
NAGALAND**

Thesis  
submitted to

**NAGALAND UNIVERSITY**

in partial fulfillment of requirements for the Degree

of

**DOCTOR OF PHILOSOPHY**

in

**SOIL AND WATER CONSERVATION**

by

**RIZONGBA KICHU**

**Admn. No. Ph - 257/18 Regn. No. Ph.D./SWC/00216**



Department of Soil and Water Conservation  
School of Agricultural Sciences and Rural Development  
Nagaland University, Medziphema Campus – 797106  
Nagaland  
**2022**

**NAGALAND UNIVERSITY**  
**Medziphema Campus**  
**School of Agricultural Sciences and Rural Development**

**Medziphema – 797106, Nagaland**

Dr. Manoj Dutta  
Professor  
Department of Soil and Water Conservation

**CERTIFICATE – I**

This is to certify that the thesis entitled “**Assessment of surface runoff and soil erosion in Dzumah watershed of Upper Dhansiri, Nagaland**” submitted to Nagaland University in partial fulfillment of the requirements for the award of degree of Doctor of Philosophy in Soil and Water Conservation is the record of research work carried out by **Mr. Rizongba Kichu**, Registration No. Ph.D./SWC/00216 under my personal supervision and guidance.

The results of the investigation reported in the thesis have not been submitted for any other degree or diploma. The assistance of all kinds received by the student has been duly acknowledged.

Date: 18/07/2022

Place: Medziphema

  
.....18/07/2022  
(Dr. MANOJ DUTTA)

Supervisor

**NAGALAND UNIVERSITY**  
**Medziphema Campus**  
**School of Agricultural Sciences and Rural Development**  
**Medziphema – 797 106, Nagaland**

**CERTIFICATE – II**

**VIVA VOCE ON THESIS OF DOCTOR OF PHILOSOPHY IN SOIL  
AND WATER CONSERVATION**


This is to certify that the thesis entitled “**Assessment of surface runoff and soil erosion in Dzumah watershed of Upper Dhansiri, Nagaland**” submitted by **Mr. Rizongba Kichu**, Admission No. **Ph-257/18** Registration No. **Ph.D./SWC/00216**, to the NAGALAND UNIVERSITY in partial fulfilment of the requirements for the award of degree of Doctor of Philosophy (Agriculture) in Soil and Water Conservation has been examined by the Advisory Board and External Examiner on **01-11-2022**.

The performance of the student has been found **Satisfactory/Unsatisfactory**.

**Members**

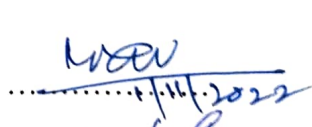
1. Prof. Manoj Dutta  
(Supervisor)
2. Prof. Sanjay Swami  
(External Examiner)
3. Prof. L. Daiho  
Dean, SASRD  
(Pro Vice -Chancellor Nominee)
4. Prof. R. C. Nayak
5. Prof. A. K. Singh
6. Prof. Amod Sharma

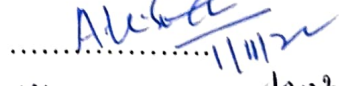
Signature

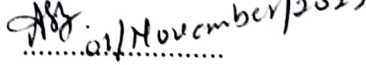
  
..... 01/11/2022

  
..... 01/11/2022

  
..... 01/11/22

  
..... 01/11/2022

  
..... 11/11/22

  
..... 01/November/2022



Head  
Department of Soil and Water Conservation

Dean  
School of Agricultural  
Sciences and Rural  
Development

## DECLARATION

I, **RIZONGBA KICHU**, hereby declare that the subject matter of this thesis is the record of work done by me, that the contents of this thesis did not form the basis of the award of any previous degree to me or to the best of my knowledge to anybody else, and that the thesis had not been submitted by me for any research degree in any other university/institute.

This is being submitted to Nagaland University for the degree of Doctor of Philosophy in **SOIL AND WATER CONSERVATION**.

Date: 18/07/2022

Place: Medziphema



(**RIZONGBA KICHU**)



.....

Supervisor

## **Acknowledgements**

All praises and glory to God Almighty for His immense blessings bestowed on me throughout my research work.

I, with all due respect and honour, would like to express my heartfelt gratitude to my supervisor Dr. Manoj Dutta, Professor, Department of Soil and Water Conservation, SASRD, Medziphema Campus, Nagaland University for his guidance, suggestions and encouragement throughout my research work.

My sincere gratitude and appreciation to all the members of my Advisory committee Prof. R. C. Nayak, Department of Soil and Water Conservation, Prof. A. K. Singh, Department of Agricultural Chemistry and Soil Sciences and Prof. Amod Sharma, Department of Agricultural Economics for their valuable suggestions and support during the course of my research work.

I also would like to express my heartfelt gratitude to the Dean, Prof. Akali Sema and the Pro Vice-Chancellor, Prof. M. Aleinla Ao for the facilities offered for my research work.

I am very thankful and indebted to Mr. S. Patton, STA, Department of Soil and Water Conservation and all the non-teaching staff members in the department for rendering their help and support in varied ways whenever needed.

I would like to extend my deep sense of gratitude and appreciation to the Outreach Team at North Eastern Space Applications

Centre (NESAC), Umiam, Meghalaya for imparting technical trainings related to my research work.

Finally, I would like to express my gratitude to all my friends and fellow scholars for their immense help and support whenever needed.

Date: 18/07/2022

Place: Medziphema



Rizongba Kichu

## LIST OF TABLES

<b>TABLE NO.</b>	<b>TITLE</b>	<b>PAGES</b>
3.1	Details of satellite data	20
3.2	Soil sampling location coordinates	20
3.3a	Morphometric analysis of linear aspects of watershed	22
3.3b	Morphometric analysis of areal aspects of watershed	23
3.3c	Morphometric analysis of relief aspects of watershed	23
3.4	Classification of Antecedent Moisture Condition	27
4.1	Linear aspects of Dzumah watershed	38
4.2	Areal and relief aspects of Dzumah watershed.	43
4.3	Land use land cover classes of Dzumah watershed	46
4.4	Soil texture and HSG of Dzumah watershed	46
4.5	CN value modification	48
4.6	Rainfall and runoff depth for the year 2019	48
4.7	Rainfall and runoff depth for the year 2020	48
4.8	Year-wise rainfall erosivity factor (R) of Dzumah watershed	51

---

---

4.9	Soil properties and K factor of Dzumah watershed	53
4.10	Slope classes of Dzumah watershed based on USDA classification	54
4.11	Year-wise average annual soil loss of Dzumah watershed	57
4.12	Mean area under different classes of erosion in Dzumah watershed	58
4.13	Area under different classes of erosion in Dzumah watershed for the year 2019	58
4.14	Area under different classes of erosion in Dzumah watershed for the year 2020	58

---



## LIST OF FIGURES

---

<b>FIGURE NO.</b>	<b>TITLE</b>	<b>IN BETWEEN PAGES</b>
3.1	Spatial extent of Dzumah watershed	18 – 19
4.1	Drainage network map of Dzumah watershed	35 – 36
4.2	Elevation map of Dzumah watershed	43 – 44
4.3	Land use/land cover map of Dzumah watershed	45 – 46
4.4a	Rainfall-runoff correlation using standard CN for the year 2019	50 – 51
4.4b	Rainfall-runoff correlation using standard CN for the year 2020	50 – 51
4.5a	Rainfall-runoff correlation using modified CN for the year 2019	50 - 51
4.5b	Rainfall-runoff correlation using modified CN for the year 2020	50 - 51
4.6	Soil erodibility factor (K) map of the Dzumah watershed	53 – 54
4.7	Slope map of Dzumah watershed	54 – 55
4.8	Slope length and steepness factor(LS) map of Dzumah watershed	54 – 55
4.9	NDVI map of Dzumah watershed	55 – 56
4.10	Crop management factor (C) map of Dzumah watershed	55 – 56

---

---

4.11	Conservation practice factor (P) map of Dzumah watershed	55 – 56
4.12	Average annual soil erosion map of Dzumah watershed	57 – 58
4.13	Average annual soil erosion map of Dzumah watershed for the year 2019	58 -59
4.14	Average annual soil erosion map of Dzumah watershed for the year 2020	58 -59
4.15	Correlation between rainfall erosivity factor (R) and average annual soil loss	58 - 59

---

## LIST OF ABBREVIATIONS

---

AMC	-	Antecedent Moisture Condition
CN	-	Curve number
DEM	-	Digital Elevation Model
ESRI	-	Environmental Systems Research Institute
<i>et al.</i>	-	And others
FCC	-	False Colour Composite
Fig.	-	Figure
GIS	-	Geographic Information System
Ha	-	Hectare
HSG	-	Hydrologic Soil Group
ICAR	-	Indian Council of Agricultural Research
IDW	-	Inverse Distance Weighted
km <sup>2</sup>	-	Square Kilometer
LULC	-	Land Use Land Cover
m	-	Meter
m.m <sup>-1</sup>	-	Meter per meter
mm	-	Millimeter
MJ mm ha <sup>-1</sup> h <sup>-1</sup> yr <sup>-1</sup>	-	Megajoule millimeter hectare <sup>-1</sup> hour <sup>-1</sup> year <sup>-1</sup>
NDVI	-	Normalized Difference Vegetation Index
NIR	-	Near Infrared
NRCS	-	Natural Resource Conservation Service

---

SCP	-	Semi-Automatic Classification Plugin
SCS	-	Soil Conservation Service
SRTM	-	Shuttle Radar Topographic Mission
$t\ ha^{-1}\ yr^{-1}$	-	Ton per hectare per year
$t\ ha\ h\ ha^{-1}\ MJ^{-1}\ mm^{-1}$	-	Ton hectare hour hectare <sup>-1</sup> Megajoule <sup>-1</sup> millimeter <sup>-1</sup>
USDA	-	United States Department of Agriculture
USLE	-	Universal Soil Loss Equation
USGS	-	United States Geological Survey
UTM	-	Universal Transverse Mercator
WGS	-	World Geodetic System

---

## CONTENTS

---

CHAPTER	TITLE	PAGE NO.
1	INTRODUCTION	1 – 4
2	REVIEW OF LITERATURE	5 – 17
	2.1 Watershed characterization using GIS technique	5
	2.2 Surface runoff estimation using NRCS-CN method	10
	2.3 Estimation of average annual soil loss using the USLE method	14
3	MATERIALS AND METHODS	18 – 34
	3.1 About the study area	18
	3.2 Collection of data	18
	3.2.1 Remote sensing data	18
	3.2.2 Rainfall data	18
	3.2.3 Soil	19
	3.2.4 Thematic maps	19
	3.2.5 Software and systems	19
	3.3 Methodology	21
	3.3.1 Watershed characterization	21
	3.3.2 Estimation of surface runoff and water yield potential	21
	3.3.3 Estimation of soil erosion using the Universal Soil Loss Equation	30
4	RESULTS AND DISCUSSION	35 – 58
	4.1 Watershed characterization	35

---

---

	4.1.1 Linear aspects	35
	4.1.2 Areal aspects	40
	4.1.3 Relief aspects	42
	4.2 Runoff estimation	44
	4.2.1 Land use land cover	45
	4.2.2 Hydrologic soil group	45
	4.2.3 CN values	47
	4.2.4 Runoff depth and water yield potential	47
	4.3 Soil loss estimation	50 – 58
	4.3.1 Rainfall erosivity factor (R)	52
	4.3.2 Soil erodibility factor (K)	52
	4.3.3 Slope length and steepness factor (LS)	52
	4.3.4 Crop management factor (C)	52
	4.3.5 Conservation practice factor (P)	55
	4.3.6 Average annual soil loss	55
5	SUMMARY AND CONCLUSION	59 – 63
	5.1 Summary	59
	5.2 Conclusion	61
	REFERENCES	i - xiii
	APPENDICES	xiv - xxv

---

## ABSTRACT

In the present study, an attempt was made to quantify the morphometric characteristics of Dzumah watershed located in Nagaland, India, and estimate surface runoff and average annual soil erosion from the watershed. The Shuttle Radar Topographic Mission (SRTM) Digital Elevation Model (DEM) of 30 m spatial resolution was used in ArcGIS environment for evaluating the morphometric parameters and generating topographic thematic layers. Cloud-free remote sensing satellite data of Sentinel-2A was used for Land Use Land Cover (LULC) image classification and generation of Normalized Difference Vegetation Index (NDVI) maps. Soil samples were collected from 19 random locations and analyzed for textural classes and organic matter content. Hydrologic Soil Group (HSG) for runoff estimation and soil erodibility (K) parameter of Universal Soil Loss Equation (USLE) method was derived from soil texture data following standard procedures. Daily rainfall data of two years (2019-2020) was considered for estimation of surface runoff using the Natural Resources Conservation Service – Curve Number (NRCS-CN) method. Rainfall events from the month of June to October were considered for estimating the rainfall (P) parameter. Surface runoff estimation was computed using the standard CN method as well as with  $\lambda$  and slope-adjusted CN. A  $\lambda$  value of 0.05 was considered for the study. Annual rainfall data of 23 years (1998-2020) was considered for estimating rainfall erosivity and average annual soil loss was calculated for each year separately from 1998 to 2020 using the USLE method.

The study showed that Dzumah watershed is a fifth order drainage basin with an area of 6555 ha and having 228 stream segments (total stream number) with a total stream length of 130.71 km. A low drainage density of 1.99 km/km<sup>2</sup> indicates coarse drainage texture revealing that the watershed has good infiltration/permeability and vegetation cover. The analysis of various areal aspects such as form factor, circularity ratio and elongation ratio revealed that the watershed is elongated in shape. The analysis of relief aspects revealed that the lowest and highest elevation in the watershed is 328 m and 2345 m above mean sea level, respectively. The observed values for relief ratio and ruggedness number are 0.14 and 4.02, respectively, indicating that the watershed has rough, steep and uneven topography. The high permeability as inferred by low values of drainage density could be negated by high rainfall and steep uneven terrain characteristics of the watershed which would not only decrease the absorption time but also increase the velocity of accumulated surface run off. The overall results from the study showed that the watershed is characterized by rugged uneven terrain with steep slopes which would favour considerable increase in flow velocity, thus increasing the risk of soil erosion.

Five land use and land cover classes were observed in the study area *viz.* cultivated area, dense forest, open forest, buildup area and water body,

occupying 322.50, 3998.55, 1553.54, 392.65, 287.76 ha, respectively. The total area under forest was 5552.09 ha accounting for 84.7 per cent of the total geographical area of the watershed. The soils in the watershed were found to be medium to fine textured and consisted of textural classes *viz.* loam, clay loam, silty clay loam and silt loam. The entire watershed was under HSG-C and had a moderately high runoff potential. The standard CN values for the watershed ranged from 70 to 100, while the  $\lambda_{0.05}$  and slope-adjusted CN ranged from 91.02 to 100. Out of 1159 mm of total rainfall received in the year 2019, the standard CN method estimated a runoff depth of 109.95 mm accounting to a mere 9.49% of the total rainfall received, while the  $\lambda_{0.05}$  and slope-adjusted CN estimated a runoff depth of 505.34 mm accounting to 43.60% of the total rainfall. Similarly, in the year 2020, out of 879.70 mm of total rainfall, the standard CN method estimated a runoff depth of 33.25 mm accounting to 3.78% of the total rainfall, while the  $\lambda_{0.05}$  and slope-adjusted CN estimated a runoff depth of 340.97 mm accounting to 38.76% of the total rainfall. The observed  $R^2$  values for the standard CN method and  $\lambda_{0.05}$  and slope-adjusted CN in the year 2019 were 0.166 and 0.858, respectively. Similarly, the  $R^2$  values for the standard CN method and  $\lambda_{0.05}$  and slope-adjusted CN in the year 2020 were 0.650 and 0.994, respectively. The  $R^2$  values observed in both the years clearly indicate that the  $\lambda_{0.05}$  and slope-adjusted CN gave a better correlation between rainfall and runoff. Based on the findings, it can be stated that the standard CN method is unfit for runoff estimation in steep sloping forested watersheds and that  $\lambda$  and slope adjustments to the CN value is significantly important under such conditions. The prediction accuracy of the model could not be validated due to the absence of hydrologic gauging stations and non-availability of daily flow records. However, the model presented a fair simulation of hydrologic response of the watershed to rainfall events and the results can be used for conservation and management purposes, though not for computation of flood design structures.

The rainfall erosivity factor (R) values ranged from 734.02 and 4157.30 MJ mm ha<sup>-1</sup> h<sup>-1</sup> yr<sup>-1</sup> with a mean of 2465.95 MJ mm ha<sup>-1</sup> h<sup>-1</sup> yr<sup>-1</sup>. The K factor values of the watershed ranged from 0.03 to 0.074 t ha h ha<sup>-1</sup> MJ<sup>-1</sup> mm<sup>-1</sup>. The slope length and steepness factor (LS) values ranged from 0.03 to 54.44. The cover management factor (C) was generated using NDVI map and its value ranged from 0.07 to 0.53. The values for conservation practice factor (P) were assigned as 0.28 for cultivated lands and 1.0 for other areas. The average annual soil loss for the year 2019 and 2020 were 3.74 and 3.04 t ha<sup>-1</sup> yr<sup>-1</sup>, respectively. It was also observed that in both years, >95% of the watershed area was under light and moderate erosion class. This could be attributed to the excellent forest cover in the steep sloping higher reaches of the watershed and the flatter plains under cultivation and settlements. Maximum soil loss in both years could be observed only in locations with extreme steep slopes and disturbed sites caused by construction activities. Considering the



average annual soil loss estimated for 23 years (1998-2020), the average potential soil erosion for Dzumah watershed was found to be  $5.38 \text{ t ha}^{-1} \text{ yr}^{-1}$ . Given the soil loss threshold limit of  $15 \text{ t ha}^{-1} \text{ yr}^{-1}$  for mountainous Himalayan regions, the watershed is considered to be stable. These findings can serve as vital information for implementing precautionary measures in future developmental activities or efforts to alter the present land use system in the watershed. The GIS platform proved to be a very effective, time and cost saving tool for computation and analysis of various morphometric characteristics of the watershed, estimation of surface runoff and soil erosion.

## INTRODUCTION

Land and water are two most important and basic natural resources in a watershed. In fact, good quality land and water is a fundamental requirement not only to maintain the existing ecosystem in a watershed but also to endorse anthropological changes to suit human needs without causing imbalances to the system. In recent times, the advent of climate change induced anomalies such as erratic spatial and temporal distribution of rainfall, sudden outbursts of high intensity rainfall, flash floods during rainy seasons and prolonged dry spells during off seasons has greatly accentuated the necessity for immediate planning and adoption of soil and water conservation strategies. Such planning and implementation is best achieved by investigating the causes and effects at smaller watershed levels.

Watershed is a term used to describe an area of land that contains a common set of channels, streams or rivers that all drain into a common outlet. Surface runoff is the flow of water that occurs when excess storm water or other sources of water flow on the land surface after fulfilling all surface and sub surface losses. The intensity, duration and distribution of rainstorms greatly influence the occurrence and quantity of surface runoff generated in a watershed. Runoff is an important hydrologic variable that needs to be assessed for various ecological and sustainability purposes. Reliable information on the rate and quantity of runoff flowing into streams or rivers is essential for addressing many watershed development and management problems. However, in ungauged watersheds, generating such vital information/data is difficult and time consuming. Extensive meteorological and hydrological data are required by conventional methods for prediction of river discharge. Collection of these data is a difficult, expensive and time consuming process.

There are only a few selected sites in India installed with recording and automatic hydrologic gauging stations which bottlenecks the availability of

accurate information in most parts of the country. Thus, acquiring information on surface runoff and sediment yield has become inevitably crucial for facilitating watershed management strategies (Zade *et al.*, 2005). Most watersheds in India are ungauged and therefore, no past documentations of rainfall-runoff processes are available (Sarangi *et al.*, 2005). However, the necessity for obtaining runoff information is gaining momentum due to advances in natural resource conservation and watershed management programmes. The lack of rainfall and runoff records in most watersheds in India has instigated the advances in surface runoff estimation techniques from ungauged watersheds (Chattopadhyay and Choudhury, 2006). Estimating runoff using remote sensing data yields reliable results and is comparatively a less exhaustive and less time consuming method. The increasing accessibility of spatial data and evolution of computational power have made it feasible for accurate prediction of runoff. The capability and versatility of Geographic Information System (GIS) in combining different types of data has significantly increased its use in hydrological applications.

Soil erosion echoes multiple environmental concerns threatening natural resources and food security. It is difficult to assess the severity of erosion because soil erosion often occurs at unnoticeable rates. Besides, the spatial distribution of the rates of soil erosion is so scattered and the rate of erosion differs from place to place. Cultivation of land without proper conservation practices to check erosion may render the land economically unproductive. Soil erosion results in decrease of soil fertility and reduction of crop yields. The on-site effects of erosion poses severe problems having long-term impacts on cultivated lands such as top soil loss, reduction in soil depth and rooting volume, disintegration of soil structure, loss of organic matter and an overall decline in soil fertility status. Land degradation induced by water erosion is a worldwide problem for sustainable agriculture (Wei *et al.*, 2019). Erosion reduces the moisture holding capacity of soil thus increasing the

susceptibility of the land to drought prone conditions. At initial stages, the loss in crop productivity could be negated by using more input of fertilizers to maintain crop yields. However, the increase in expenditure on fertilizers and simultaneous deterioration of soil properties eventually leads to a severely degraded land unsuitable for cultivation. The off-site consequences of soil erosion arises due to deposition of sediments in downstream areas, which shortens the design life of reservoir dams, reducing capacity of water bodies, increase flooding and other related problems.

A sound knowledge on the processes of erosion is necessary for selection and implementation of appropriate soil conservation practices. Various scientists have developed models for predicting soil erosion from watershed based on parameters such as land use and land cover; soil type, drainage characteristics, topographical and climatic information. Investigation and observation of these important factors on a spatial scale has been made possible through remote sensing techniques, which helps in quick assessment and prioritization of the watershed. In most cases, it is not practical to employ watershed development activities in the entire watershed area due to limitation of resources, including manpower and financial resources. Runoff and erosion rates are not constant, but vary throughout the area of a watershed depending on the spatial variation of the influential parameters such as amount and intensity of rainfall, soil type, vegetation cover, topography etc. Therefore, prioritizing and focusing on specific areas more prone to erosion hazards is important. Despite being a natural process, the rate of erosion, its spatial and temporal variation is greatly influenced by human activities. A very close relation exists between land use and erosion such that, mismanagement of land could lead to accelerated rates of soil erosion, which in turn would dictate changes in land use.

Nagaland, a NE state in India, is characterized by steep and uneven terrain with hilly topography. The state is said to be geologically highly susceptible to soil erosion as only 8.48 per cent of the total geographical area of 16,579 km<sup>2</sup> can be considered plain and the rest is constituted by undulating and hilly terrain with altitudes varying from 200 to 3,840 m. The state receives high amount of annual rainfall (1700mm-2600mm) but it is unevenly distributed throughout the year. Monsoon season (June to September) account for 68% of total annual rainfall, post monsoon (October to November) accounts for 22% leaving only 5% during winter season (December to January) and pre monsoon season (March to May) (Verma, 2007). High rainfall during summer generates excess surface runoff and increases erosivity thereby rendering the soil surface more susceptible to erosion whereas in winter, the state faces drought-like situations due to less rainfall. Based on the scenario described above, the present investigation entitled “Assessment of surface runoff and soil erosion in Dzumah watershed of Upper Dhansiri, Nagaland” is being undertaken with the following objectives:

1. Characterization of the Dzumah watershed.
2. Estimation of surface runoff, soil erosion and water yield potential of the watershed.

## REVIEW OF LITERATURE

The literature pertaining to the present investigation entitled “Assessment of surface runoff and soil erosion in Dzumah watershed of Upper Dhansiri, Nagaland” has been reviewed in this chapter under the following heads:

### 2.1 Watershed characterization using GIS technique

Saxena *et al.* (2000) carried out watershed characterization and management study in Gondkhairi watershed of Nagpur district using IRS-1C satellite data. Watershed components like drainage density and pattern, slope percentage and direction, physiography, soils, land use and land cover, were visually interpreted using the geocoded false colour composites (FCCs) of IRS-1B LISS II and IRS-1C LISS III at 1:50 000 scale. Based on their findings on soil types, percentage slope, drainage density, bifurcation ratio and constant channel maintenance ratio, various soil conservation modules were suggested and successfully implemented.

Reddy *et al.* (2004) from a study conducted in Vena river basin of Maharashtra using GIS platform categorized the watershed into seven classes *viz.*, extremely severe, very severe, severe, moderator severe, moderate, slight and very slight. The study also demonstrated that remotely sensed data and GIS based approach is found to be more appropriate than the conventional methods in evaluation and analysis of drainage morphometry, landforms and land resources and to understand their inter-relationships for planning and management at river basin level.

Chopra *et al.* (2005) studied the morphometric characteristics of Bhagra-Phungotri and Hara Majha sub-watersheds in Gurdaspur district of Punjab using Remote Sensing and GIS techniques. It was observed that both the sub-watersheds showed dendritic to sub-dendritic drainage pattern with

moderate drainage texture. High bifurcation ratio indicated a strong structural control on the drainage. Logarithm of number of stream vs. stream order showed deviation from straight line indicating regional upliftment. In spite of mountainous relief, low drainage density values indicated that the area was underlain by impermeable sub-surface material. Circulatory and elongation ratios showed that both the subwatersheds have elongated shape.

Javed *et al.* (2009) carried out prioritization of sub-watersheds (SW) in Kanera watershed of Madhya Pradesh based on morphometric and land use analysis using Remote Sensing and GIS techniques. The study demonstrated the significant land use changes especially in cultivated lands, open scrub, open forest, water bodies and wastelands from 1989 to 2001. Based on morphometric and land use/land cover analysis, the sub-watersheds were classified into three categories as high, medium and low in terms of priority for conservation and management of natural resources. Out of the seven sub-watersheds, two sub-watersheds viz., SW1 and SW6 qualified for high priority, whereas SW7 was categorized as medium priority based on the integration of morphometric and land use change analysis.

Thomas *et al.* (2010) studied the morphometric aspects of Muthirapuzha watershed in Kerala, India. The study revealed that the watershed was moderate to well-drained and exhibited a geomorphic maturity in its physiographic development. The shape parameters revealed the elongated nature and drainage network development in the watershed. The study strongly highlighted the tendency of the watershed to soil loss and the hydrological makeup of the sub-watersheds, which helped to formulate a comprehensive watershed management plan.

Vincy *et al.* (2012) used GIS techniques for morphometric characterization of Tikovil and Payappara sub-watersheds of Meenachil river basin in Kottayam district of Kerala. Drainage density varied between

1.69 and 2.62 km.km<sup>-2</sup>. The drainage texture of the drainage basins were 2.3 km<sup>-1</sup> and 6.98 km<sup>-1</sup> and categorized as coarse to very fine texture. The form factor value varied in between 0.42 and 0.55 suggesting an elongated shape for Payappara sub-watershed and a rather more circular shape for Tikovil sub-watershed. The mean bifurcation ratio of 3.5 indicated that both the sub-watersheds were within the natural stream system.

Patil and Mali (2013) characterized and prioritized the Tulasi micro-watershed basin of Kolhapur district in Maharashtra based on morphometric characteristics. Their study revealed sub-basins that were under high risk of soil erosion requiring high priority for land conservation practices. They suggested that these studies were significant for formulating soil erosion control and rainwater harvesting methods and techniques.

Sarma *et al.* (2013) carried out a geospatial study on morphometric characteristics of Umtrew river basin of Meghalaya in India. Their findings suggested that the basin has highly permeable sub-soil material and thick vegetative cover in most of its areas. The circularity ratio value revealed that the basin was elongated in shape and a predominance of highly permeable homogenous geologic material. They concluded that GIS based approach facilitated analysis of different morphometric parameters and to explore the relationship between drainage morphometry and properties of landforms, soils and eroded lands. GIS techniques characterized by very high accuracy of mapping and measurement proved to be a competent tool in morphometric analysis.

Soni *et al.* (2013) computed the fluvial morphometric characteristics of Rachhar Nala mini watershed in Anuppur district of Madhya Pradesh using GIS techniques. They affirmed that GIS technique was useful for the identification of morphological features and thus important for basin area planning and management.



Kaliraj *et al.* (2015) studied the morphometric parameters of Thamirabarani sub-basin in Kanyakumari district of Tamil Nadu using remote sensing and GIS techniques. The sub-basin was found to be strongly elongated in shape with a length of 42.78 km, circularity ratio of 0.33 and elongation ratio as 0.57. The textural dissection of the landforms showed low drainage density in the elevated hilly terrains and higher values in the plain areas. The morphometric parameters-induced denudation rate of the study area was  $65.14 \text{ t}^{-1}\text{km}^{-2}\text{year}$  and indicated the occurrence of a wide range of denudation intensities throughout the sub-basin. Based on the realistic output, it was concluded that remote sensing and GIS are effective tools for morphometric studies of the drainage basin.

Da Cunha and Bacani (2016) conducted a morphometric characterization of Indaiá watershed in Brazil using SRTM data and GIS techniques. Classical morphometric parameters were calculated and specialized through spatial analysis in geographic information systems. The integrated analysis of the variables (morphometric and relief) revealed that the watershed had low susceptibility to flooding but that the morphology of the relief and lithological structure favored the development of erosion processes in the watershed.

Yadav *et al.* (2016) carried out prioritization of sub-watersheds (SW) in Upper Tons River Basin of North India based on morphometric parameters with respect to groundwater derived from topographic sheets and CARTOSAT data. 10 SWs were delineated in the region, of which SWs 1, 2, 3, 5 and 9 were identified as areas with poor groundwater potentialities. SW-2 has been identified as poorest groundwater potential zone; whereas SWs 4, 6, 7 and 8 were identified as areas possibly having good ground water potential. Further, the areal parameters indicated elongated shape of the basin, hilly region has

moderate to steeper ground slope. The outcomes of the study had the potential to manage groundwater and to ameliorate flash flood and droughts.

Lodhi and Reza (2017) studied the morphometric characteristics of Singki river catchment of Arunachal Pradesh using GIS platform. Their study revealed that the catchment has an area of 79.8 sq.km<sup>-1</sup> and exhibited a dendritic drainage pattern.

Patil and Toradmal (2020) performed a Digital Terrain Analysis and characterized Vincharna river basin in Maharashtra using Digital Elevation Model (DEM). Analysis of surface morphology, chances of rainfall, particular direction and accumulation of water flow, saturation and concentration of water zones in area were done based on the calculated parameters. It was concluded that such kind of study played a very convenient and vital role in watershed management and prompted further research in rural area planning.

Hamad (2020) carried out multiple morphometric characterization and analysis of Malakan Valley drainage basin in Kurdistan region of Iraq using GIS and remote sensing techniques. Various aspects such as linear, areal, and relief morphometric parameters were calculated using hydrological tool and slope-aspect in ArcGIS. The study showed that the integration of RS and GIS was an effective approach for analyzing the morphometric pattern and land use change. Future investigation was instigated to broaden over all sub-watersheds of the current study giving more importance to land use in the watersheds.

Bogale (2021) analyzed the morphometric parameters of Gilgel Abay watershed in Ethiopia using GIS technique. The results showed that the Gilgel Abay is a fifth-order drainage basin with a total of 662 drainage networks. The mean bifurcation ratio was 5.16, indicating that the basin is mountainous and susceptible to flooding. The observed drainage density was 0.6 km.km<sup>-2</sup>, indicating that the basin is highly permeable with healthy vegetation cover.

Areal aspects of the basin revealed that the study area has slight potential to flooding and soil erosion.

Ismail *et al.* (2022) performed quantitative morphometric analysis of Veshav and Rembi Ara watersheds in India using quantum GIS software. Their findings on areal aspects indicated that Veshav watershed is comparatively a more circular-shaped basin than Rembi Ara watershed which has an elongated shape. The values of length of overland flow ( $L_g$ ) and relief parameters reflected that Rembi Ara watershed has higher flow velocity than Veshav watershed. Based on their findings, it was observed that Veshav watershed has more effective surface runoff discharge capacity.

## **2.2 Surface runoff estimation by NRCS-CN method**

Nayak and Jaiswal (2003) performed rainfall-runoff modeling for Bebas river in Madhya Pradesh using remote sensing and GIS techniques. Remotely sensed satellite data was used for acquiring spatial information on land use land cover and soil parameters to generate the curve number. Their findings revealed good correlation between the measured and estimated runoff volume with seasonal correlation coefficient varying from 0.92 to 0.94.

Ramakrishnan *et al.* (2009) estimated runoff from Kali sub-watershed in the semi-arid region of Gujarat using GIS based NRCS CN method. Their findings helped in the selection of suitable sites for construction of different water harvesting structures in the watershed. The derived sites were field investigated and the accuracy of the site selection at implementation level varied from 80–100%.

Shi *et al.* (2009) made an attempt to determine the ratio of initial abstraction ( $I_a$ ) and to compare the performance of traditional and modified  $I_a/S$  values with observed rainfall-runoff data in the Three Gorges Area of China. Their findings showed that the  $I_a/S$  values varied from 0.010 to 0.154, with a

median and average of 0.048 and 0.053, respectively. Their study also revealed that the standard NRCS-CN method underestimated large runoff events, yielded a slope of the regression line of 0.559 and an intercept of 0.301. The modified  $I_a/S$  value was about 0.05 that better predicted runoff depths with an  $R^2$  of 0.804 and a linear regression slope of 0.834. The model efficiency coefficient (E) was also improved from 0.482 for traditional  $I_a/S$  value to 0.768. They concluded that the  $I_a/S$ -adjusted NRCS-CN method was better suited for runoff prediction in the Three Gorges Area of China.

Garg *et al.* (2013) investigated the efficiency of slope adjustment and modification of NRCS-CN method for runoff estimation in Solani watershed of Uttarakhand and concluded that slope factor affects runoff estimation significantly.

Tirkey *et al.*, (2013) demonstrated the use of NRCS-CN technique for runoff estimation using high resolution satellite data in Daltonganj watershed of Jharkhand. Their study revealed strong correlation between both rainfall and runoff as well as between observed and estimated runoff indicating high accuracy of runoff estimation by the NRCS CN technique.

Gitika and Ranjan (2014) demonstrated the successful integration of remote sensing and GIS based methodology for estimation of runoff in Buriganga watershed, Assam. Their study reported relatively low recharge capacity in the northern part of the watershed due to dissected, hilly and hard rock terrain with moderate to high degree of slope whereas the southern part of the watershed produced high surface runoff covered due to exposed bare surface and crop land in gentle slopes.

Akbari *et al.* (2016) investigated the effect of slope on CN in Kuantan river basin of Malaysia using Huang and Sharply-Williams methods to examine the changes in CN values. Their study revealed that both the methods resulted in expanding the CN value domain in the lower and upper limits of the

standard CN value range. It was also observed that the range of the upper limit exceeded well beyond the maximum possible value for CN in both methods. The slope adjustment of CN also resulted in decrease of CN values in flat and mild slopes while CN values increased in areas with relatively steep slopes.

Bartlett *et al.* (2016) highlighted the limitations of the SCS-CN method of runoff estimation mentioning that the method is restricted to certain geographic regions and land use types and does not describe the spatial variability of runoff. To overcome these limitations, they presented a new theoretical framework for spatially lumped, event-based rainfall-runoff modeling. They demonstrated the concept in four forested watersheds and suggested the resulting model which could better represent geographic regions and site types that previously have been beyond the scope of the traditional SCS-CN method.

Oliveira *et al.* (2016) used experimental plots to measure natural runoff rates under undisturbed Brazilian savanna (Cerrado) conditions. Their study confirmed the suitability of CN values obtained from the USDA Natural Resources Conservation Service (NRCS) standard table for estimating runoff from bare soil, soybeans and sugarcane cultivated lands. However, CN values calibrated from measured rainfall-runoff data provided better runoff estimates than the CN values from the standard table. They also observed that the standard CN method was not satisfactory in estimating runoff from undisturbed Cerrado, bare soil with hydrologic soil group A, millet cultivated areas and pasture lands.

Abraham *et al.* (2017) estimated surface runoff from a sub-basin of the Periyar river basin in Kerala using the SCS-CN method integrated with GIS techniques. Their results showed good correlation between rainfall and runoff. The correlation coefficient ( $R^2$ ) for yearly, monthly and daily runoff was observed to be 0.993, 0.957 and 0.901, respectively.

Raju *et al.* (2018) estimated the surface runoff from the Mandavi basin in Andhra Pradesh for a period of 20 years (1995 - 2014) using the NRCS-CN method coupled with remote sensing and GIS techniques. Their findings revealed that the ungauged watershed exhibited an annual average rainfall, runoff, runoff volume and runoff coefficient values of 688.82 mm, 478.06 mm, 699.75 m<sup>3</sup> and 0.69, respectively.

Verma *et al.* (2018) studied the efficacy of the standard NRCS-CN model and three slope-adjusted CN models with four different values of initial abstraction coefficient ( $\lambda$ ), *i.e.*, 0.05, 0.1, 0.2 and 0.3 for runoff estimation in the Kalu watershed of Maharashtra, using remote sensing and GIS techniques. Their results showed that the Sharpley-Williams slope-adjusted CN model with a  $\lambda$  value of 0.3 performed the best as compared to the other models, while the standard NRCS-CN model performed the worst.

Ajmal *et al.* (2020) investigated the effects of different values of initial abstraction coefficient ( $\lambda$ ) and watershed slope factor in runoff estimation from 39 watersheds on the Korean Peninsula with slopes varying between 7.50% and 53.53%. Their study showed that the use of  $\lambda$  value of 0.05 instead of the standard  $\lambda$  value of 0.2 and the consequent adjustment of CN-II values to CN<sub>0.05</sub> moderately improved the runoff estimation, but not well enough for estimating runoff from steep-sloped watersheds. Based on their findings, they proposed a slope-adjusted CN (CN<sub>II $\alpha$</sub> ) approach to improve the runoff prediction capability of the CN model in steep-sloped watersheds.

Kumar *et al.* (2021) estimated surface runoff for ten years *i.e.*, 2005 – 2014, in Sind river basin of India using GIS integrated SCS-CN technique. It was observed that the average annual surface runoff from the Sind river basin was 133.71 mm representing 17.21% of the total average annual rainfall. The maximum and minimum surface runoff was observed in the years 2009 and 2006 with values 231.43 and 32.41 mm, respectively.

Khazr *et al.* (2022) estimated runoff in the Sulaymaniyah sub-basin of the Kurdistan region of Iraq using SCS-CN and GIS techniques. Their findings revealed that increased urbanization in the study area during the period 1999 – 2019 has increased the impermeability of the land by 40.9% and the resultant runoff depth was 40.2% higher in 2019 as compared to the runoff depth observed in 1999. It was concluded that the increase in built-up areas and diminishing vegetation cover resulted in greater runoff depth in urban catchments.

### **2.3 Estimation of average annual soil loss using the USLE method**

Baban and Yosuf (2001) successfully demonstrated the effectiveness of integrating remote sensing and GIS with the USLE in generating essential quantitative information on soil erosion in Langkawi Island, Malaysia.

Fistikoglu and Harmancioglu (2002) integrated GIS with the USLE model for estimation of soil loss and concluded that GIS permits more effective and accurate applications of the USLE model for small watersheds provided that sufficient spatial data are available.

Ozcan *et al.* (2008) performed soil loss assessment in five different lands uses in Indagi Mountain Pass, Turkey using GIS based USLE methodology. It was observed that the spatial average of soil loss among the land uses were 1.99, 1.29, 1.21, 1.20, 0.89 t ha<sup>-1</sup> yr<sup>-1</sup> for the cropland, grassland, recreation, plantation and forest, respectively.

Dabral *et al.* (2008) carried out soil erosion assessment of Dikrong river basin of Arunachal Pradesh using remote sensing and GIS techniques. Their study generated vital information on spatial distribution of soil erosion rates in the watershed and reported an average potential soil erosion of 51 t ha<sup>-1</sup> yr<sup>-1</sup>. They concluded that remote sensing and GIS helped in generation of USLE parameters for soil erosion assessment in remote areas.

Sheikh *et al.* (2011) integrated GIS with USLE method for soil loss estimation in IEL 7 watershed of Lidder catchment in the Himalayan region. Their findings showed that the annual soil loss of the study area varied between 0 and 61 t ha<sup>-1</sup> yr<sup>-1</sup>. It was observed that soil loss from agriculture land was highest whereas forest areas showed the least amount of annual soil loss.

Ghosh *et al.* (2013) carried out soil loss assessment in the Dhalai river basin of Tripura using USLE method. It was observed that the average annual soil loss ranged between 11 and 836 t ha<sup>-1</sup> yr<sup>-1</sup>. Low annual soil loss rates of <50 t ha<sup>-1</sup> yr<sup>-1</sup> were mostly recorded from densely forested areas.

Devatha *et al.* (2015) used remote sensing and GIS techniques for soil loss assessment in Kulhan basin of Chhattisgarh. It was observed that 83.97 % of total area was under slight erosion risk class and only 0.45 % of total area was under very severe class.

Ali and Hagos (2016) carried out soil erosion assessment using USLE and GIS in the Awassa catchment of Central Ethiopia. Based on their findings, the study area was categorized into six ordinal classes of soil erosion risk zones *viz.*, extremely high risk, extreme risk, very high risk, high risk, moderate risk and low risk with soil loss values 91-202, 56-91, 30-56, 10-30, 5-10 and 0-5 t ha<sup>-1</sup> yr<sup>-1</sup>, respectively. It was observed that 94.83% of the total area was under low risk of soil erosion and therefore, it was concluded that the amount of soil loss was tolerable at its current situation.

Belasri and Lakhouili (2016) estimated annual soil loss using the USLE method integrated with remote sensing and GIS techniques in the Oued El Makhazine watershed of Morocco. It was concluded that spatial erosion maps generated with GIS based USLE method could provide vital inputs for planning and management strategies in the environmentally sensitive mountainous areas.



Singh and Panda (2017) investigated the spatial heterogeneity of annual soil erosion on grid-cell basis in a small agricultural watershed of eastern India by integrating universal soil loss equation (USLE) model with GIS and generated information that can be used for prioritizing critical erosion prone areas and for determining appropriate soil erosion prevention and control measures.

Bagegnehu *et al.* (2019) estimated soil loss using GIS based USLE method for soil conservation planning in Karesa watershed of South West Ethiopia. Based on their findings, the soil loss rate was classified into four erosion severity classes as very less, less, moderate and high. It was observed that very less to less soil loss was recorded from areas having slopes of 0-15 and 15-30% with a soil loss rate of 0-6.25 t ha<sup>-1</sup> yr<sup>-1</sup>. On the other hand, moderate to high soil loss was recorded from areas having >30% slope with a soil loss rate of 6.25-25 t ha<sup>-1</sup> yr<sup>-1</sup>.

Girmay *et al.* (2020) estimated soil loss rate using the USLE model in Agewmariyam watershed of Northern Ethiopia. Their results showed that about 33.5% of total area of the watershed was prone to severe erosion because of cultivation on steep slopes, sparse vegetation cover and absence of conservation measures. It was proposed that immediate soil and water conservation measures should be adopted in such areas.

Ebrahimi *et al.* (2021) performed an assessment of soil loss-prone zones using the USLE model in North-Eastern Iran. The annual soil loss was classified into five classes from slight soil losses (0–3 t ha<sup>-1</sup> yr<sup>-1</sup>) to severe soil losses (25–55 t ha<sup>-1</sup> yr<sup>-1</sup>). It was observed that about 9.36% of the study area was under critical erosion-prone zones of high and severe soil losses. Their findings also revealed that a very strong and significant relationship ( $R = 0.997$ ) was observed between high/severe soil losses and xeroll soils of the study area.

Jemai *et al.* (2021) carried out soil erosion estimation in the Oued El Hamma catchment of South-Eastern Tunisia. It was observed that erosion risk was minimal in most of the catchment with an approximate soil loss rate of  $0.2 \text{ t ha}^{-1} \text{ yr}^{-1}$ . The maximum soil loss in the study area was observed in the Matmata mountainous regions with a soil loss rate of  $17 \text{ t ha}^{-1} \text{ yr}^{-1}$ .

Dos Santos *et al.* (2022) analyzed soil erosion in Verdinho basin of the Brazilian Cerrado. Based on their findings, the soil loss rates were classified from slight ( $0\text{--}2.5 \text{ t ha}^{-1} \text{ yr}^{-1}$ ) to extremely high ( $>100 \text{ t ha}^{-1} \text{ yr}^{-1}$ ). It was observed that the highest soil losses were recorded from areas under cultivation, pasture and other exposed land surfaces in potentially erosive environments.

## **MATERIALS AND METHODS**

The details of the materials and methods used in the present investigation are given in this chapter under the following sections:

### **3.1 About the study area**

The Dzumah watershed selected for the study is located in Medziphema, under Dimapur district of Nagaland. The watershed is located between 93° 51' 33" to 94° 00' 16" E longitude and 25° 40' 45" to 25° 47' 01" N latitude occupying an area of 6555 ha (65.55 sq km). The elevation of the watershed is at a height of 328 m above mean sea level at the confluence and increases up to a height of 2345 m above mean sea level. The watershed area has a typical humid sub-tropical and associated agro-ecological setup. The watershed exhibits a dendritic drainage pattern. The location and spatial extent of the study area is as shown in Fig. 3.1.

### **3.2 Collection of data**

The present investigation requires data on rainfall, soil, land use/land cover, relief and topography of the study area. Collection of relevant data was performed as follows:

#### **3.2.1 Remote sensing data**

Cloud-free high resolution multispectral satellite data (Sentinel-2A) downloaded from the USGS website ([earthexplorer.usgs.gov](http://earthexplorer.usgs.gov)) had been used in the present study for classification of land use and land cover. The details of the satellite dataset are as given in Table 3.1.

#### **3.2.2 Rainfall data**

Monthly rainfall data of 23 years (1998-2020) and daily rainfall data of two years (2019-2020) was collected from ICAR, Jharnapani, Medziphema,

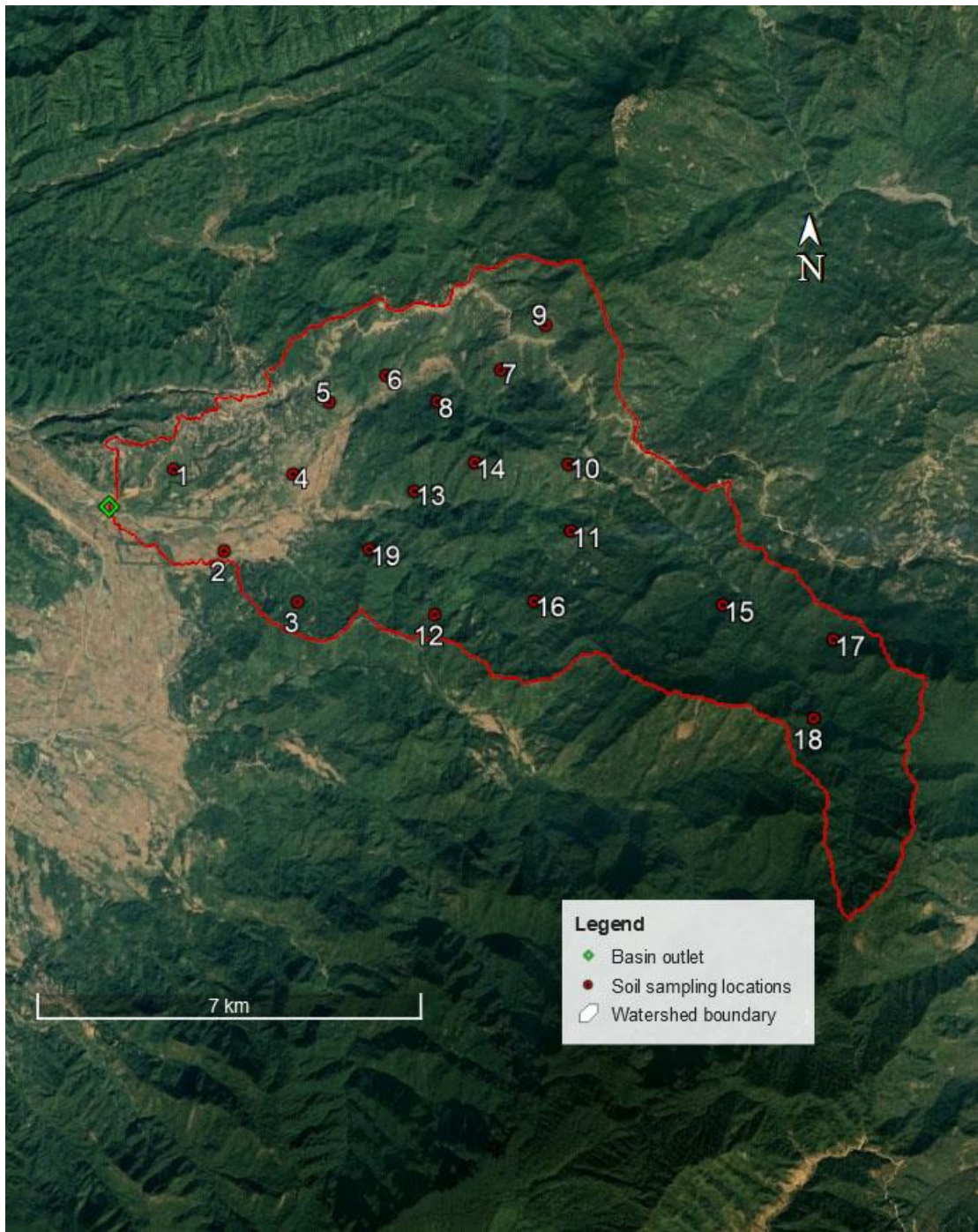


Fig. 3.1: Spatial extent of Dzumah watershed

Nagaland. The monthly and daily rainfall data were used for calculating rainfall erosivity and studying the rainfall-runoff relationship of the watershed, respectively.

### **3.2.3 Soil**

A total of 19 sampling locations as represented in Fig. 3.1, were randomly selected from the watershed area for collection of soil samples. The coordinates of the sampling points and the corresponding sample number are presented in Table 3.2.

### **3.2.4 Thematic maps**

The basic thematic maps for hydrological studies were generated as follows:

- Land use/land cover map was prepared using the Sentinel-2A (10 m resolution) images.
- Soil map was prepared from laboratory analysis of soil samples collected from the watershed.
- Watershed delineation, slope map and drainage map were generated using SRTM DEM (30 m resolution) downloaded from USGS website ([earthexplorer.usgs.gov](http://earthexplorer.usgs.gov)).

### **3.2.5 Software and systems**

ArcGIS 10.8, QuantumGIS (QGIS) and MS-Office suite were used for digital analysis, data creation and output generation. ArcGIS 10.8 and QGIS are software applications that allow to perform GIS tasks such as mapping, geographic analysis, hydrology and spatial analysis, data editing and compilation, data management, visualization, and geo-processing. MS-Office suite was used for statistical analysis, documentation and for presentation purpose.

Table 3.1: Details of satellite dataset

Sl.No.	Satellite	Product level	Tile ID	Absolute Orbit Number	Acquisition time	Resolution
1.	Sentinel-2A	L1C	T46REP	A022967	15/11/2019	10 m

Table 3.2: Soil sampling location coordinates

Sample Number	Coordinates (Decimal degrees)	
	Longitude	Latitude
1	93.8720862	25.7497276
2	93.8811345	25.7364345
3	93.8945354	25.7281952
4	93.8936231	25.748924
5	93.900196	25.7605496
6	93.9104677	25.7648868
7	93.9310979	25.7656707
8	93.9197039	25.7605732
9	93.9390183	25.7725566
10	93.9431405	25.7503422
11	93.9435515	25.7396345
12	93.9192593	25.7261942
13	93.9155765	25.7460998
14	93.926405	25.7506485
15	93.9703183	25.727786
16	93.9369824	25.7283717
17	93.9895084	25.7223661
18	93.9856627	25.7100644
19	93.9074576	25.7367460

### **3.3 Methodology**

#### **3.3.1 Watershed characterization**

Watershed characterization describes the very nature of the watershed and its components. Morphometric parameters of a watershed influence the rate and quantity of water flowing out of a watershed. These physical features determine the reaction of a watershed to rainfall events and its vulnerability to natural calamity like floods and erosion. These parameters describe the physical features of a watershed in terms of its overall shape, ruggedness, dissection and drainage qualities.

Watershed delineation, relief/slope aspects, drainage pattern and stream network generation was carried out using SRTM DEM of 30m resolution in QGIS. Stream ordering scheme proposed by Strahler was adopted for assigning orders to drainage. All the thematic layers generated were projected to a common spatial reference system (WGS-84/UTM) for overlay in GIS environment. Based on this dataset, the morphometric analysis of the Dzumah watershed was carried out. Important linear, areal and relief parameters were computed using respective formula and interpreted with reference to the watershed as given in Table 3.3a, 3.3b and 3.3c.

#### **3.3.2 Estimation of surface runoff and water yield potential**

##### **3.3.2.1 The NRCS-CN method**

The Soil Conservation Service Curve Number (SCS-CN) method, now called as Natural Resource Conservation Service Curve Number (NRCS-CN) was developed by the U.S. Department of Agriculture in 1969 for estimation of direct runoff volume based on storm rainfall depth. Due to its simplicity and versatility, it has become a widely used procedure for predicting runoff. The curve number method has been adopted and used in models to simulate runoff behavior and flow response of watershed to ordinary as well as heavy rainfall

Table 3.3a: Morphometric analysis of linear aspects of watershed

Sl.No.	Morphometric parameters	Formula	Description	References
1	Stream order (u)	-	Hierarchical rank	Strahler (1964)
2	Stream length (Lu)	-	Length of the major stream	Horton (1945)
3	Stream number (Nu)	-	Total number of stream segments of order 'u'	Horton (1945)
4	Mean stream length (Lsm)	$L_{sm} = L_u/N_u$	Lu = Total stream length of order 'u' Nu = Total number of stream segments of order 'u'	Strahler (1964)
5	Stream length ratio (Rl)	$R_l = L_u/L_{u-1}$	Lu = Total stream length of order 'u' Lu-1 = Total stream length of its next lower order	Horton (1945)
6	Length of overland flow (Lg)	$L_g = 1/(2 \times D_d)$	Dd = Stream density	Horton (1945)
7	Bifurcation ratio (Rb)	$R_b = N_u/N_{u+1}$	Nu = Total number of stream segments of order 'u' Nu+1 = Number of stream segments of the next higher order	Schumm(1956)
8	Mean bifurcation ratio (Rbm)	-	Average of bifurcation ratios of all orders	Strahler(1957)
9	Basin length (Lb)	-	-	Schumm (1956)



Table 3.3b: Morphometric analysis of areal aspects of watershed

Sl.No.	Morphometric parameters	Formula	Description	References
1	Watershed area (A)	-	-	Schumm (1956)
2	Watershed perimeter (P)	-	-	Schumm (1956)
3	Form factor (Ff)	$Ff = A/Lb^2$	A = Area of watershed Lb = Basin length	Horton (1932)
4	Elongation ratio (Re)	$Re = (2/Lb)[(A/\pi)^{0.5}]$	A = Area of watershed Lb = Basin length	Schumm (1956)
5	Circulatory ratio (Rc)	$Rc = (4\pi A)/P^2$	A = Area of watershed P = Perimeter	Strahler (1964)
6	Drainage density (Dd)	$Dd = Lu / A$	Ratio of total stream length and area	Horton (1945)

Table 3.3c: Morphometric analysis of relief aspects of watershed

Sl.No.	Morphometric parameters	Formula	Description	References
1	Basin relief (Bh)	$Bh = H-h$	Vertical distance between the lowest and highest points	Strahler(1952)
2	Relief ratio (Rr)	$Rr = Bh/Lb$	Ratio of basin relief and length	Schumm (1956)
3	Ruggedness number (Rn)	$Rn = Bh \times Dd$	Bh = Basin relief Dd = Drainage density	Strahler (1958)

events. The NRCS-CN method is based on the water balance equation of the rainfall in a known interval of time  $\Delta t$ , which can be expressed as

$$P = I_a + F + Q \quad (3.1)$$

Where,

$P$  = total precipitation

$I_a$  = initial abstraction,

$F$  = cumulative infiltration excluded in  $I_a$

$Q$  = direct surface runoff

Two other concepts as below are also used with equation (3.1):

1. The first concept is that the ratio of actual amount of direct runoff ( $Q$ ) to maximum potential runoff ( $P - I_a$ ) is equal to the ratio of actual infiltration ( $F$ ) to the potential maximum retention or infiltration ( $S$ ), thus

$$\frac{Q}{P - I_a} = \frac{F}{S} \quad (3.2)$$

2. The second concept is that the amount of initial abstraction ( $I_a$ ) is some fraction of potential maximum retention, thus

$$I_a = \lambda S \quad (3.3)$$

Combining equation (3.1) and (3.2) and using (3.3),

$$Q = \frac{(P - I_a)^2}{P - I_a + S} = \frac{(P - S)^2}{P - I_a + S} \quad \text{when } P > I_a \quad (3.4)$$

$$Q = \frac{(P - 0.2S)^2}{P + 0.8S} \quad \text{when } P > I_a \quad (3.5)$$

Where,

$Q$  = runoff depth (mm)

$P$  = rainfall (mm)

$S$  = maximum recharge capacity of watershed after 5 days antecedent rainfall (mm)

$I_a = 0.2S$  (Initial abstraction of rainfall by soil and vegetation, mm)

Subsequently, the water yield potential of the watershed was estimated by converting runoff depth in millimeter (mm) to cubic meter ( $m^3$ ). The formula used for this conversion is given as follows:

$$W = A \times 10^4 \times \frac{Q}{1000} \quad (3.6)$$

Where,

$W$  = Water yield potential ( $m^3$ )

$A$  = Area of catchment (ha)

$Q$  = Total runoff depth (mm)

### **3.3.2.2 Development of model database for NRCS-CN method**

#### **3.3.2.2.1 Rainfall parameter (P)**

Daily rainfall data for the year 2019 and 2020 was collected from ICAR, Jharnapani, Medziphema, Nagaland. Most of the annual rainfall in the study area is received during the month of June to October. Therefore, the rainfall events from the month of June to October were considered for estimating the rainfall (P) parameter.

#### **3.3.2.2.2 Potential maximum retention (S)**

Potential maximum retention (S) was calculated for all the three antecedent moisture conditions *i.e.*, normal, dry and wet conditions for the study area using the equation as follows:

$$S = \frac{25400}{CN} - 254 \quad (3.7)$$

$$CN = \frac{25400}{S+254} \quad (3.8)$$

Where,

S = Maximum recharge capacity of watershed after 5 days rainfall antecedent (mm)

CN = Curve Number

### **3.3.2.2.3 Curve number (CN)**

The curve number (CN) is dimensionless with values varying from 0 to 100. The curve number is derived from a number of collective factors which influences runoff generation in a watershed *i.e.*, antecedent moisture condition, land use/land cover and treatments, soil type and surface condition of the watershed. As defined by NRCS soil scientists, soils are classified into four Hydrologic Groups as A, B, C, and D (USDA, 2009) depending on the soil physical characteristics that influence infiltration and drainage capacities of the soil. Group A soils have the highest infiltration rates, thus producing the least runoff, whereas Group D soils have lowest infiltration rate and produces the highest runoff. Soil texture data obtained from laboratory analysis and classification method as described by Ross *et al.* (2018) was used to derive the hydrological soil groups of the study area. The hydrological soil-cover complex was generated using land use/land cover map.

Antecedent Moisture Condition (AMC) is the relative wetness or dryness of a watershed and has a significant effect on amount of runoff generated in a watershed. Recognizing its significance, SCS developed a guide for adjusting CN according to AMC based on the total rainfall in the 5-day period preceding a storm. Three levels of AMC are used in the CN method: AMC-I for dry, AMC-II for normal, and AMC-III for wet conditions. Table 3.4 gives seasonal rainfall limits for these three antecedent moisture conditions.

The CN values are always documented for the case of AMC-II (USDA, 1985). Rainfall data is required to determine the most appropriate AMC related

Table 3.4: Classification of Antecedent Moisture Condition

AMC	5-days Antecedent Rainfall (mm)	
	Active growing season	Dormant season
I	Dry ( < 35 )	Dry ( < 12.5 )
II	Medium ( 35 to 52.5 )	Medium ( 12.5 to 27.5 )
III	Wet ( > 52.5 )	Wet ( > 27.5 )

to the watershed. To calculate CN values for AMC-I and AMC-III conditions, the following equations are used (Hawkins *et al.*, 1985):

$$\text{CN for AMC – I:} \quad CN_I = \frac{CN_{II}}{2.281 - 0.01281 CN_{II}} \quad (3.9)$$

$$\text{CN for AMC – III:} \quad CN_{III} = \frac{CN_{II}}{0.427 + 0.00573 CN_{II}} \quad (3.10)$$

Where,

$CN_I$  = curve number for dry condition

$CN_{II}$  = curve number for normal condition

$CN_{III}$  = curve number for wet condition

#### 3.3.2.2.4 Initial abstraction parameter ( $I_a$ )

The amount of initial abstraction ( $I_a$ ) is some fraction of the potential maximum retention and it is expressed as:

$$I_a = \lambda S \quad (3.11)$$

Where,

$\lambda$  = initial abstraction ratio

$S$  = potential maximum retention

The  $\lambda$  value of 0.2, which is treated as a constant, is widely debated among researchers because of great variations in the  $\lambda$  value reported across the world (Verma *et al.*, 2018). Recent research has found that a  $\lambda$  value of 0.05 instead of 0.2 gave more appropriate results (Woodward *et al.*, 2003). This adjustment of  $\lambda$  value has recently been adopted by the Task Group on Curve Number Hydrology (Hawkins *et al.*, 2019), which recommends a new relation as follows:

$$S_{0.05} = 1.42S_{0.2} \quad (3.12)$$

This modification in the  $\lambda$  value and the resultant change in the  $CN_{II}$  have been adopted for estimation of runoff in the present study and is given as follows:

$$CN_{II0.05} = \frac{100}{1.42 - 0.0042CN_{0.2}} \quad (3.13)$$

### 3.3.2.2.5 Slope-adjusted CN

The SCS-CN method was originally developed for use in agricultural lands having slopes less than 5% and as such, slope was not factored into the equation. However, slope has significant influence on surface runoff generation and therefore, integrating slope factor and adjusting CN values is imperative for runoff estimation. The Huang *et al.* (2006) approach was used to integrate the slope factor into the investigation and is given as follows:

$$CN_{II\alpha} = CN_{II} \left( \frac{322.79 + 15.63\alpha}{\alpha + 323.52} \right) \quad (3.14)$$

Where,

$CN_{II\alpha}$  = Slope adjusted  $CN_{II}$

$\alpha$  = slope ( $m \cdot m^{-1}$ )

Weighted slope was computed as follows:

$$\text{Weighted slope} = \frac{\sum_{i=1}^n a_i X s_i}{A} \quad (3.15)$$

Where,

$a_i$  = area of slope (ha)

$s_i$  = slope (%)

$A$  = polygon area (ha)

Weighted slope was applied in equation (3.14) to compute slope-adjusted  $CN_{II}$  values.

### 3.3.2.2.6 Land use/land cover

The land use/land cover map of the study area was prepared using Sentinel-2A imagery. The cloud-free satellite data captured on 15<sup>th</sup> November, 2019 having a spatial resolution of 10m in three spectral bands (band 1: 560 nm; band 2: 665 nm; band 3: 842 nm) were obtained from the USGS website (earthexplorer.usgs.gov). QGIS 3.10 software was used for generating the standard false color composite (FCC) image of the study area. The FCC thus obtained was used for the land use/land cover classification. In the present study, the Semi-Automatic Classification Plugin (SCP) was used for performing a supervised classification of the image. The Maximum Likelihood algorithm was considered for classification of the image.

### 3.3.3 Estimation of soil erosion using the Universal Soil Loss Equation

The Universal Soil Loss Equation (USLE) is an empirical soil erosion prediction method developed by Weischmeier and Smith (1978) to predict long-term average annual rate of soil losses. The equation is a product of five input factors and is expressed as follows:

$$A = R \times K \times LS \times C \times P \quad (3.16)$$

Where,

A = the average annual soil loss ( $t \text{ ha}^{-1} \text{ yr}^{-1}$ )

R= the rainfall erosivity factor ( $\text{MJ mm ha}^{-1} \text{ h}^{-1} \text{ yr}^{-1}$ )

K= the soil erodibility factor ( $t \text{ ha h ha}^{-1} \text{ MJ}^{-1} \text{ mm}^{-1}$ )

LS = the slope length steepness factor (dimensionless)

C= the cover management factor (dimensionless, ranging between 0 and 1)

P= conservation practice factor (dimensionless, ranging between 0 and 1)

In this study, the Universal Soil Loss Equation (USLE) was combined with GIS technologies to estimate the potential soil loss from the watershed. A cell size of 30 x 30 m was considered as basic operational unit for erosion



analysis. Average annual soil losses were grouped into different classes as suggested by Prasanakumar *et al.* (2011).

### 3.3.3.1 Rainfall erosivity factor (R)

Annual rainfall data of 23 years (1998–2020) was collected from ICAR, Jharnapani for calculating the R-factor. As there was no record of rainfall intensity, monthly rainfall data was used for calculating annual R-factor using the following relationship developed by Wischmeier and Smith (1978):

$$R = \sum_{i=1}^{12} 1.735 \times 10^{[1.5 \log_{10} (P_i^2/P) - 0.08188]} \quad (3.17)$$

Where,

R = Rainfall erosivity factor (MJ mm ha<sup>-1</sup> h<sup>-1</sup> yr<sup>-1</sup>)

P<sub>i</sub> = Monthly rainfall (mm)

P = Annual rainfall (mm)

### 3.3.3.2 Soil erodibility factor (K)

The K-factor was calculated using the following equation as given by Wischmeier and Mannering (1969):

$$K = \frac{2.1 \times 10^{-4} (12 - \text{OM}) M^{1.14} + 3.25(s-2) + 2.5(p-3)}{759.4} \quad (3.18)$$

Where,

K = soil erodibility (t ha h ha<sup>-1</sup> MJ<sup>-1</sup> mm<sup>-1</sup>)

OM = percentage of organic matter

S = soil structure code

P = permeability code

M = function of the fraction of the primary particle size

Soil samples collected from the watershed were analyzed in the laboratory of the Department of Soil and Water Conservation, SASRD,

Nagaland University. The mechanical composition of the soil was analyzed using International Pipette Method (Piper, 1996) and thereafter, soil textural classes were assigned using the soil texture triangle. This information on soil texture was used for calculating the function of the primary particle size fraction (M) using the following equation:

$$M = (\% \text{ silt} + \% \text{ sand}) \times (100 - \% \text{ clay}) \quad (3.19)$$

The soil structure and permeability codes of different soil types were assigned according to their particle size as suggested by Wischmeier and Mannering (1969). Organic carbon was determined using Walkley and Black method (1934) and the organic matter content was derived by multiplying the organic carbon content with the van Bemmelen factor. The K values thus obtained were interpolated using Inverse Distance Weight (IDW) technique in ArcGIS to derive the K-factor map.

### **3.3.3.3 Slope length and steepness factor (LS)**

The slope length factor (L) and slope steepness factor (S) accounts for the effect of topography on erosion in the USLE method. Slope length (L) and slope steepness (S) and were determined and combined to form a single factor known as the topographic factor (LS). In the present study, the LS factor was computed in Spatial Analyst module of ArcGIS using SRTM DEM of 30 m resolution. The slope length factor (L) is calculated using following equation

$$L = (\lambda/22.13)^m \quad (3.20)$$

Where,

22.13 = the USLE unit plot length (m)

$m$  = a variable slope-length exponent.

Slope length  $\lambda$  is defined as the horizontal distance from the origin of overland flow to the point where the slope gradient decreases enough that deposition begins or runoff becomes concentrated in a defined channel.

The slope length exponent  $m$  is calculated as follows:

$$m = \frac{\beta}{1+\beta} \quad (3.21)$$

$\beta$  is calculated as follows:

$$\beta = (\sin \theta / 0.0896) / [3.0(\sin \theta)^{0.8} + 0.56] \quad (3.22)$$

Where,

$\theta$  = slope angle

The slope steepness factor  $S$  is evaluated by the relationship developed by McCool *et al.* (1987) as follows:

$$S = 10.8\sin\theta + 0.03 \quad S < 9\% \quad (i.e. \tan\theta < 0.09) \quad (3.23a)$$

$$S = (\sin\theta / \sin 5.143)^{0.6} \quad S \geq 9\% \quad (i.e. \tan\theta \geq 0.09) \quad (3.23b)$$

To calculate LS factor, flow accumulation map and slope map (degrees) were derived from DEM. The L factor map is derived by applying equation 3.20 on flow accumulation map and slope length exponent ( $m$ ) map in raster calculator environment of ArcGIS 10.8. Equation 3.20 is converted to a form of grid equation as follows:

$$L = (\text{Flow accumulation} \times \text{Grid size} / 22.13)^m \quad (3.24)$$

### 3.3.3.4 Cover management factor (C)

The C-factor represents the effects of vegetation and soil cover on soil erosion. Currently, due to wide variations in the spatial and temporal patterns

of land cover, remote sensing satellite datasets are used for estimation of C factor (Karydas *et al.*, 2009; Tian *et al.*, 2009). The Normalized Difference Vegetation Index (NDVI) is an indicator of the vegetation health and is expressed as follows:

$$NDVI = \frac{NIR-R}{NIR+R} \quad (3.25)$$

Where,

NDVI = Normalized Difference Vegetation Index

NIR = Near Infrared Band

R = Red Band

The C-factor of the study area was calculated based on the works of Durigon *et al.* (2014) and is given as follows:

$$C = \frac{(-NDVI+1)}{2} \quad (3.26)$$

Where,

C = Crop management factor

### **3.3.3.5 Conservation practice factor (P)**

The P-factor reflects the effects of conservation practices to decrease the runoff and erosion (Renard *et al.*, 1997; Yue-Qing *et al.*, 2008). The P-factor values range from 0.25 to 1. Higher P-factor values correspond to areas with no conservation practices (forest/natural vegetation) whereas lower values correspond to crop land with strip and contour cropping. The P-factor values for different management practices in the study area were adopted as suggested by Rao (1981).

## RESULTS AND DISCUSSION

In the present study, an attempt has been made to characterize the Dzumah watershed, estimate surface runoff following a rainfall event and consequently estimate soil loss from the watershed. The NRCS-CN method and USLE equation has been used to estimate surface runoff and soil loss as described in different sections of the previous chapter. The results of the present investigations are presented and discussed in the following sections:

### 4.1 Watershed characterization

#### 4.1.1 Linear aspects

The linear aspects of the Dzumah watershed are discussed below:

##### 4.1.1.1 Stream order (Su)

Stream order refers to the hierarchical position of streams within a drainage basin. All the tiny unbranched stream segments are referred to as the first order streams. The shape and dimensions of a watershed and its relief characteristics influences the stream order of that watershed (Haghipour and Burg, 2014). The Dzumah watershed is a 5<sup>th</sup> order basin and a representation of its drainage network map is depicted in Fig. 4.1. Many studies have reported the higher increase in stream orders in humid environments of mountain-plain settings as compared to plateau-plain topographical settings under sub-humid conditions (Wakode *et al.*, 2013).

##### 4.1.1.2 Stream number (Nu)

Stream number refers to the total count of stream segments in each order. The Dzumah watershed consisted of 184, 36, 5, 2 and 1 stream segments of 1<sup>st</sup>, 2<sup>nd</sup>, 3<sup>rd</sup>, 4<sup>th</sup> and 5<sup>th</sup> stream order, respectively (Table 4.1). The total number of stream segments of all the order in the watershed was 228. It was observed that the number of stream segments decreased as the stream order increase to higher orders. The hilly, uneven and dissected terrain of the watershed is responsible for the higher count of lower stream orders. The

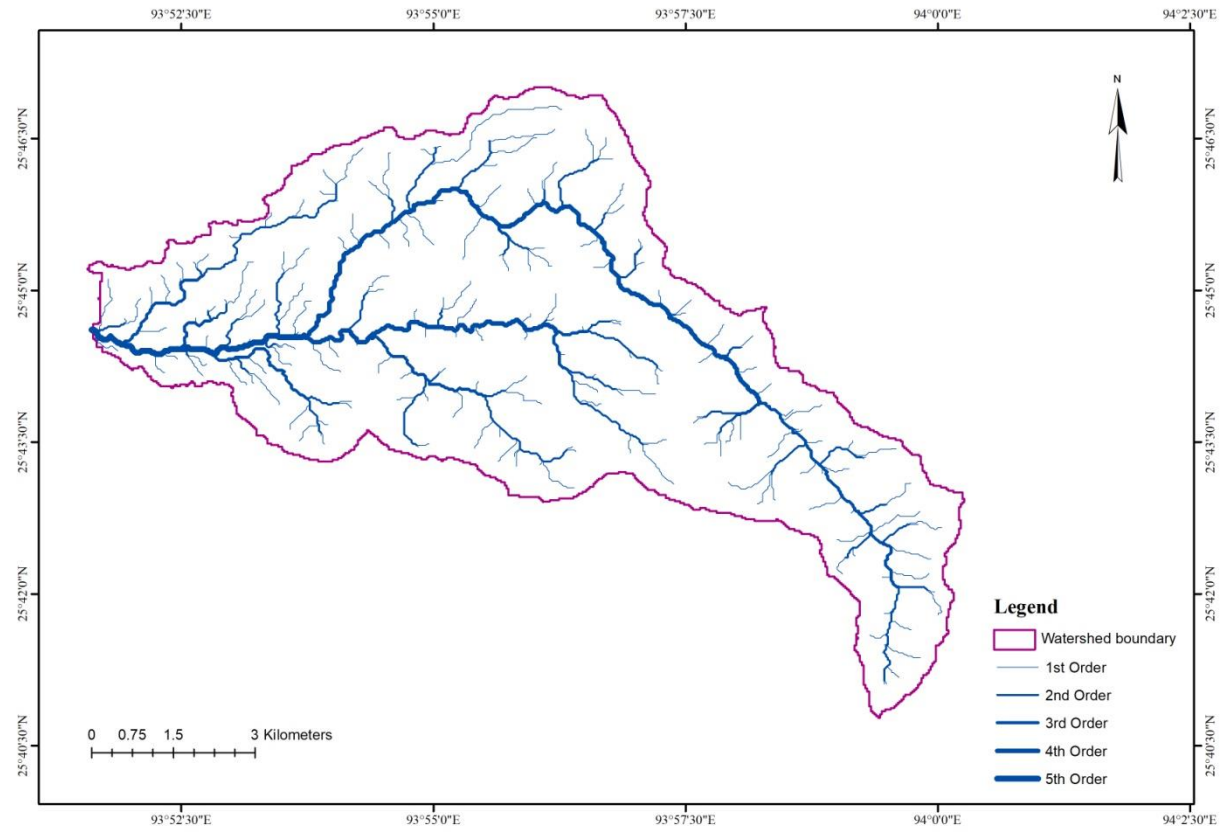


Fig. 4.1: Drainage network map of Dzumah watershed

higher count of stream segments in the higher zones of the watershed indicates the occurrence of young topography (Mahala, 2020). It was observed that there was a sudden drop in stream numbers as the stream order increases, which indicated major morphological change within the watershed. The Dzumah watershed is expected to have less infiltration and high runoff capacity with possibilities of sudden flooding during high intensity rainfall events, as indicated by the much higher count of lower order streams.

#### **4.1.1.3 Stream length (Lu)**

The length of all the stream segments in the watershed was calculated using GIS software. The stream length was found to be 66.20, 34.40, 19.84, 6.35 and 3.9 km for the 1<sup>st</sup>, 2<sup>nd</sup>, 3<sup>rd</sup>, 4<sup>th</sup> and 5<sup>th</sup> stream order, respectively (Table 4.1). The total stream length of the watershed was 130.72 km. The total stream length is usually higher in 1<sup>st</sup> order streams and then it declines as the stream order goes higher up the hierarchy. Any abnormality in this trend denotes inconsistency in lithology of the area (Mahala, 2020). Similarly, in the present study it was observed that 1<sup>st</sup> order streams has the maximum stream length and then it decreased with increasing stream order, which indicated that there was no lithological irregularities in the watershed. This observation is similar with that of Babu *et al.*, (2016), Chitra *et al.*, (2011) and Magesh *et al.* (2013). Several studies have verified that mountain–plain environments have higher stream length as compared to plateau–plain environments (Vittala *et al.*, 2004; Sreedevi *et al.*, 2005).

#### **4.1.1.4 Mean stream length (Lsm)**

The mean stream length of the 1<sup>st</sup>, 2<sup>nd</sup>, 3<sup>rd</sup>, 4<sup>th</sup> and 5<sup>th</sup> order streams of the Dzumah watershed was found to be 0.36, 0.96, 3.97, 3.18 and 3.92 km, respectively (Table 4.1). The increase in Lsm from 1<sup>st</sup> order to the 5<sup>th</sup> order indicated that 1<sup>st</sup> order streams are numerous but short whereas higher order streams are fewer in number but longer in length as described by Strahler (1964). This could be attributed to the decrease in slope of the watershed from

the divideline towards the confluence of the watershed, and indicated young developmental phase of the watershed (Gizachew and Berhan, 2018). Moreover, streams of shorter lengths indicate the presence of steep slopes whereas longer stream lengths indicate that the area has low gradient slopes (Withanage *et al.*, 2014). The mean stream length generally increases with increase in the stream order (Shrestha *et al.*, 2010). Many studies have reported that mountainous regions have lower mean stream length as compared to regions with plains and plateaus (Rai *et al.*, 2017). In the present investigation, it was observed that the upper reaches of the Dzumah watershed has low values of mean stream length, suggesting juvenile stage of geomorphological development of the watershed. It was also observed that there was some inconsistency in the mean stream length among the different stream orders of the watershed. This inconsistency suggested changes in slope gradient in the channel network, highlighting the possibilities of sudden changes in flow pattern and characteristics (Mahala, 2020).

#### **4.1.1.5 Length of overland flow (Lg)**

Lg is a measure of the soil's susceptibility to erosion and hence, it is an important variable affecting the geomorphological development of a watershed (Gutema, 2015). Lg is categorized into three classes as low, moderate and high with values  $< 0.2$ ,  $0.2$  to  $0.3$  and  $> 0.3$ , respectively (Chandrashekar *et al.*, 2015). Low values of Lg suggests that an area has steep slopes, short stream lengths, lower infiltration and higher surface runoff capacity whereas, a high value of Lg denotes a flatter terrain with longer stream length, higher infiltration and lower runoff (Sukristiyanti *et al.*, 2018). In the present study, it was found that the Dzumah watershed falls under moderate class with a Lg value of 0.25, which indicated that the watershed is prone to moderate hazards of surface runoff and soil erosion. The shorter the length of overland flow, the quicker the surface runoff from the streams (Kumar *et al.*, 2011).



Table 4.1: Linear aspects of Dzumah watershed

Stream Order (Su)	Stream Number (Nu)	Stream Length (Lu) (Km)	Mean stream length (Lsm) (Km)	Stream Length ratio (Rl)	Bifurcation ratio (Rb)		Mean Bifurcation ratio (Rbm)	Basin length (Lb) (Km)	Length of overland flow ((Lg) (Km)
1st	184	66.20	0.36	-	-	-	4.20	14.74	0.25
2nd	36	34.40	0.96	0.52	1:2	5.1			
3rd	5	19.84	3.97	0.58	2:3	7.2			
4th	2	6.35	3.18	0.32	3:4	2.5			
5th	1	3.92	3.92	0.62	4:5	2.0			
Total	228	130.71							

#### **4.1.1.6 Stream length ratio (RI)**

In this present investigation, the values of stream length ratio in the Dzumah watershed was found to be 0.52 for 1<sup>st</sup> to 2<sup>nd</sup> order streams, 0.58 for 2<sup>nd</sup> to 3<sup>rd</sup> order, 0.32 for 3<sup>rd</sup> to 4<sup>th</sup> order and 0.62 for 4<sup>th</sup> to 5<sup>th</sup> order streams (Table 4.1). The increase in the values of RI from lower order to higher order streams denotes the geomorphic maturity of the basin (Vinutha and Janardhana, 2014). Therefore, there is no classification for RI (Sukristiyanti *et al.*, 2018). In case of the Dzumah watershed, it was observed that the stream length ratio increased from 1<sup>st</sup> order up to the 3<sup>rd</sup> stream order. A drop in the stream length ratio was however, observed between the 3<sup>rd</sup> and 4<sup>th</sup> stream order which yet again increased between the 4<sup>th</sup> and 5<sup>th</sup> stream order. These changes in the stream length ratio indicated the early geomorphic developmental stage of the watershed (Mahala, 2020). Studies have reported that areas with mountain–plain settings showed higher tendencies of irregular stream length ratio as compared to flat plain and plateau environments (Magesh and Chandrasekhar, 2014).

#### **4.1.1.7 Bifurcation ratio (Rb)**

Bifurcation ratio is a dimensionless variable representing the degree of integration among the numerous stream segments of different stream orders present in a watershed (Gutema *et al.*, 2017). The value range of the Rb classifications varies among the researchers (Sukristiyanti *et al.*, 2018). In general, the values of bifurcation ratio is categorized into two classes *i.e.*, low and high. Rb values less than 5 are considered low whereas Rb values greater than 5 are considered high. Low values of Rb indicates that the drainage pattern is not affected by the geologic structures (Rai *et al.*, 2017; Vittala *et al.*, 2004; Abboud and Nofal, 2017; Yangchan *et al.*, 2015), whereas the high values of Rb indicates that the drainage pattern is controlled by the geologic structures.

The bifurcation ratio of the Dzumah watershed was found to be 5.1 for 1<sup>st</sup> to 2<sup>nd</sup> stream order; 7.2 for 2<sup>nd</sup> to 3<sup>rd</sup> stream order; 2.5 for 3<sup>rd</sup> to 4<sup>th</sup> stream order and 2.0 for the 4<sup>th</sup> to 5<sup>th</sup> stream order (Table 4.1). The average bifurcation ratio of the watershed was 4.2. It was observed that the lower stream orders had greater values of bifurcation ratio as compared to the streams of higher order. Thus, it could be inferred that the drainage pattern of lower order streams, which occupy higher reaches of the basin are influenced by geologic structures whereas the drainage pattern of the higher order streams occupying flatter and plain areas of the basin are independent of geologic structures.

#### **4.1.2 Areal aspects**

The areal aspects include watershed area, watershed perimeter, form factor, elongation ratio, texture ratio, circulatory ratio and drainage density which are discussed as follows:

##### **4.1.2.1 Watershed area (A) and perimeter (P)**

Watershed area is important for hydrological studies as the area coverage determines the amount of rainfall received by the watershed and the amount of runoff that would be generated. The Dzumah watershed has an area of 6555 hectares. The perimeter of the watershed was calculated from the delineated watershed layer and was found to be 59.58 km.

##### **4.1.2.2 Form factor (Rf)**

The value of Rf for a perfectly circular watershed is always less than 0.7854 (Bali *et al.*, 2011), which implies that under natural geographical conditions, the value of Rf of a watershed cannot be more than 0.7854. Elongated basins tend to have lower values of Rf. A circular-shaped basin will have greater values of Rf and is often characterized by having high peak flows in shorter duration of time, whereas elongated basins generally have lower Rf values with comparatively lower peak flow but for a longer duration (Bali *et al.*, 2011). In the present study, the Rf value of the Dzumah watershed was

found to be 0.30 (Table 4.2), denoting that the study area is elongated in shape. Based on this finding, it is expected that the Dzumah watershed should have a flatter peak flow for longer time duration.

#### **4.1.2.3 Elongation ratio (Re)**

The elongation ratio is a dimensionless property and its value ranges from 0.6 to 1.0 over a large variety of climatic condition and geologic structure (Strahler, 1964). There are four classes of Re viz., elongated, less elongated, oval and circular with value ranges  $<0.7$ ,  $0.7$  to  $0.8$ ,  $0.8$  to  $0.9$  and  $> 0.9$ , respectively (Sukristiyanti *et al.*, 2018). In the present investigation, the Re value of Dzumah watershed was found to be 0.62, indicating that the watershed is elongated in shape (Table 4.2).

#### **4.1.2.4 Circularity ratio (Rc)**

Circulatory ratio is also a dimensionless property. The value of Rc varies from '0' (minimum circularity) to '1' (Maximum circularity) (Mahala, 2020). Rc values  $< 0.4$  indicates that a watershed is elongated in shape, Rc values varying between  $0.4$  - $0.75$  indicates that the watershed has an intermediate shape and Rc values  $> 0.75$  indicate a circular-shaped basin (Miller, 1953). Lower Rc values implies a greater susceptibility to soil erosion (Kadam *et al.*, 2019). The circulatory ratio of the Dzumah watershed was found to be 0.23, which also denoted that the watershed is elongated in shape (Table 4.2). The low value of Rc also indicated higher risks of soil erosion and further validates the highly irregular nature of the watershed.

#### **4.1.2.5 Drainage density (Dd)**

Drainage density is an expression of the closeness of spacing of channel within a basin (Horton, 1945). The drainage density is classified into three categories *i.e.*, coarse if the value of  $Dd < 5 \text{ km.km}^{-2}$ , medium if the value of  $Dd$  varies between  $5$ - $10 \text{ km.km}^{-2}$  and fine if  $Dd$  value is  $> 10 \text{ km.km}^{-2}$  (Yousuf *et al.*, 2020). Drainage density greatly influences the runoff characteristics of a

watershed. High drainage density facilitates rapid removal of excess runoff, effectively minimizing the basin lag time and increasing the peak flow (Chorley, 1969). Several studies have reported that areas with permeable soil, healthy vegetation cover and flat terrains have low drainage density whereas, those regions with comparatively less permeable surfaces, thin vegetation and high relief showed higher values of drainage density (Asfaw and Workineh, 2019; Babu *et al.*, 2016; Gizachew and Berhan, 2018; Kaur *et al.*, 2014; Magesh and Chandrasekhar, 2014; Prasad *et al.*, 2008). Studies have also confirmed that drainage density has close correlation with rainfall intensity, rock resistivity and an inverse relationship with the developmental extent of drainage network, infiltration capacity, vegetation cover, landscape dissection and spacing of streams (Prabhakaran and Jawahar, 2018). The overall drainage density value of Dzumah watershed was found to be 1.99, indicating that it has a coarse drainage texture (Table 4.2).

#### **4.1.3 Relief aspects**

Relief characteristics of a watershed play a significant role in controlling the velocity of water draining through the basin. Surface runoff usually flows with greater velocity in steeper slopes, producing higher discharge with greater erosive power. The relief aspects of the Dzumah watershed are discussed below:

##### **4.1.3.1 Basin relief (Bh)**

In the present study, it was observed that the lowest and the highest elevation points in the Dzumah watershed was located at elevations of 328 m and 2345 m above mean sea level, resulting in a basin relief of 2017 m for the watershed. An elevation map of the Dzumah watershed is depicted in Fig. 4.2.

##### **4.1.3.2 Relief ratio (Rr)**

It refers to the ratio between basin relief and basin length. It is an indicator of the general steepness or flatness of a watershed (Babu *et al.*, 2016).

Table 4.2: Areal and relief aspects of Dzumah watershed

Areal aspects	
Basin Area (A) km <sup>2</sup>	65.55
Basin Perimeter (P) km	59.58
Form factor (Rf)	0.30
Elongation ratio (Re)	0.62
Circulatory ratio (Rc)	0.23
Drainage Density (Dd) km.km <sup>-2</sup>	1.99
Relief aspects	
Basin relief (Bh) (m)	2017
Relief ratio (Rh)	0.14
Ruggedness number (Rn)	4.02

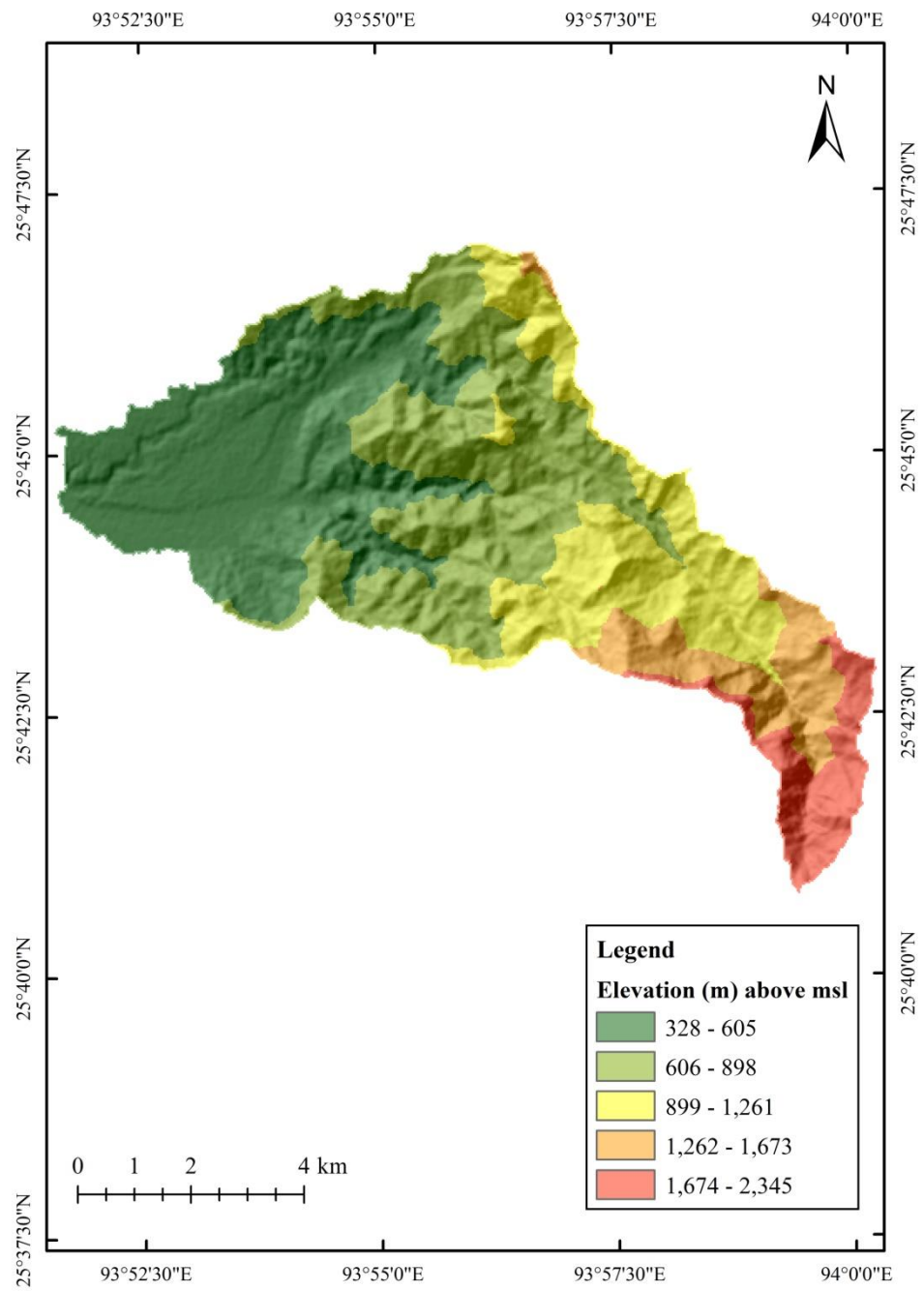


Fig. 4.2: Elevation map of the Dzumah watershed

There is no mention about the value range of relief ratio and research workers performed relative classification based on the values of relief ratio observed in their respective study area (Sukristiyanti *et al.*, 2018). Generally, the low values of relief ratio indicate low relief whereas high values indicate steep slope and high relief. Considering the values of relief ratio reported by other research workers, it was observed that the Rr values varied from as low as 0.0028 (Mahala, 2020) to as high as 0.19 (Adhikari, 2020), with the latter indicating high relief and steep slopes. In the present study, it was observed that the Dzumah watershed has a relief ratio value of 0.14 (Table 4.2). Based on relative assessment and comparison with the findings of other researchers, it can be inferred that the Dzumah watershed has a high relief ratio, indicating the presence of strong relief and steep slopes in the watershed.

#### **4.1.3.3 Ruggedness number (Rn)**

The Rn merges the effects of slope length and steepness representing the degree of instability of the land surface (Strahler, 1957). It is a measure of the smoothness or unevenness of the watershed terrain and its susceptibility to erosion (Asfaw and Workineh, 2019). Low Rn values indicate less vulnerability to erosion (Pareta and Pareta, 2011) and vice-versa. The Rn value of the Dzumah watershed was found to be 4.02, which is high, indicating that the watershed has a rough and dissected terrain thus rendering the area susceptible to erosion hazards.

## **4.2 Runoff estimation**

In the present study, the NRCS-CN model was used for surface runoff estimation. The various watershed parameters required in the model and the resultant rainfall-runoff relationship are discussed as follows:

### **4.2.1 Land use land cover**



Major land use land cover classes identified in the Dzumah watershed is depicted in Fig. 4.3. There were five land use land cover classes in the study area *viz.* cultivated area, dense forest, open forest, buildup area and water body. Forest area was the predominant and most conspicuous land use identified in the watershed. The forest area was categorized into dense and open forest based on canopy coverage. The total area under forest was 5552.09 ha accounting for 84.7 per cent of the total watershed geographical area. The dominance of forest cover and the inability to convert to cultivation or other land uses could be attributed to the highly undulating terrain and steep topography of the watershed. Major cultivated areas in the watershed was noticed in the lower reaches of the watershed having nearly level to gentle slopes, covering an area of 322.5 ha constituting a mere 4.92% of the total watershed area. The buildup area includes rural establishments, roads and other related construction sites, covering an area of 392.65 ha constituting 5.99% of the total watershed area. Area statistics of land use/land cover classes of the watershed is given in Table 4.3.

#### **4.2.2 Hydrologic soil group**

The Hydrologic soil group (HSG) of the watershed was derived from the soil texture data obtained from the laboratory analysis of soil samples collected from the watershed. The results of the soil textural analysis are presented in Table-4.4. The soils in the watershed were found to be medium to fine textured, predominantly clay loam in texture; and consisted of textural classes *viz.* loam, clay loam, silty clay loam and silt loam. With the exception of Sample no. 15, which showed clay content of 42.60%, all samples showed clay contents ranging from 20- 40%. The sand and silt content among the samples varied from 19.0 % to 35.80 % and 28.00 to 47.7%, respectively. Based on these findings, it can be inferred that the entire watershed falls under Hydrological Group – C and has a moderately high runoff potential.

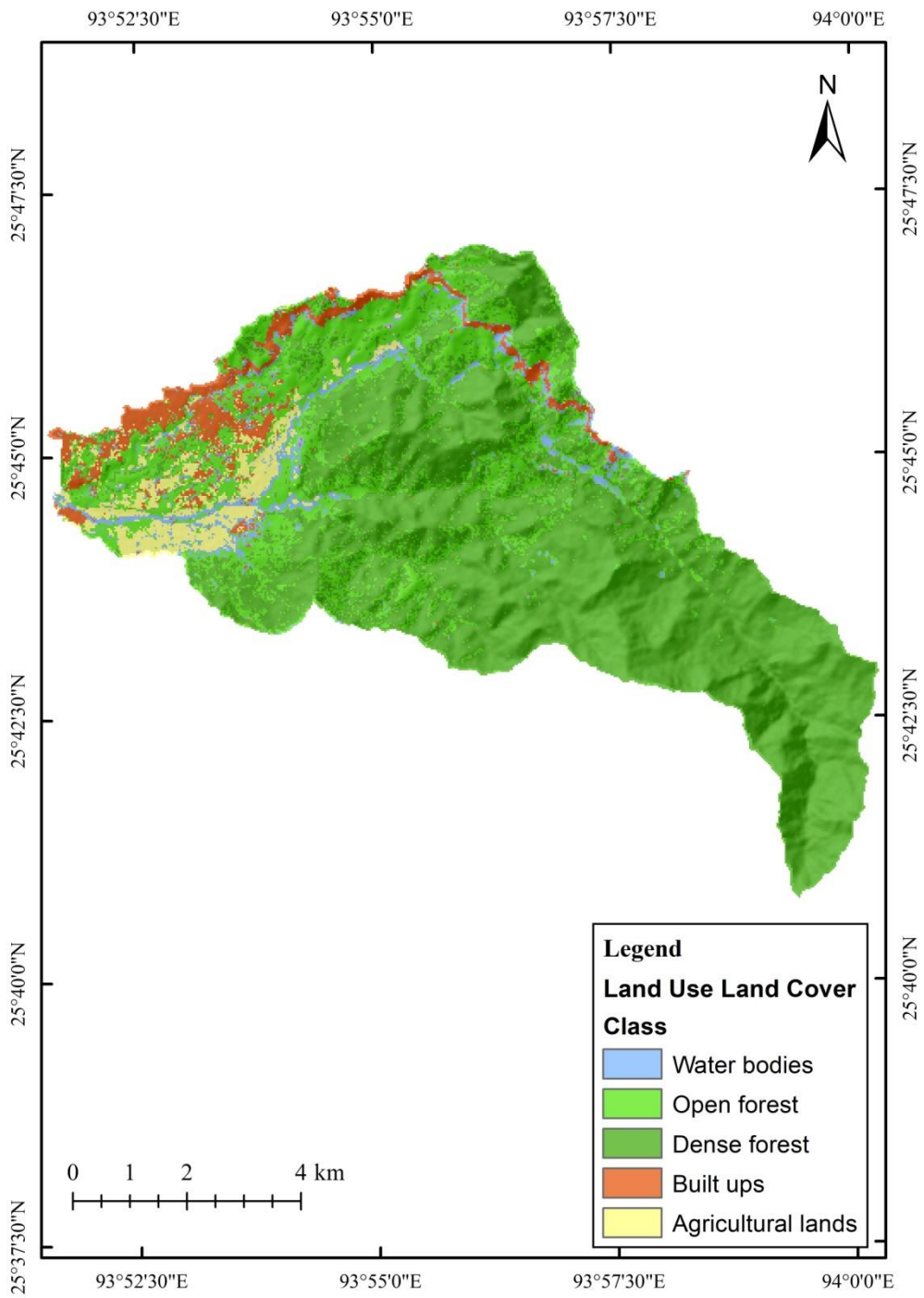


Fig. 4.3: Land use/land cover map of the Dzumah watershed

Table 4.3: Land use/land cover classes of Dzumah watershed

Sl.No.	Land use class	Area (ha)	% of total geographical area
1	Cultivated area	322.50	4.92
2	Dense forest	3998.55	61
3	Open forest	1553.54	23.70
4	Buildup area	392.65	5.99
5	Water body	287.76	4.39
Total		6555.00	100.00

Table 4.4: Soil texture of Dzumah watershed

Sample Number	Sand (%)	Silt (%)	Clay (%)	Textural Class	HSG
1	35.80	42.50	20.10	Loam	C
2	19.70	46.20	32.50	Silty Clay Loam	C
3	27.70	38.80	32.50	Clay Loam	C
4	33.80	41.20	22.70	Loam	C
5	18.80	46.70	33.30	Silty Clay Loam	C
6	19.00	51.40	28.30	Silty Clay Loam	C
7	34.70	29.80	34.10	Clay Loam	C
8	35.50	33.40	28.60	Clay Loam	C
9	30.00	34.50	32.80	Clay Loam	C
10	32.40	34.20	29.40	Clay Loam	C
11	20.00	44.30	33.80	Silty Clay Loam	C
12	21.00	52.30	24.20	Silt Loam	C/D
13	35.00	28.00	35.20	Clay Loam	C
14	35.80	28.40	33.50	Clay Loam	C
15	19.40	36.50	42.60	Silty Clay Loam	C
16	27.30	33.10	38.20	Clay Loam	C
17	19.30	47.70	31.80	Silty Clay Loam	C
18	24.60	38.50	35.50	Clay Loam	C
19	27.10	33.50	37.80	Clay Loam	C

### 4.2.3 CN values

The NRCS-CN model represents an empirical equation that requires rainfall and watershed characteristics as inputs for computing surface runoff. The watershed characteristics are combined to generate a single dimensionless value called the Curve Number (CN), which represents the runoff potential of the watershed. Higher the CN values, higher will be the runoff produced from the watershed. Based on the standard TR-55 table (USDA-NRCS, 1986), the CN values for normal/AMC-II condition ( $I_a = 0.2S$ ) were assigned taking into account the different land uses and HSG of the watershed. These CN-II values were used for computing  $CN-II_{0.05}$  values as described in previous chapter. Similarly, the  $CN-II_{0.05}$  values were further subjected to slope adjustment to generate the final and slope-adjusted CN as  $CN-II_\alpha$ . Weighted curve number for each land use was calculated as a product of percent area covered by each land use classes and the corresponding curve number. The weighted  $CN-II_\alpha$  value was used for computing CN-I and CN-III values corresponding to AMC-I and AMC-III conditions of the watershed, respectively. The modification of the original CN values to  $CN-II_{0.05}$  and slope-adjusted  $CN-II_\alpha$  for different land use classes are presented in Table-4.5. The original CN-II values of the watershed based on the standard TR-55 table (USDA-NRCS, 1986) varied from 73 to 100, whereas the modified CN-II values with  $\lambda_{0.05}$  and slope adjustments ranged from 91.02 to 100.

### 4.2.4 Runoff depth and water yield potential

In the present study, daily rainfall data of the watershed was obtained for the year 2019 and 2020 and surface runoff was estimated using the NRCS-CN method. The runoff estimation was computed exclusively for the monsoon months *i.e.*, from the month of June to October, in which majority of the rainfall events occur in the watershed. Daily rainfall and subsequent runoff

Table 4.5: CN value modification

Sl.No.	LULC	CN-II	CN-II <sub>0.05</sub>	CN-II <sub>α</sub>
1	Cultivated area	84	93.70	95.61
2	Dense forest	70	88.81	91.02
3	Open forest	73	89.81	92.04
4	Buildup area	86	94.45	96.8
5	Water body	100	100	100

Table 4.6: Rainfall and runoff depth for the year 2019

Month	Total Rainfall (mm)	Mod. CN Runoff (mm)	Std. CN Runoff (mm)	Mod. CN Runoff %	Std. CN Runoff %
June	195.0	69.56	5.57	35.67	2.85
July	271.3	124.40	8.40	45.85	3.10
August	274.5	120.76	27.72	43.99	10.10
September	173.4	57.64	4.61	33.24	2.66
October	244.8	132.98	63.66	54.32	26.01
Total	1159.0	505.34	109.95	43.60	9.49

Table 4.7: Rainfall and runoff depth for the year 2020

Month	Total Rainfall (mm)	Mod. CN Runoff (mm)	Std. CN Runoff (mm)	Mod. CN Runoff %	Std. CN Runoff %
June	266.2	124.89	25.35	46.92	9.52
July	199.9	69.67	1.88	34.85	0.94
August	80.3	13.97	0.00	17.40	0.00
September	157.6	51.87	0.48	32.91	0.30
October	175.7	80.57	5.54	45.86	3.15
Total	879.7	340.97	33.25	38.76	3.78

estimations aggregated on monthly basis for the year 2019 and 2020 are presented in Tables 4.6 and 4.7, respectively. Despite the lack of proper hydrological station and stream gauging data, it was validated through field survey and visual observation that the runoff depth computation using the standard CN values clearly underestimated the actual discharge occurring at the confluence of the watershed. The runoff values estimated using the standard CN for the years 2019 and 2020 were only 109.95 mm and 33.25 mm, respectively; accounting for a mere 9.49 and 3.78% of the total rainfall received in each year (Table 4.6 and 4.7). Runoff estimation using the modified CN value gave a better representation of the actual discharge and the findings are described below.

In the year 2019, the total rainfall received in the watershed during the month of June to October was 1159 mm with a mean average rainfall of 231.80 mm. The surface runoff estimation using the NRCS-CN method showed a runoff depth of 505.34 mm implying that 43.60% of the total rainfall received was converted to surface runoff. This gave an effective water yield potential of 3,31,24,912.66 m<sup>3</sup> for the watershed. The lowest rainfall as well as the lowest estimated runoff was observed in the month of September with 173.4 mm and 57.64 mm, respectively. The highest estimated runoff with a value of 132.98 mm was observed in the month of October which had a total monthly rainfall of 244.80 mm. It was observed that the months of July and August had higher monthly rainfall as compared to the month of October with values 271.30 mm and 274.50 mm, respectively. However, the frequency and temporal distribution of rainfall events coupled with wide variations in the amount of rainfall received during rainfall events in those months affected the AMC condition of the watershed which resulted in lower rainfall-runoff conversion.

In the year 2020, the watershed received a total rainfall of 879.70 mm during the month of June to October with a mean average rainfall of 175.90

mm. The total surface runoff observed was 340.97 mm, which was 38.76% of the total rainfall received during June to October. This resulted in an estimated water yield potential of 2,23,50,524.49 m<sup>3</sup> from the watershed. The highest rainfall and the highest estimated runoff was observed in the month of June with values 266.20 mm and 124.89 mm, respectively, implying a rainfall-runoff conversion of 46.92%. Similarly, the lowest rainfall and runoff were observed in the month of August with values 80.30 mm and 13.97 mm, respectively, resulting in a rainfall-runoff conversion of 17.40%.

Correlation between rainfall and runoff was determined for runoff depth estimated using both the standard CN and modified CN values. The R<sup>2</sup> values for runoff estimated using standard CN values for the years 2019 and 2020 were 0.166 and 0.650, respectively (Fig. 4.4a and 4.4b). The R<sup>2</sup> values for runoff estimated using modified CN values for the years 2019 and 2020 were 0.858 and 0.944, respectively (Fig. 4.5a and 4.5b). This study clearly indicated that runoff depth estimation using slope and  $\lambda$  adjusted CN values gives a better rainfall runoff correlation as compared to runoff estimated using standard CN values. The standard CN method failed to estimate surface runoff to represent real world scenario. The adjustment of  $\lambda$  value in initial abstraction and slope-adjusted CN gave better results. This finding is supportive of the results reported by Jacobs and Srinivasan (2005), Lim *et al.* (2006), Shi *et al.* (2009), Ebrahimian *et al.* (2012) and Ajmal *et al.* (2020).

### **4.3 Soil loss estimation**

In the present study, GIS based USLE method was used to estimate average annual soil loss from the watershed. The results of individual USLE factors and annual soil loss estimation are presented and discussed as follows:

#### **4.3.1 Rainfall erosivity factor (R)**

The R-factor of the Dzumah watershed was calculated using rainfall data of 23 years (1998 - 2020) and is presented in Table 4.8. In the

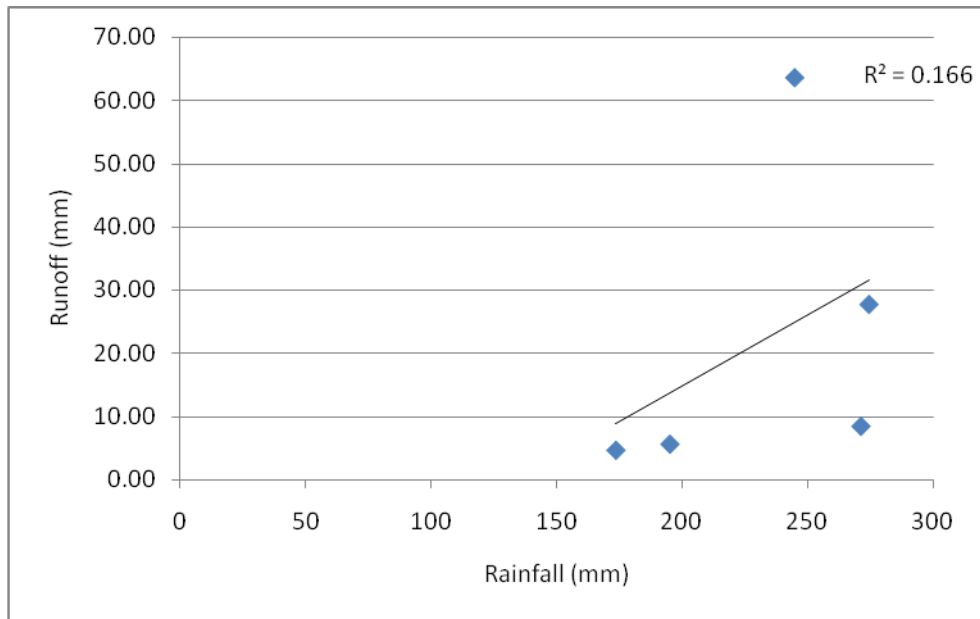


Fig 4.4a: Rainfall-runoff correlation using standard CN for the year 2019

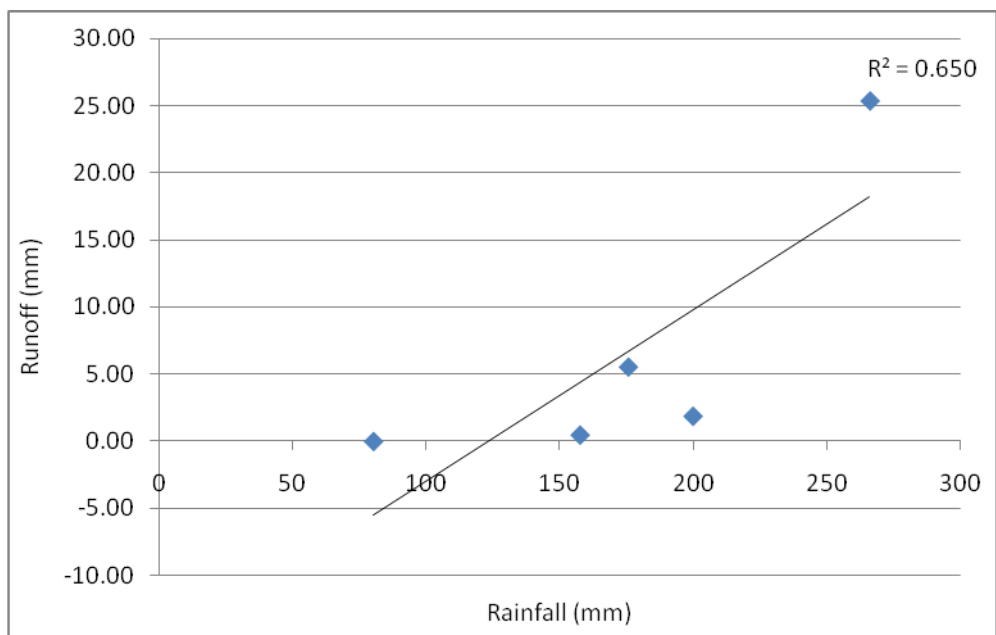


Fig 4.4b: Rainfall-runoff correlation using standard CN for the year 2020



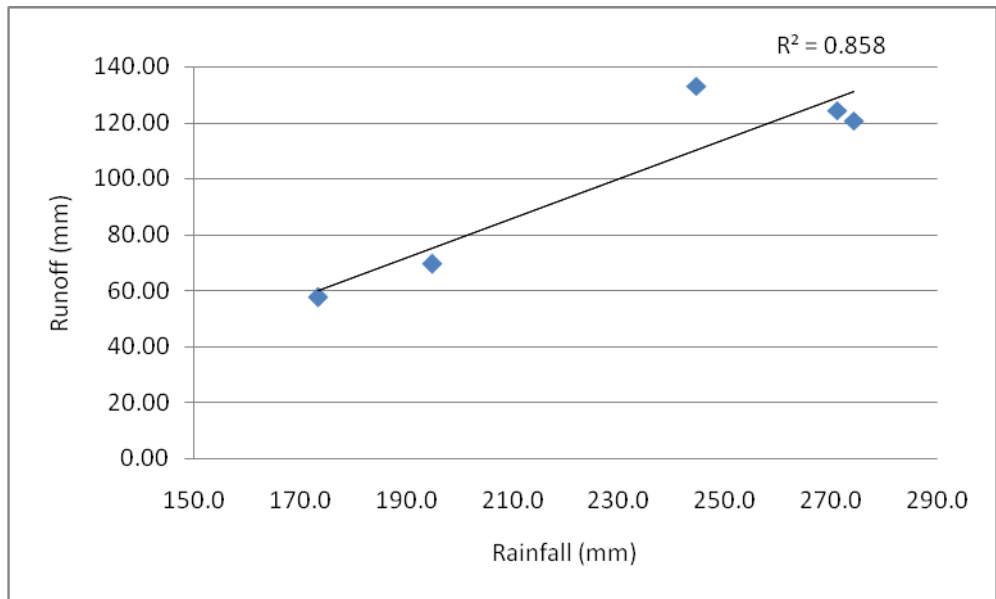


Fig 4.5a: Rainfall-runoff correlation using modified CN for the year 2019

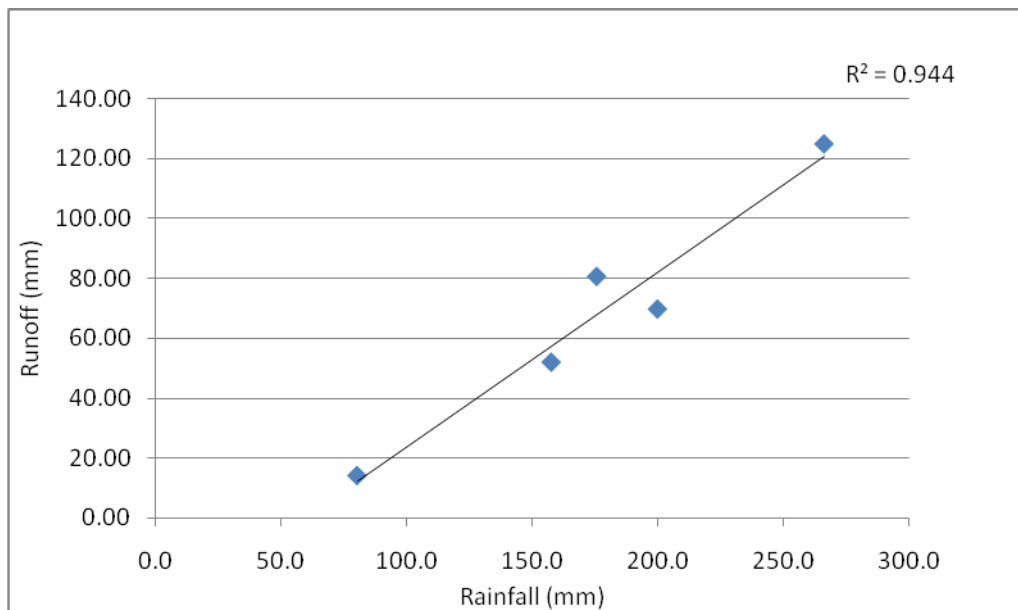


Fig 4.5b: Rainfall-runoff correlation using modified CN for the year 2020

Table 4.8: Year-wise Rainfall Erosivity factor(R) of Dzumah watershed

Sl.No.	Year	Annual R (MJ mm ha <sup>-1</sup> h <sup>-1</sup> yr <sup>-1</sup> )
1	1998	734.02
2	1999	2517.19
3	2000	3595.31
4	2001	2051.86
5	2002	2421.80
6	2003	1546.70
7	2004	3716.96
8	2005	2337.36
9	2006	2359.64
10	2007	3499.41
11	2008	1950.60
12	2009	1263.36
13	2010	3070.67
14	2011	3509.38
15	2012	2374.70
16	2013	3526.01
17	2014	2070.16
18	2015	1863.00
19	2016	2559.88
20	2017	4157.30
21	2018	2473.81
22	2019	1729.50
23	2020	1388.16
Average		2465.95

present study, the R-factor was considered to be homogenous given the relatively small area of the watershed, the absence of multiple gauging stations and the inconvenience of setting up gauging stations within the watershed. The lowest and the highest annual R-factor was observed in the year 1998 and 2017 with values 734.02 and 4157.30 MJ mm ha<sup>-1</sup> h<sup>-1</sup> yr<sup>-1</sup>, respectively.

#### **4.3.2 Soil erodibility factor (K)**

The K-factor depends on soil physical properties and organic matter content of the soil. The soil in the Dzumah watershed was predominantly clay loam in nature. The organic carbon content varied from 0.53 to 2.57% (Table 4.9). The soil erodibility factor (K) of the Dzumah watershed ranged from 0.03 to 0.074 with an average of 0.045 (Table 4.9). K-factor map is presented in Fig. 4.6.

#### **4.3.3 Slope length and steepness factor (LS)**

The combination of slope length and steepness is called the topographic factor and was computed using the DEM of the watershed area. The slope classes were categorized according to the USDA classification as adopted by Pamela *et al.* (2018). The slope map generated using the DEM showed that most areas of the watershed falls under hilly, moderately steep and steep classes with areas covering 24.51, 27.50 and 19.72 % of the total watershed area, respectively (Table 4.10). A slope map of the Dzumah watershed is presented in Fig. 4.7. The LS-factor of the Dzumah watershed varied from 0.03 to 54.44 (Fig. 4.8). Steeper slopes are concentrated on the north and southeastern part of the watershed and it gradually decreased and flattened towards the west.

#### **4.3.4 Cover management factor (C)**

In the present study, Normalized Difference Vegetation Index (NDVI), which measures vegetation health and vigour, has been used for determining

Table 4.9: Soil properties and K factor of Dzumah watershed

Sample point	Sand (%)	Silt (%)	Clay (%)	Textural Class	OC (%)	Permeability	Soil Structure Code	M	K
1	35.80	42.50	20.10	Loam	0.53	3	2	6256.17	0.068
2	19.70	46.20	32.50	Silty Clay Loam	1.31	3	2	4448.25	0.043
3	27.70	38.80	32.50	Clay Loam	1.74	4	2	4488.75	0.045
4	33.80	52.20	11.70	Silt Loam	2.03	3	2	7593.8	0.074
5	18.80	46.70	33.30	Silty Clay Loam	1.64	3	2	4368.85	0.041
6	19.00	51.40	28.30	Silty Clay Loam	1.48	3	2	5047.68	0.049
7	34.70	29.80	34.10	Clay Loam	2.57	4	2	4250.55	0.039
8	35.50	33.40	28.60	Clay Loam	1.72	4	2	4919.46	0.050
9	30.00	34.50	32.80	Clay Loam	2.38	4	2	4334.4	0.041
10	32.40	34.20	29.40	Clay Loam	1.35	4	2	4701.96	0.049
11	20.00	44.30	33.80	Silty Clay Loam	1.58	3	2	4256.66	0.040
12	21.00	52.30	24.20	Silt Loam	2.44	3	2	5556.14	0.050
13	35.00	28.00	35.20	Clay Loam	1.66	4	2	4082.4	0.041
14	35.80	28.40	33.50	Clay Loam	1.79	4	2	4269.3	0.043
15	19.40	36.50	42.60	Silty Clay Loam	1.27	3	2	3208.66	0.030
16	27.30	33.10	38.20	Clay Loam	2.15	4	2	3732.72	0.036
17	19.30	47.70	31.80	Silty Clay Loam	1.87	3	2	4569.4	0.042
18	24.60	38.50	35.50	Clay Loam	2.4	4	2	4069.95	0.038
19	27.10	33.50	37.80	Clay Loam	2.36	4	2	3769.32	0.036
Average									0.045

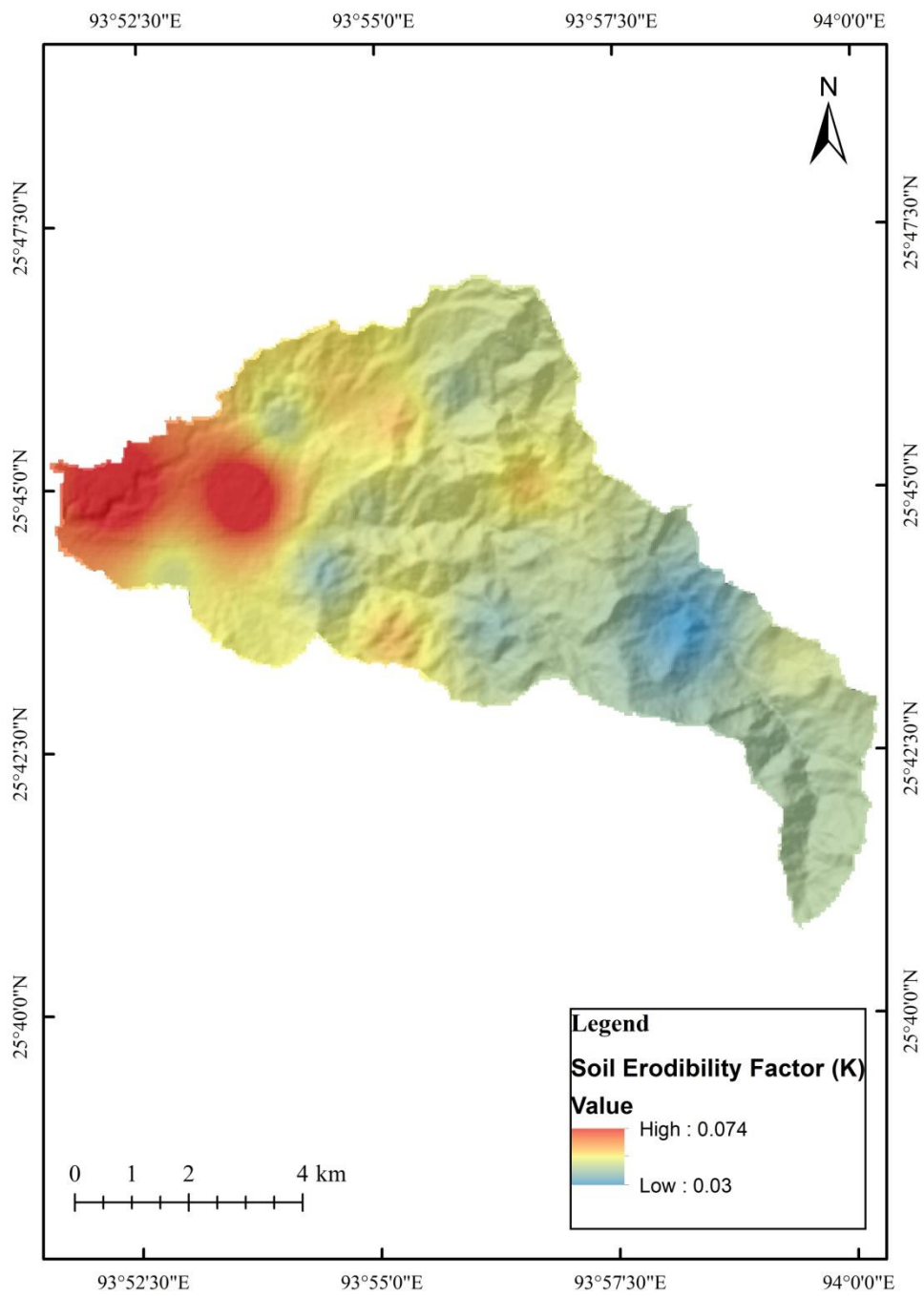


Fig. 4.6: Soil erodibility factor (K) map of Dzumah watershed

Table 4.10: Slope classes of Dzumah watershed based on USDA classification

Description	Slope		Area (ha)	Percent Area
	Percent	Degree		
Flat	0-3	<2	208.40	3.18
Undulating	3-8	2-5	616.68	9.40
Moderately Sloping	8-15	5-8	495.14	7.55
Hilly	15-30	8-17	1606.78	24.51
Moderately Steep	30-45	17-24	1802.54	27.50
Steep	45-65	24-33	1292.3	19.72
Very Steep	>65	>33	533.57	8.14

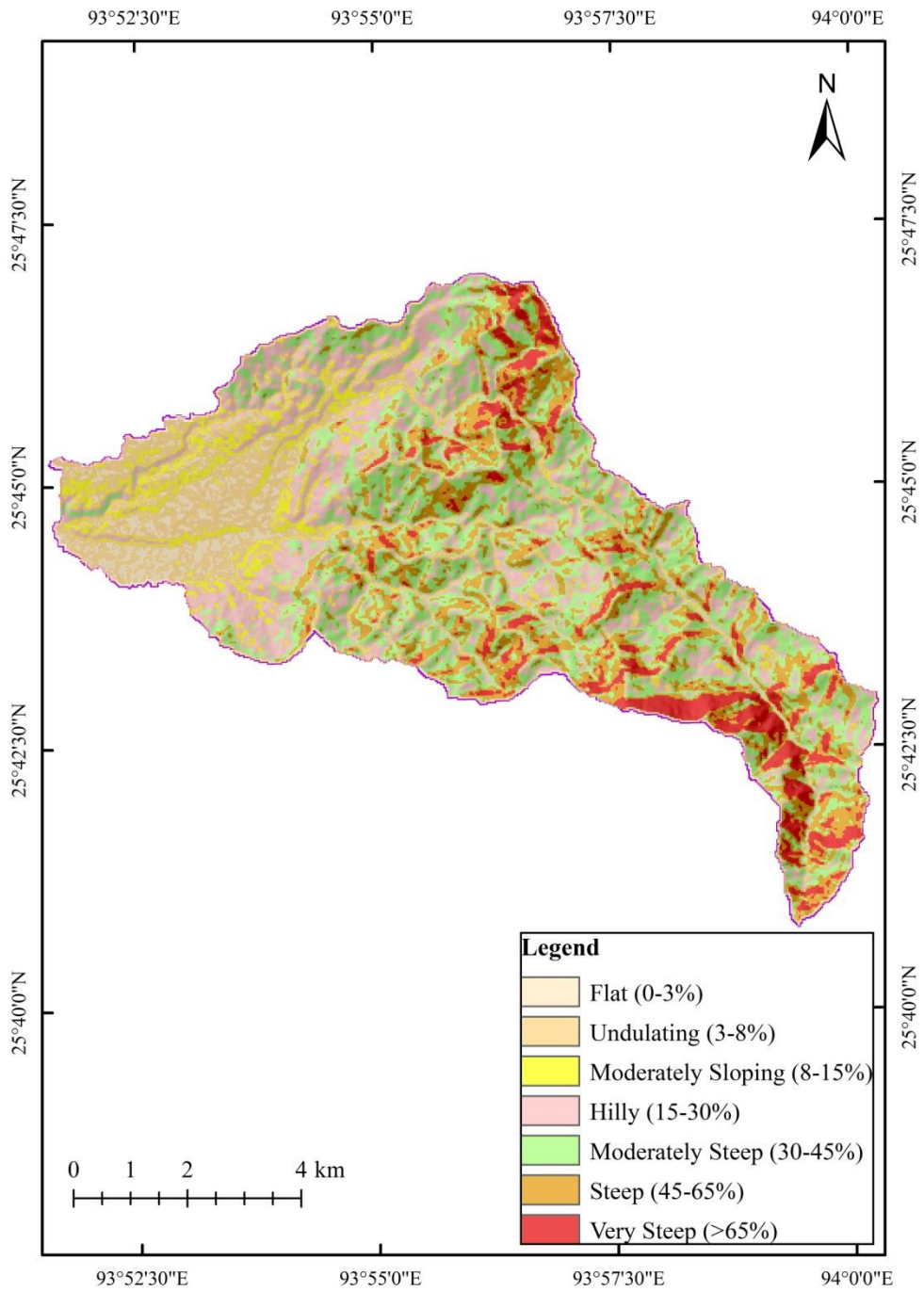


Fig. 4.7: Slope map of Dzumah watershed

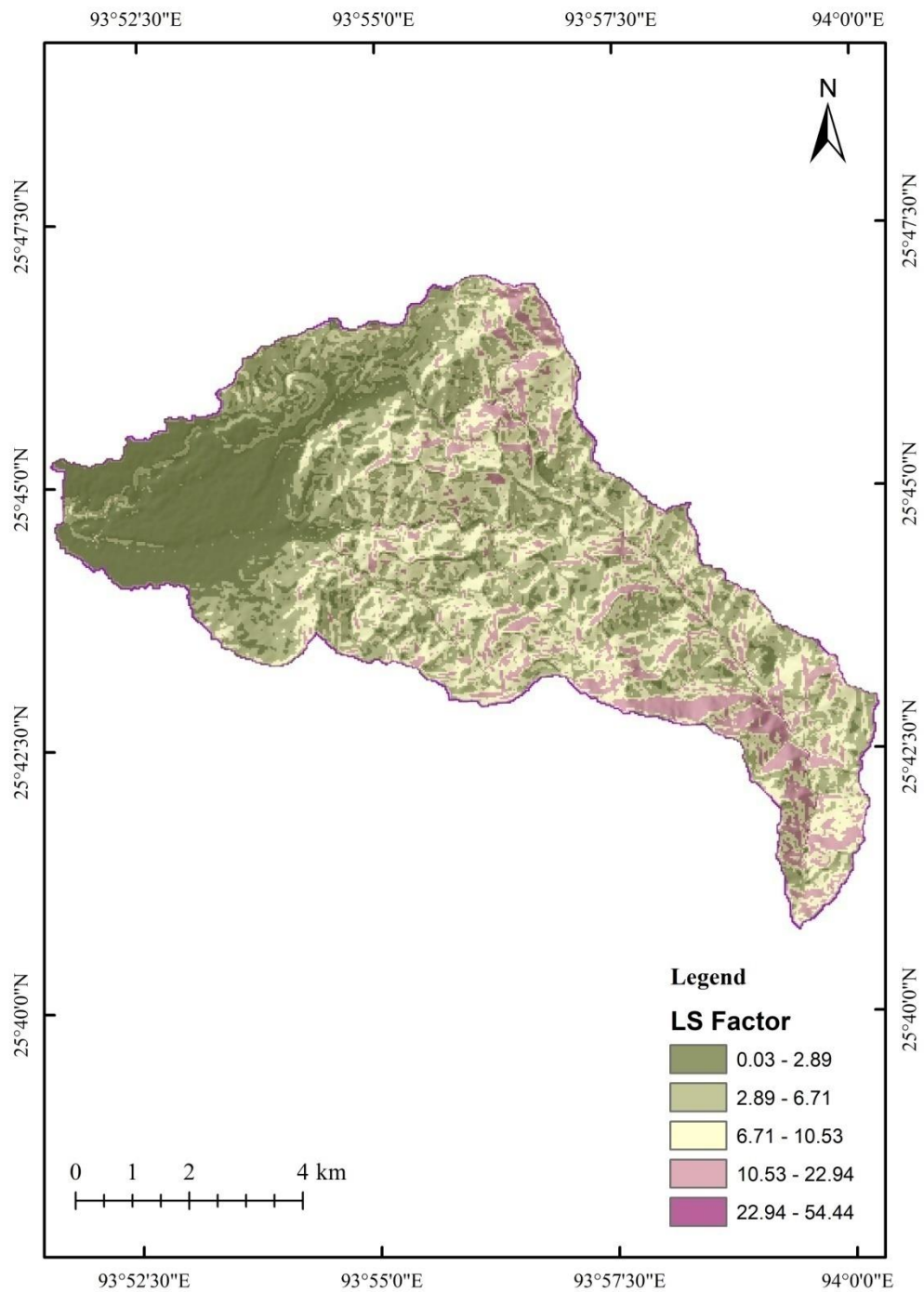


Fig. 4.8: Slope length and steepness factor (LS) map of Dzumah watershed



the C-factor of the watershed. Many researchers have developed techniques to compute C-factor using NDVI (De Jong *et al.*, 1999; Wang *et al.*, 2002; Lin *et al.* 2002; Karaburun, 2010). Better estimates of C-factor could be achieved by employing remote sensing techniques and using vegetation indices such as the NDVI (Almagro *et al.*, 2019). The NDVI image of the Dzumah watershed is presented in Fig. 4.9, showing values ranging from - 0.08 to 0.87. The resultant NDVI map was used for calculating the C-factor map of the watershed. The C-factor map of the watershed is presented in Fig.4.10, showing values ranging from 0.07 to 0.52.

#### **4.3.5 Conservation practice factor (P)**

Adoption and practice of different soil conservation measures can control soil erosion processes and reduce the rates of erosion. The P factor values were assigned depending upon the major conservation practice adopted in an area. There were no major conservation measures adopted in the study area and therefore, in view of the present land use and land cover pattern of the study area, the values for P-factor were assigned as 0.28 for cultivated lands and 1.0 for other areas. P factor map is presented in Fig. 4.11.

#### **4.3.6 Average annual soil loss**

The average annual soil loss of the Dzumah watershed was calculated separately for each year *i.e.*, from the year 1998 to 2020, by multiplying the USLE parameters generated in the GIS database using the raster calculator in ArcGIS environment. The final spatial soil erosion map was generated by calculating cell statistics from all the resultant soil erosion raster layers using the Spatial Analyst Toolbox in ArcGIS. Considering the average annual soil losses estimated from 1998-2020, the average potential soil erosion for Dzumah watershed was found to be  $5.38 \text{ t ha}^{-1} \text{ yr}^{-1}$  (Table 4.11). The total area under light and moderate erosion classes were 1777.34 and 4089.67 ha, respectively which collectively comprised nearly 90% of the total geographical

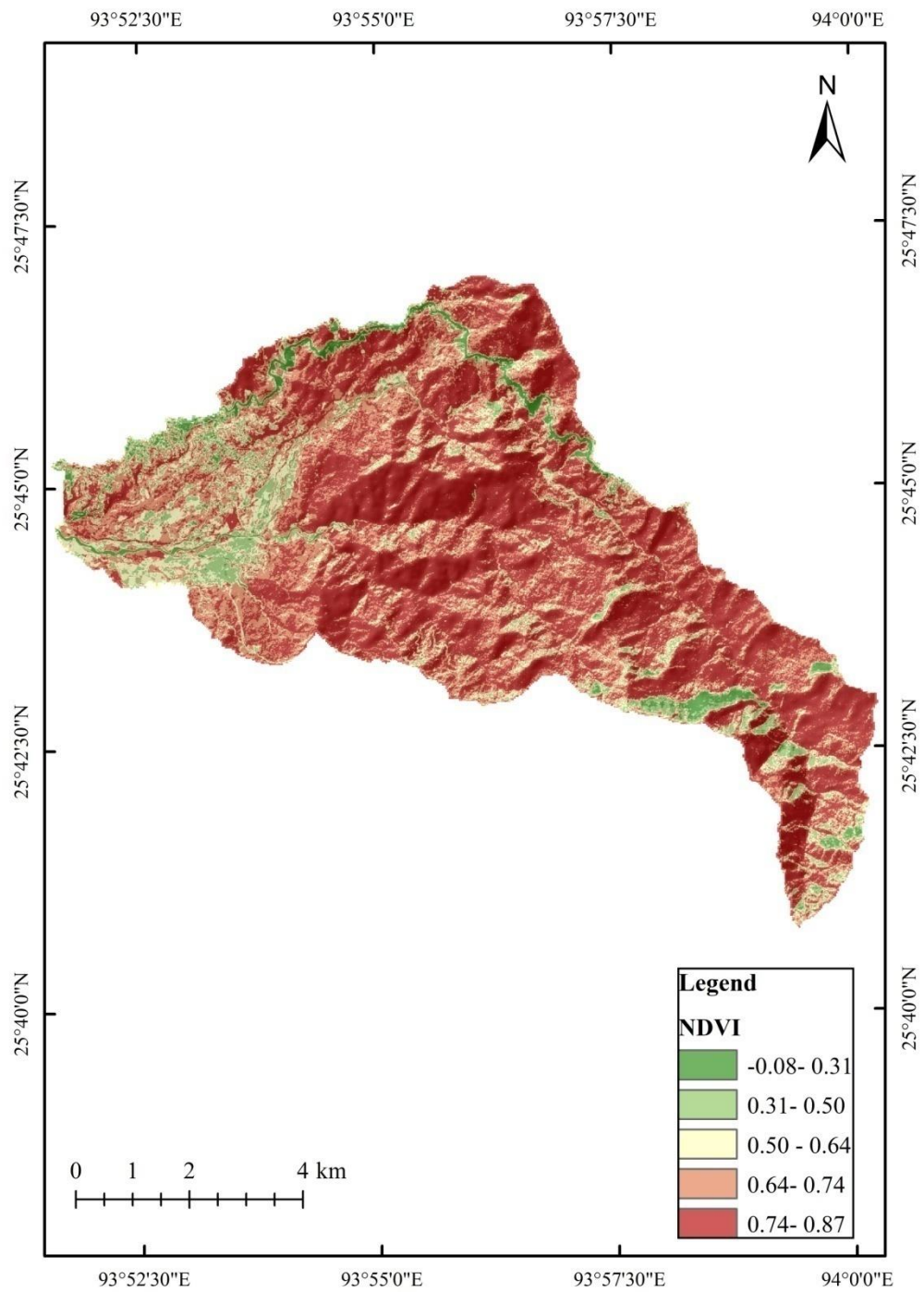


Fig. 4.9: NDVI map of Dzumah watershed

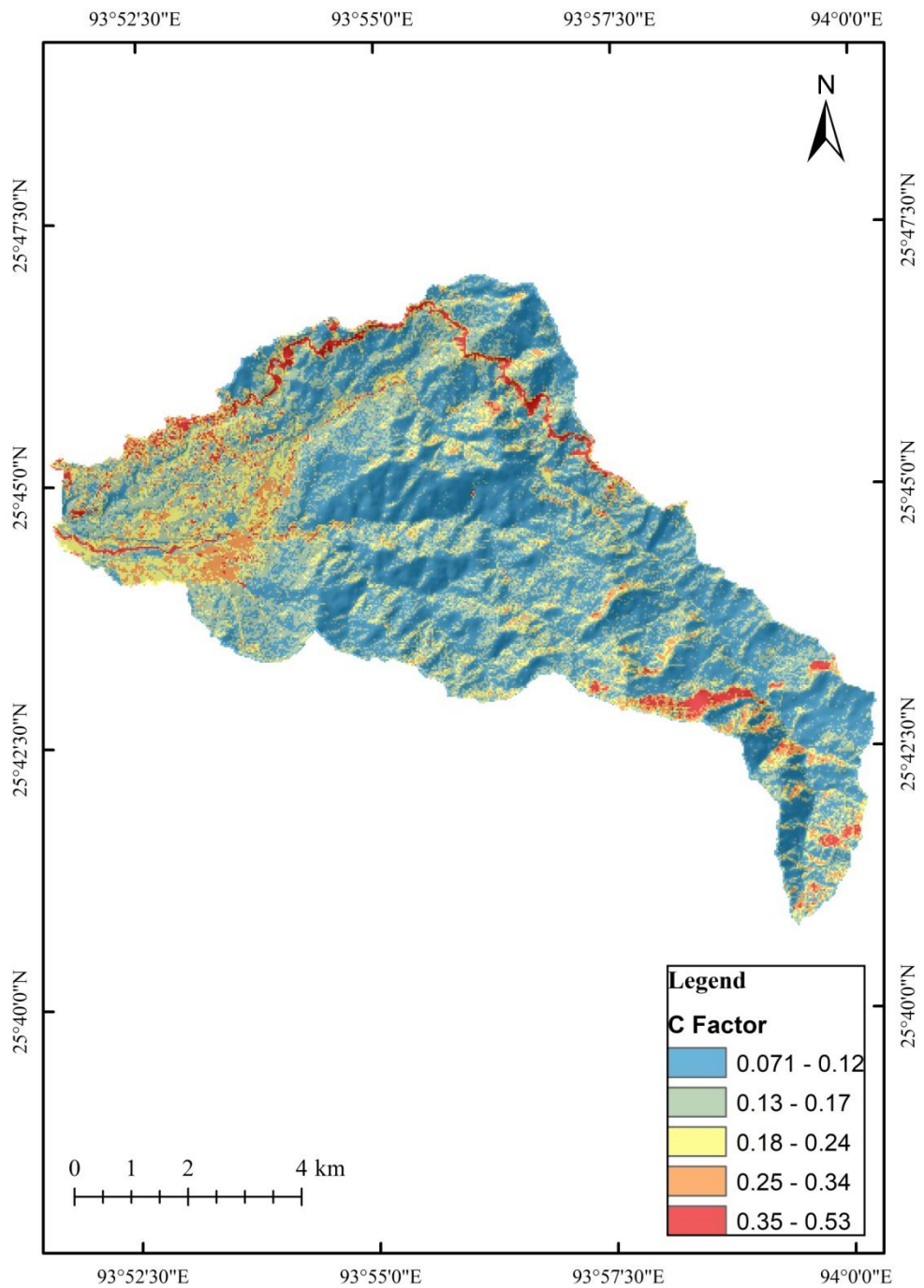


Fig. 4.10: Crop management factor (C) map of Dzumah watershed

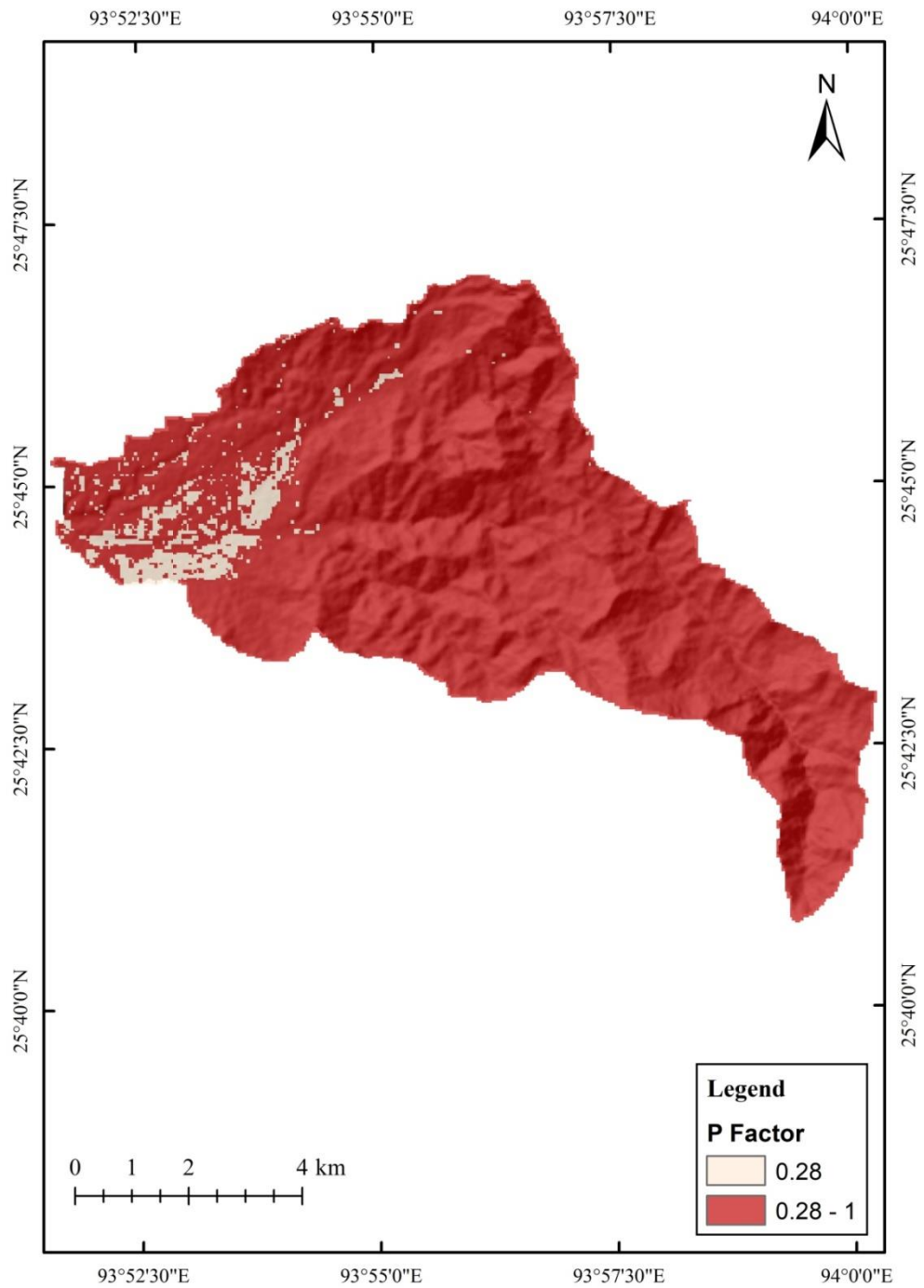


Fig. 4.11: Conservation practice factor (P) map of Dzumah watershed

area of the watershed (Table 4.12, Fig. 4.12). The average annual soil losses as obtained from the raster statistics for the year 2019 and 2020 were 3.78 and 3.04 t h<sup>-1</sup> yr<sup>-1</sup>, respectively (Table 4.11). In both these years, it was observed that more than 95% of the watershed area was under light to moderate erosion classes (Table 4.13 and 4.14; Fig. 4.13 and 4.14). Severe erosion in the watershed was observed only in areas with extreme steep slopes and disturbed sites caused by construction activities. The permissible soil loss for the mountainous Himalayan regions is 15 t ha<sup>-1</sup> yr<sup>-1</sup> (Jasrotia *et al.*, 2006). Considering this threshold limit, the Dzumah watershed can be considered stable with no major threats of erosion hazards. A very strong correlation was observed between rainfall erosivity and soil loss with an R<sup>2</sup> value of 0.99 (Fig 4.15). The highest and the lowest rainfall erosivity were recorded in the year 2017 and 1998 with values 4157.30 and 734.02 MJ mm ha<sup>-1</sup> h<sup>-1</sup> yr<sup>-1</sup>, respectively (Table 4.8). Similarly, the highest and lowest average annual soil losses were recorded in the year 2017 and 1998 with values 9.07 and 1.6 t ha<sup>-1</sup> yr<sup>-1</sup>, respectively (Table 4.11).

Table 4.11: Year-wise average annual soil loss of Dzumah watershed

Sl. No.	Year	Average annual soil loss (t ha <sup>-1</sup> yr <sup>-1</sup> )
1	1998	1.60
2	1999	5.49
3	2000	7.84
4	2001	4.48
5	2002	5.29
6	2003	3.38
7	2004	8.11
8	2005	5.10
9	2006	5.15
10	2007	7.64
11	2008	4.26
12	2009	2.78
13	2010	6.70
14	2011	7.66
15	2012	5.18
16	2013	7.70
17	2014	4.52
18	2015	4.07
19	2016	5.59
20	2017	9.07
21	2018	5.40
22	2019	3.78
23	2020	3.04
	Average	5.38

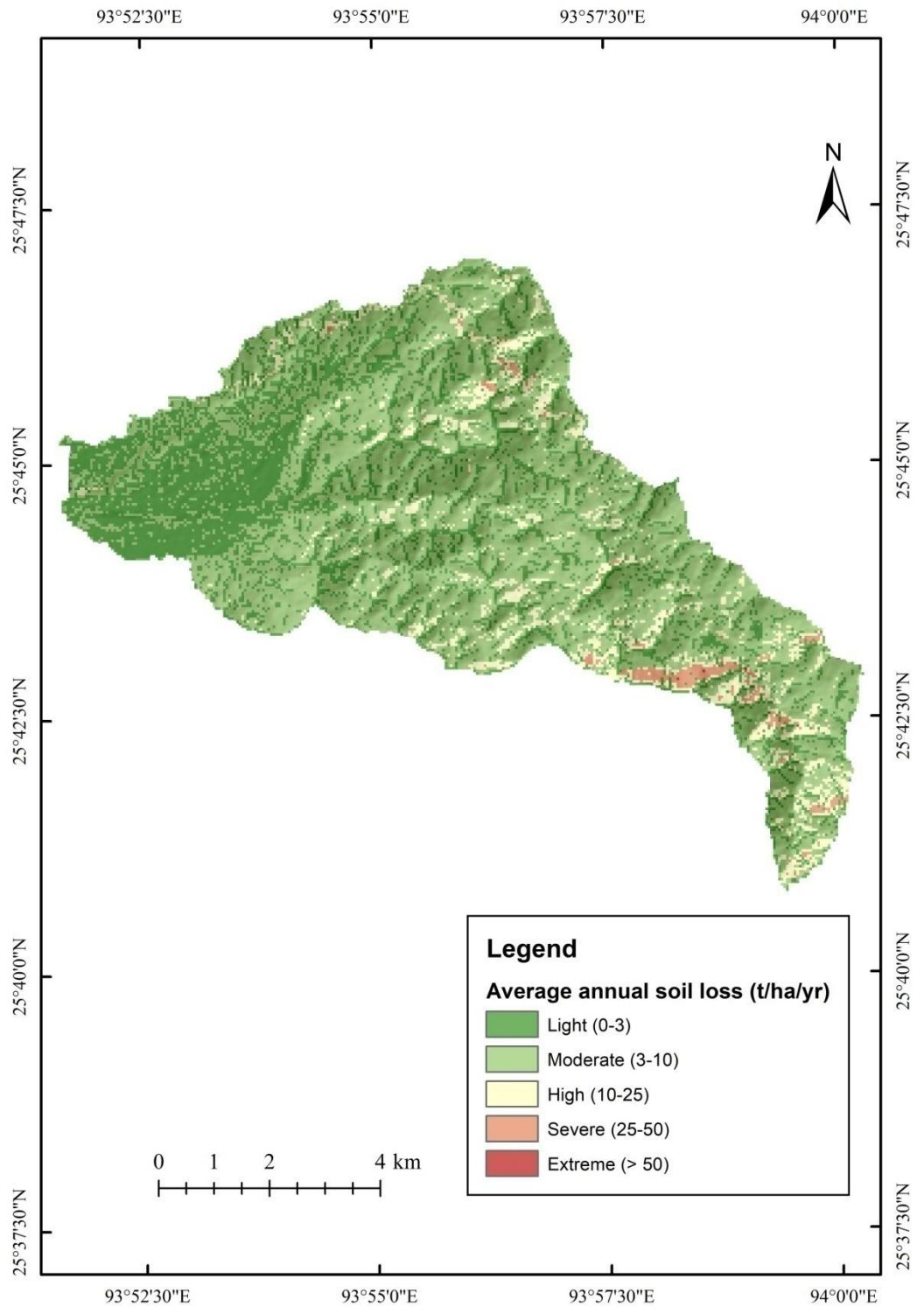


Fig. 4.12: Average annual soil erosion map of Dzumah watershed

Table 4.12: Mean area under different classes of erosion in Dzumah watershed

Soil loss (t ha <sup>-1</sup> yr <sup>-1</sup> )	Area (ha)	% Area	Soil erosion class
0-3	1777.34	27.11	Light
3-10	4089.67	62.39	Moderate
10-25	588.82	8.98	High
25-50	98.33	1.50	Severe
>50	0.84	0.01	Extreme

Table 4.13: Area under different classes of erosion in Dzumah watershed for the year 2019

Soil loss (t ha <sup>-1</sup> yr <sup>-1</sup> )	Area (ha)	% Area	Soil erosion class
0-3	2862.16	43.66	Light
3-10	3367.95	51.38	Moderate
10-25	294.55	4.49	High
25-50	31.07	0.47	Severe
>50	-	-	Extreme

Table 4.14: Area under different classes of erosion in Dzumah watershed for the year 2020

Soil loss (t ha <sup>-1</sup> yr <sup>-1</sup> )	Area (ha)	% Area	Soil erosion class
0-3	3900.23	59.5	Light
3-10	2409.62	36.76	Moderate
10-25	239.92	3.66	High
25-50	5.26	0.08	Severe
>50	-	-	Extreme



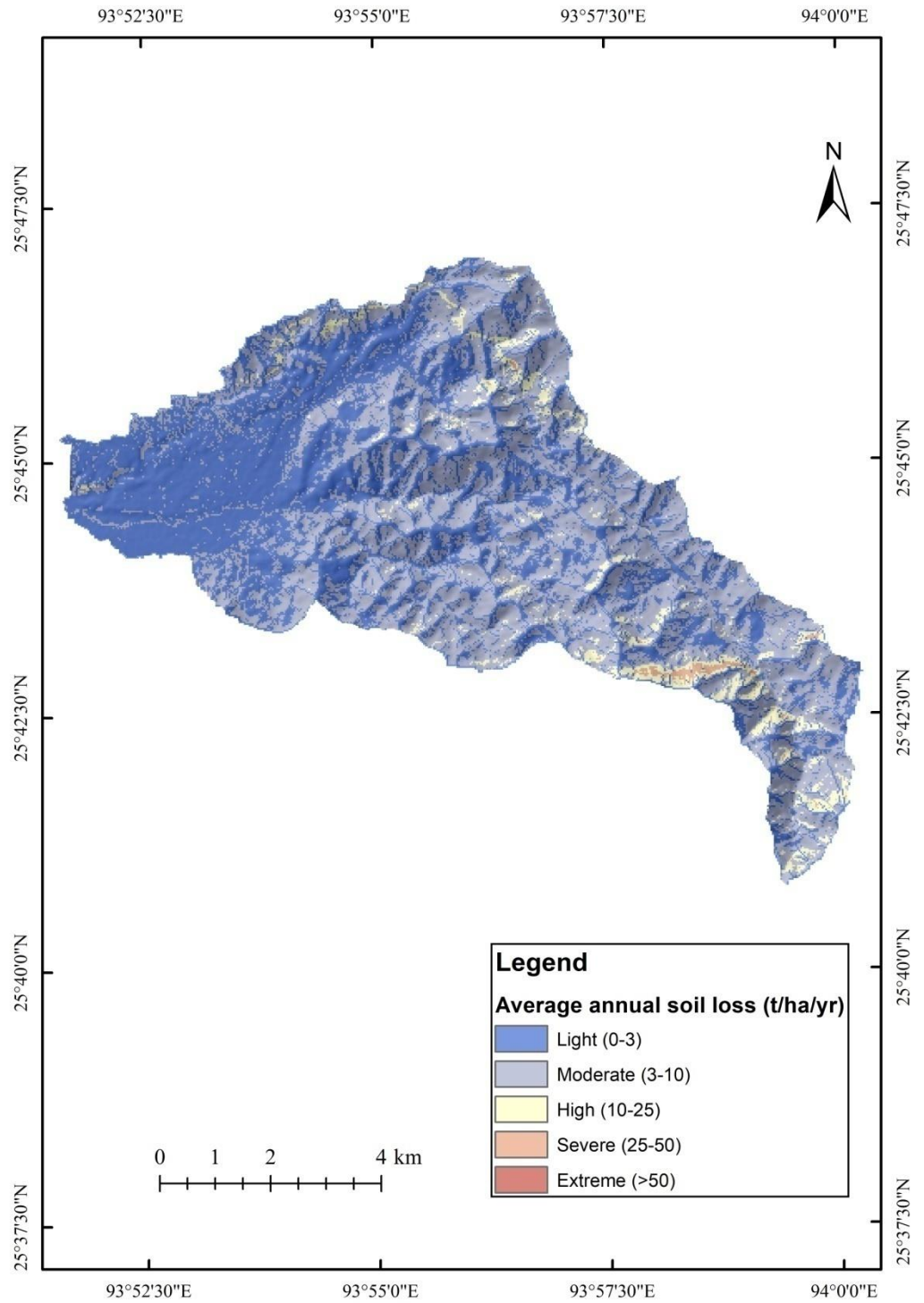


Fig. 4.13: Average annual soil loss map of Dzumah watershed for the year 2019

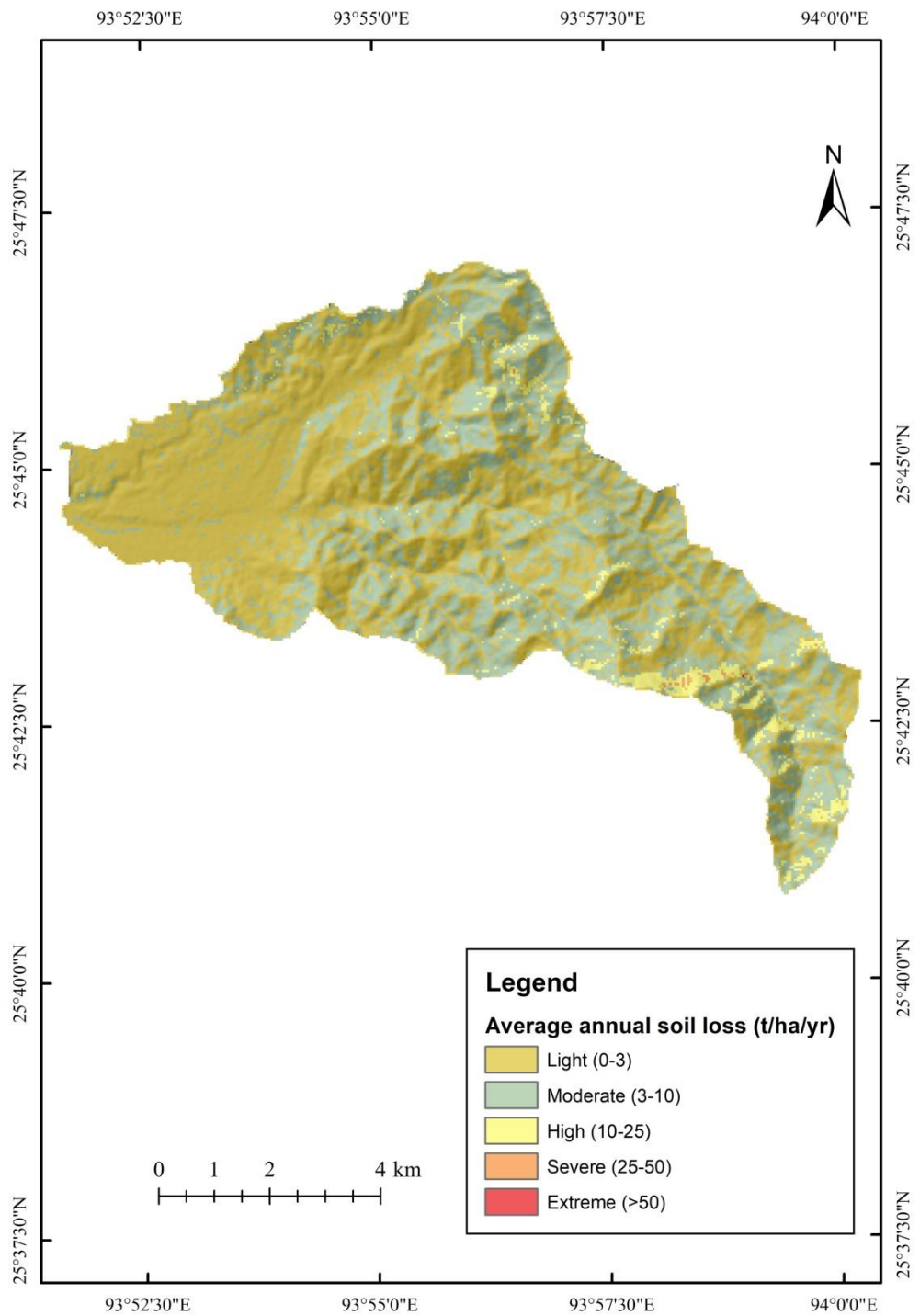


Fig. 4.14: Average annual soil loss map of Dzumah watershed for the year 2020

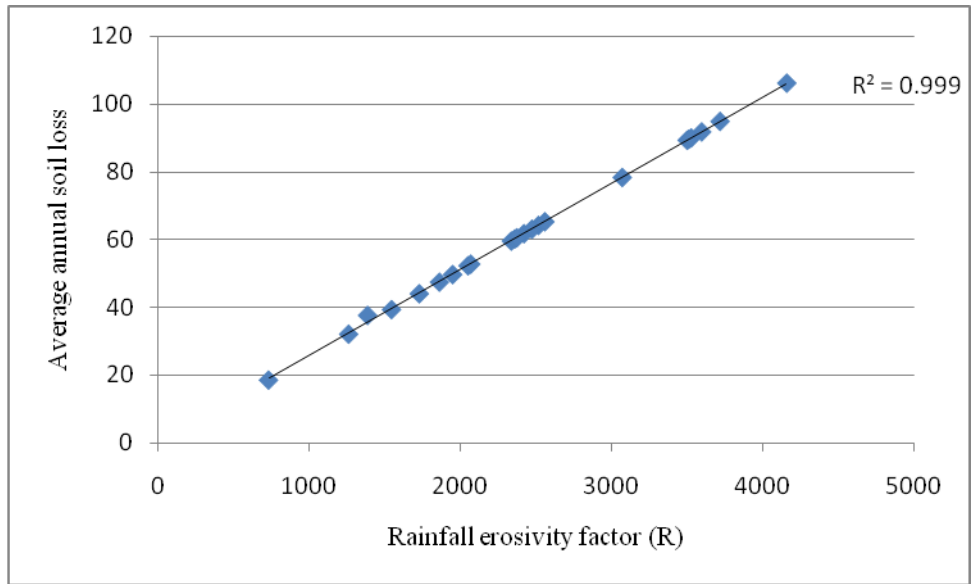


Fig. 4.15: Correlation between rainfall erosivity factor (R) and average annual soil loss

## SUMMARY AND CONCLUSION

### 5.1 Summary

The present research work was undertaken to study the morphometric characteristics of Dzumah watershed of Upper Dhansiri, Nagaland and estimate surface runoff and average annual soil loss from the watershed. The watershed boundary was delineated using SRTM DEM of 30 m resolution. QGIS software was used for generation of stream network and digitization of drainage map of the watershed area. Rainfall data collected from ICAR, Jharnapani, Medziphema, Nagaland was used for calculation of all rainfall related parameters. Soil samples from 19 pre-defined coordinates were collected and analyzed to fulfill all soil related parameters required in the study. Remotely sensed satellite data was used for preparing land use land cover map. The NRCS-CN method and USLE method were used to estimate surface runoff and average soil loss of the watershed. The salient findings of this study are summarized below:

#### 5.1.1 Watershed characterization

1. The Dzumah watershed is a 5<sup>th</sup> order basin with an area and perimeter of 6555 ha and 59.58 km, respectively.
2. The 1<sup>st</sup>, 2<sup>nd</sup>, 3<sup>rd</sup>, 4<sup>th</sup> and 5<sup>th</sup> order streams consisted of 184, 36, 5, 2 and 1 stream segments, respectively. The higher number of lower order streams indicated its hilly and undulating terrain, suggesting less infiltration and high runoff.
3. The value of length of overland flow (Lg) was 0.25, suggesting that the watershed is prone to moderate risks of runoff and erosion.
4. The values of all the areal aspects observed in the study suggested that the Dzumah watershed is elongated in shape. The value of form factor (Rf) suggested that the discharge from the watershed should have flatter peak flows for longer period. The value of drainage density (Dd)

suggested that the watershed should have good infiltration and excellent vegetation cover.

5. The values of Relief ratio (Rr) and Ruggedness number (Rn) suggested that the watershed has strong relief with rough and uneven topography rendering it vulnerable to soil erosion.

### **5.1.2 Runoff estimation and water yield potential**

1. It was observed that the Dzumah watershed is predominantly a forested watershed with forest cover occupying 85% of the total geographical area of the watershed.
2. The soil type included loam, clay loam, silty clay loam and silt loam, all of which falls under Hydrologic Soil Group C, indicating a moderately high runoff potential.
3. The original CN-II values of the watershed based on the standard TR-55 table (USDA-NRCS, 1986) varied from 73 to 100, whereas the modified CN-II values after  $\lambda_{0.05}$  and slope adjustments ranged from 91.02 to 100.
4. Runoff estimation using standard CN values underestimated the actual discharge occurring in the watershed. The total runoff depth estimated during the years 2019 and 2020 was just 9.49 and 3.78% of the total rainfall received in each year. Runoff estimation using the modified CN value gave better results representing actual discharge.
5. Using the modified CN value, the total runoff estimated in the years 2019 and 2020 were 43.60% and 38.76% of the total rainfall received during each respective years.
6. The water yield potential observed during the years 2019 and 2020 were 3,31,24,912.66 and 2,23,50,524.49 m<sup>3</sup>, respectively.
7. The runoff estimation using modified CN values also resulted in better rainfall-runoff correlation as compared to runoff estimated by standard CN values.

### 5.1.3 Average annual soil loss

1. For the years 1998 to 2020, the R-factor values ranged from 734.0 and 4157.3 MJ mm ha<sup>-1</sup> h<sup>-1</sup> yr<sup>-1</sup> with an average of 2465.9 MJ mm ha<sup>-1</sup> h<sup>-1</sup> yr<sup>-1</sup>.
2. The K-factor values of the watershed ranged from 0.03 to 0.074 t ha h ha<sup>-1</sup> MJ<sup>-1</sup> mm<sup>-1</sup>.
3. The slope map of the Dzumah watershed revealed that most of the watershed falls under hilly, moderately steep and steep classes with areas covering 24.51, 27.50 and 19.72 % of the total watershed area, respectively. The LS-factor values ranged from 0.03 to 54.44.
4. C-factor map was generated using NDVI map and its value ranged from 0.071 to 0.53.
5. It was observed that no major conservation practices were followed in the study area. Therefore, P-factor value was taken as 0.28 for cultivated areas and 1 for other land uses.
6. The average annual soil losses for the year 2019 and 2020 were 3.78 and 3.04 t h<sup>-1</sup> yr<sup>-1</sup>, respectively.
7. Considering the average annual soil losses estimated from 1998-2020, the average potential soil erosion for Dzumah watershed was found to be 5.38 t ha<sup>-1</sup> yr<sup>-1</sup>.

### 5.2 Conclusion

The present investigation revealed that the Dzumah watershed has an elongated configuration, characterized by hilly and dissected topography with steep slopes in the upper north and southeastern zones. These inherent properties of the watershed could facilitate the increase in surface flow velocity, thereby effectively reducing the absorption time while increasing erosion hazards. The study on drainage aspects revealed that the watershed is prone to moderate risks of soil erosion. The standard CN method failed to estimate surface runoff to represent real world scenario. The adjustment of  $\lambda$

value in initial abstraction and slope-adjusted CN gave better results. The prediction accuracy of the model could not be validated due to the absence of hydrologic gauging stations and daily flow records. However, the model presented a fair simulation of the hydrologic response of the watershed to rainfall events and the results can be used for conservation and management purposes, but not for computation of flood design structures. The Dzumah watershed is considered stable since almost 90% of the watershed area has light to moderate levels of erosion. Severe erosion is observed only in extreme steep slopes and disturbed sites caused by construction activities. These findings can serve as vital information for implementing precautionary measures in future developmental activities or efforts to alter the present land use system in the watershed. The GIS platform has proved to be a very effective, time and cost saving tool for computation and analysis of various morphometric characteristics of the watershed, estimation of surface runoff and soil erosion.

### **Recommendations:**

During monsoon, the watershed generates amply excessive surface runoff while it experiences drought-like conditions during months of December to May. Given the high water yield potential of the catchment, it is recommended that suitable water harvesting structures or in-situ conservation techniques be employed so as to store water for domestic and agricultural use during the lean period. Construction of check dams at suitable sites is also recommended so as to arrest the uncontrolled flow, minimize flow turbulence and facilitate ground water recharge.

Despite the rugged and steep topographical settings of the Dzumah watershed, it was found that the area is fairly stable. However, given the fragile mountainous environment of the watershed, maintaining the existing

forest cover and early adoption of soil conserving land use system is highly recommended for sustaining the current stability of the watershed.

**Future line of work:**

Validation of the rainfall-runoff model needs to be carried out for which a continuous recording gauging station is vitally important. Investigations regarding region-specific  $\lambda$  value in the initial abstraction parameter of the CN method for Nagaland conditions also need to be undertaken.

The USLE model considers only the soil losses caused by sheet and rill erosion. Therefore, other sources of soil losses from the watershed such as gully and stream bank erosion needs to be investigated. It is also significantly important to undertake a detailed analysis of all the individual USLE parameters under Nagaland conditions to determine the changes/modifications to their empirical derivation thereof; and validate the model under diverse land use patterns of Nagaland.



## REFERENCES

- Abboud, I. A. and Nofal, R. A. 2017. Morphometric analysis of Wadi Khumal basin, western coast of Saudi Arabia, using remote sensing and GIS techniques. *African Journal of Earth Science*. **126**: 58-74.
- Abraham, A., Thomas, D., Hariraj, E., Thuruthel, L. S. and Vysakh, K. B. 2017. Runoff estimation by SCS-Curve number method by GIS. *Journal of Water Resources and Pollution Studies*. **2**(2):1-9.
- Adhikari, S. 2020. Morphometric Analysis of a Drainage Basin: A Study of Ghatganga River, Bajhang District, Nepal. *The Geographic Base*. **7**: 127-144. Doi: 10.3126/tgb.v7i0.34280
- Ajmal, M., Waseem, M., Kim, D. and Kim, T. W. 2020. A Pragmatic Slope-Adjusted Curve Number Model to Reduce Uncertainty in Predicting Flood Runoff from Steep Watersheds. *Water*. **12**(5):1469.
- Akbari, A., Samah, A. A. and Ngien, S. K. 2016. Effect of slope adjustment on curve number using global digital elevation data: New look into Sharply-Williams and Huang methods. **In**: Proceedings of the Second International Conference on Science, Engineering & Environment, Osaka, Japan. pp. 21-23.
- Ali, S. A. and Hagos, H. 2016. Estimation of soil erosion using USLE and GIS in Awassa Catchment, Rift valley, Central Ethiopia. *Geoderma Regional*. **7**(2): 159-166.
- Almagro, A., Thomé, T. C., Colman, C. B., Pereira, R. B., Marcato, J., Rodrigues, D. B. B. and Oliveira, P. T. S. 2019. Improving cover and management factor (C-factor) estimation using remote sensing approaches for tropical regions. *International Soil and Water Conservation Research*. **7** (4): 325-334.
- Asfaw, D. and Workineh, G. 2019. Quantitative analysis of morphometry on Ribb and Gumara watersheds: Implications for soil and water conservation. *International Soil and Water Conservation Research* **7**: 150–157.
- Baban, S. M. J., and Yusof K. W. 2001. Modelling soil erosion in tropical environments using remote sensing and geographical information systems. *Hydrological Sciences Journal*. **46**(2): 191-198.
- Babu, K. J., Sreekumar, S., Aslam, A. 2016. Implication of drainage basin parameters of a tropical river basin of South India. *Applied Water Science*. **6**:67–75. DOI 10.1007/s13201-014-0212-8

- Bagegnehu, B., Muluneh, A. and Wondrade, N. 2019. Geographic Information System (GIS) based soil loss estimation using Universal Soil Loss Equation model (USLE) for soil conservation planning in Karesa watershed, Dawuro zone, South West Ethiopia. *International Journal of Water Resources and Environmental Engineering*. **11**(8): 143-158.
- Bali, R., Agarwal, K. K., Ali, S. N., Rastogi, S. K. and Krishna, K. 2011. Drainage morphometry of Himalayan Glacio-fluvial basin, India: hydrologic and neotectonic implications. *Environmental Earth Sciences*. **66**(4):1163–1174.
- Bartlett, M. S., Parolari, A. J., McDonnell, J. J. and Porporato, A. 2016. Beyond the SCS-CN method: A theoretical framework for spatially lumped rainfall-runoff response. *Water Resources Research*. **52**: 4608–4627. doi:10.1002/2015WR018439
- Belasri, A. and Lakhouili, A. 2016. Estimation of soil erosion risk using the Universal Soil Loss Equation (USLE) and Geo-information technology in Oued El Makhazine Watershed, Morocco. *Journal of Geographic Information System*. **8**(1): 98-107.
- Bogale, A. 2021. Morphometric analysis of a drainage basin using Geographical Information System in Gilgel Abay watershed, Lake Tana Basin, Upper Blue Nile Basin, Ethiopia. *Applied Water Science*. **11**(7): 1-7.
- Chandrashekar, H., Lokesh, K. V., Sameena, M., Roopa, J. and Ranganna, G. 2015. **In:** Proceedings of the International Conference on Water Resources, Coastal and Ocean Engineering (Mangalore) **4**: 1345 – 1353.
- Chattopadhyay, G. S. and Choudhury, S. 2006. Application of GIS and remote sensing for watershed development project – A case study. *Map India 2006*. <http://www.gisdevelopment.net>
- Chitra, C., Alaguraja, P., Ganeshkumari, K., Yuvaraj, D. and Manivel, M. 2011. Watershed characteristics of Kundah subbasin using remote sensing and GIS techniques. *International Journal Geomatics Geosciences*. **2**(1): 311–335.
- Chopra, R., Dhiman, R. D. and Sharma, P. K. 2005. Morphometric analysis of sub-watersheds in Gurdaspur district, Punjab using remote sensing and GIS techniques. *Journal of the Indian Society of Remote Sensing*. **33**(4): 531-539. <https://doi.org/10.1007/BF02990738>

- Chorley, R. J. (Ed.), 1969. *Water, Earth and Man. A synthesis of Hydrology, Geomorphology, and Socio–Economic Geography*. 588 p., figs. Methuen and Co. Ltd., London; Barnes and Noble, New York.
- Dabral, P. P., Baithuri, N. and Pandey, A. 2008. Soil erosion assessment in a hilly catchment of North Eastern India Using USLE, GIS and Remote Sensing. *Water Resource Management*.**22**: 1783-1798.
- Da Cunha, E. and Bacani, V. 2016. Morphometric characterization of a watershed through SRTM data and Geoprocessing technique. *Journal of Geographic Information System*. **8**: 238-247. doi: [10.4236/jgis.2016.82021](https://doi.org/10.4236/jgis.2016.82021)
- De Jong, S. M., Paracchini, M. L., Bertolo, F., Folving, S., Megier, J. and De Roo, A. P. J. 1999. Regional assessment of soil erosion using the distributed model SEMMED and remotely sensed data. *Catena*. **37**: 291-308.
- Devatha, C. P., Deshpande, V. and Renukaprasad, M. S. 2015. Estimation of soil loss using USLE model for Kulhan watershed, Chattisgarh - A case study. *Aquatic Procedia*. **4**: 1429-1436.
- Dos Santos, A. W., Martins, A. P., Morais, W. A., Pôssa, É. M., Castro, R. M. and de Moura, D. M. B. 2022. USLE modelling of soil loss in a Brazilian cerrado catchment. *Remote Sensing Applications: Society and Environment*. p.100788.
- Durigon, V. L., Carvalho, D. F., Antunes, M. A. H., Oliveira, P. T. S. and Fernandes, M. M. 2014. NDVI time series for monitoring RUSLEcover management factor in a tropical watershed. *International Journal of Remote Sensing*.**35**(2): 441–453.
- Ebrahimian, M., Nuruddin, A. A., Soom, M. A. B. and Sood, A. M. 2012. Application of NRCS-Curve Number method for runoff estimation in a mountainous watershed. *Caspian Journal of Environmental Sciences*. **10**(1):103-114.
- Ebrahimi, M., Hamid, N., Ali, S. and Mohammad, R. M. D. 2021. Assessment of the soil loss-prone zones using the USLE model in Northeastern Iran. *Paddy and Water Environment*. **19**(1): 71-86.
- Fistikoglu, O. and Harmancioglu, N. B. 2002. Integration of GIS with USLE in assessment of soil erosion. *Water Resource Management*.**16**:447–467.

- Garg, V., Bhaskar R. N., Thakur, P. K. and Aggarwal, S. P. 2013. Assessment of the effect of slope on runoff potential of a watershed using NRCS-CN method. *International Journal of Hydrology, Science and Technology*. **3**(2): 141-159.
- Ghosh, K., Kumar S. D., Bandyopadhyay, S. and Saha, S. 2013. Assessment of soil loss of the Dhalai river basin, Tripura, India using USLE. *International Journal of Geosciences*. **4**(1): 11-23.
- Girmay, G., Awdenegest, M. and Alemayehu, M. 2020. Estimation of soil loss rate using the USLE model for Agew mariyam watershed, Northern Ethiopia. *Agriculture and Food Security*. **9**(1): 1-12.
- Gitika, T. and Ranjan, S. 2014. Estimation of surface runoff using NRCS \Curve Number procedure in Buriganga watershed, Assam, India - A geospatial approach. *International Research Journal of Earth Sciences*. **2**(5): 1-7.
- Gizachew, K. and Berhan, G. 2018. Hydro-geomorphological characterization of Dhidhessa River Basin, Ethiopia. *International Soil and Water Conservation Research*. **6**: 175–183.
- Gutema, D. 2015. Morphometric analysis to identify erosion prone areas on the Upper Blue Nile using GIS (Case study of Didessa and Jema sub-basin, Ethiopia). M.Sc Thesis, Jimma Institute of Technology, Jimma.
- Gutema, D., Kassa, T. and Sifan, A. K. 2017. Morphometric analysis to identify erosion prone areas on the upper blue Nile using GIS: case study of Didessa and Jema sub-basin, Ethiopia. *International Research Journal of Engineering and Technology*. **4**(8): 1773 – 1784.
- Haghipour, N. and Burg, J. P. 2014. Geomorphological analysis of the drainage system on the growing Makran accretionary wedge. *Geomorphology*. **209**:111–132.
- Hamad, R. 2020. Multiple morphometric characterization and analysis of Malakan Valley drainage basin using GIS and Remote Sensing, Kurdistan Region, Iraq. *American Journal of Water Resources*. **8**(1): 38-47. DOI:10.12691/ajwr-8-1-5
- Hawkins, R. H., Hjelmfelt, A. T. and Zevenbergen, A. W. 1985. Runoff probability, storm depth, and curve numbers. *Journal of Irrigation and Drainage Engineering*. **111**(4): 330-340.
- Hawkins, R. H., Theurer, F. D. and Rezaeianzadeh, M. 2019. Understanding the basis of the curve number method for watershed models and TMDLs. *Journal of*

*Hydrologic Engineering*. **24** (7): 06019003.

[https://doi.org/10.1061/\(ASCE\)HE.1943-5584.0001755](https://doi.org/10.1061/(ASCE)HE.1943-5584.0001755)

Horton, R. E. 1932. Drainage basin characteristics, 2nd edn. transactions, American Geophysical Union, New York.

Horton, R. E. 1945. Erosional development of streams and their drainage basins: hydro physical approach to quantitative morphology. *Bulletin of Geological Society of America*. **56**:275–370.

Huang, M., Jacques, G., Wang, Z. and Monique, G. 2006. A modification to the soil conservation service curve number method for steep slopes in the Loess plateau of China. *Hydrological Processes*. **20**(3): 579–589.

Ismail, M., Singh, H., Farooq, I. and Yousuf, N. 2022. Quantitative morphometric analysis of Veshav and Rembi Ara watersheds, India, using Quantum GIS. *Applied Geomatics*. **14**(2): 119-134.

Jacobs, J. H. and Srinivasan, R. 2005. Effects of curve number modification on runoff estimation using WSR-88D rainfall data in Texas Watersheds. *Journal of Soil and Water Conservation*. **60**: 274-278.

Jasrotia, A. S. and Singh, R. 2006. Modeling runoff and soil erosion in a catchment area, using the GIS in the Himalayan region, India. *Environmental Geology*. **51**: 29-37.

Javed, A., Khanday, M. Y. and Ahmed, R. 2009. Prioritization of Sub-watersheds based on Morphometric and Land Use Analysis using Remote Sensing and GIS Techniques. *Journal of the Indian Society of Remote Sensing*. **37**: 261–274.

Jemai, S., Amjad, K., Belgacem, A. and Habib, A. 2021. Soil erosion estimation in arid area by USLE model applying GIS and RS: Case of Oued El Hamma catchment, south-eastern Tunisia." *Journal of the Indian Society of Remote Sensing*. **49**(6): 1293-1305.

Kadam, A. K., Jaweed, T. H., Kale, S. S., Umrikar, B. N. and Sankhua, R. N. 2019. Identification of erosion-prone areas using modified morphometric prioritization method and sediment production rate: a remote sensing and GIS approach. *Geomatics, Natural Hazards and Risk*. **10**(1): 986-1006. DOI: [10.1080/19475705.2018.1555189](https://doi.org/10.1080/19475705.2018.1555189)

Kaliraj, S., Chandrasekar, N. and Magesh, N. S. 2015. Morphometric analysis of the River Thamirabarani sub-basin in Kanyakumari District, South west coast of

- Tamil Nadu, India, using remote sensing and GIS. *Environmental Earth Sciences*. **73**(11): 7375–7401.
- Karaburun, A. 2010. Estimation of C factor for soil erosion modeling using NDVI in Buyukcekmece watershed. *Ocean Journal of Applied Sciences*.**3**(1):77-85.
- Karydas, C. G., Sekuloska, T. and Silleos, G. N. 2009. Quantification and site specification of the support practice factor when mapping soil erosion risk associated with olive plantations in the Mediterranean Island of Crete. *Environmental Monitoring and Assessment*. **149**: 19–28.
- Kaur, M., Singh, S., Verma, V. K. and Pateriya, B. 2014. Quantitative geomorphological analysis & land use/ land cover change detection of two sub-watersheds in NE region of Punjab, India. *The International Archives of the Photogrammetry, Remote Sensing and Spatial Information Sciences*. **8**: 371-375.
- Khizr, B. O., Ibrahim, G. R. F., Hamid, A. A. and Ail, S. A. 2022. Runoff estimation using SCS-CN and GIS techniques in the Sulaymaniyah sub-basin of the Kurdistan region of Iraq. *Environment, Development and Sustainability*. **24**(2): 2640-2655.
- Kumar, A., Jayappa, K. S., and Deepika, B. 2011. Prioritization of sub-basins based on geomorphology and morphometric analysis using remote sensing and geographic information system (GIS) techniques. *Geocarto International*. **26**(7): 569-592. DOI: [10.1080/10106049.2011.606925](https://doi.org/10.1080/10106049.2011.606925)
- Kumar, A., Kanga, S., Taloor, A. K., Singh, S. K. and Durin, B. 2021. Surface runoff estimation of Sind river basin using integrated SCS-CN and GIS techniques. *HydroResearch*. **4**:61-74.
- Lim, K. J., Engel, B. A., Muthukrishnan, S. and Harbor, J. 2006. Effects of initial abstraction and urbanization on estimated runoff using CN technology. *Journal of the American Water Resources Association*. **42**(3):629- 643.
- Lin, C. Y., Lin, W. T. and Chou, W. C. 2002. Soil erosion prediction and sediment yield estimation: the Taiwan experience. *Soil and Tillage Research*.**68**(2): 143–152.
- Lodhi, M. S. and Reza, M. 2017. Morphometric analysis of Singki River Catchment using remote sensing and GIS: Papumpare, Arunachal Pradesh. *International Journal of Advanced Remote Sensing and GIS*. **6**(1): 2023-2032.

- Magesh, N. S. and Chandrasekhar, N. 2014. GIS model-based morphometric evaluation of Tamiraparani sub basin, Tirunelveli district, Tamil Nadu, India. *Arabian Journal of Geosciences*. **7**:131–141.
- Magesh, N. S., Jitheshlal, K. V. and Chandrasekar, N. 2013. Geographical information system-based morphometric analysis of Bharathapuzha river basin, Kerala, India. *Applied Water Science*. **3**: 467–477.
- Mahala, A. 2020. The significance of morphometric analysis to understand the hydrological and morphological characteristics in two different morpho-climatic settings. *Applied Water Science*. **10**: 33. <https://doi.org/10.1007/s13201-019-1118-2>
- McCool, D. K., Foster, G. R., Mutchler, C. K. and Meyer, L. D. 1987. Revised slope steepness factor for the Universal Soil Loss Equation. *Transactions of the American Society of Agricultural Engineers*. **30**(5):1387–1396.
- Miller, V.C. 1953. A quantitative geomorphic study on drainage basin characteristics in the Clinch mountain area, Virginia and Tennessee, Project NR 389-042. Technical report 3. Columbia University, New York.
- Nayak, T. R. and Jaiswal, R. K. 2003. Rainfall-Runoff modelling using Satellite data and GIS for Bebas River in Madhya Pradesh. *Journal of the Institution of Engineers(India), Civil Engineering Division*. **84**: 47-50.
- Oliveira, P. T. S., Nearing, M. A., Hawkins, R. H., Stone, J.J., Rodrigues, D. B. B., Panachuki, E. and Wendland E. 2016. Curve number estimation from Brazilian Cerrado rainfall and runoff data. *Journal of Soil and Water Conservation*. **71**(5): 420 – 429.
- Ozcan, A. U., Erpul, G., Basaran, M. and Erdogan, H. E. 2008. Use of USLE/GIS technology integrated with geostatistics to assess soil erosion risk in different land uses of Indagi Mountain Pass - Cankiri, Turkey. *Environmental Geology*. **53**(8):1731-1741.
- Pamela, P., Sadisun, I. A. and Arifianti, Y. 2018. Weights of evidence method for landslide susceptibility mapping in Takengon, Central Aceh, Indonesia. **In**: Proceedings of the IOP conference series: Earth Environmental Science, Bandung, Indonesia. <https://doi.org/10.1088/1755-1315/118/1/012037>

- Pareta, K. and Pareta, U. 2011. Quantitative Morphometric Analysis of a Watershed of Yamuna Basin, India using ASTER (DEM) Data and GIS. *International Journal of Geomatics and Geosciences*. **2**(1): 248-269.
- Patil, V. S. P. and Mali, S. P. 2013. Watershed characterization and prioritization of Tulasi subwatershed: A geospatial approach. *International Journal of Innovative Research in Science, Engineering and Technology*. **2**(6): 2182 – 2189.
- Patil, V. V. and Toradmal, A. B. 2020. Digital Terrain Analysis for watershed characterization and management- A case study of Vincharna river basin, Maharashtra, India. *Journal of Information and Computational Science***10**(2): 637-647
- Piper, C.C. 1996. Soil and Plant analysis. *Hans Publishers*, Mumbai.
- Prabhakaran, A. and Jawahar R. N. 2018. Drainage morphometric analysis for assessing form and processes of the watersheds of Pachamalai hills and its adjoining, Central Tamil Nadu, India. *Applied Water Science*. **8**: 31. <https://doi.org/10.1007/s13201-018-0646-5>
- Prasad, R. K., Mondal, N. C., Banerjee, P., Nandakumar, M. V. and Singh, V.S. 2008. Deciphering potential ground water zone in hard rock through the application of GIS. *Environmental Geology*. **55**: 467–475.
- Prasannakumar, V., Vijith, H., Geetha, N. and Shiny, R. 2011. Regional scale erosion assessment of a Sub-tropical Highland segment in the Western Ghats of Kerala, South India. *Water Resource Management*. **25**:3715–3727.
- Rai, P. K., Mohan, K., Mishra, S., Ahmad, A. and Mishra, V. N. 2017. A GIS based approach in drainage morphometric analysis of Kanhar River Basin, India. *Applied Water Science*. **7**:217–232.
- Raju, S. R., Raju, G. S. and Rajasekhar, M. 2018. Estimation of rainfall runoff using SCS-CN method with RS and GIS techniques for Mandavi Basin in YSR Kadapa District of Andhra Pradesh, India. *Hydrospatial Analysis*. **2**(1): 1-15.



- Ramakrishnan, D., Bandyopadhyay, A. and Kusuma, K. N. 2009. SCS-CN and GIS-based approach for identifying potential water harvesting sites in the Kali watershed, Mahi river basin, India. *Journal of Earth System Science*. **118**: 355-368.
- Rao, Y. P. 1981. Evaluation of cropping management factor in Universal Soil Loss Equation under natural rainfall condition of Kharagpur, India. **In**: Proceedings of the Southeast Asian Regional Symposium on Problems of Soil Erosion and Sedimentation. Asian Institute of Technology, Bangkok. pp 241–254.
- Reddy, G. P. O., Maji, A. K. and Gajbhiye, K. S. 2004. Drainage morphometry and its influence on landform characteristics in a basaltic terrain, Central India – A remote sensing and GIS approach. *International Journal of Applied Earth Observation and Geoinformation*. **6**(1): 1–16.
- Renard, K. G., Foster, G. R., Weesies, G. A., McCool, D. K. and Yoder, D. C. 1997. Predicting soil erosion by water: A guide to conservation planning with the Revised Universal Soil Loss Equation (RUSLE). USDA Agricultural Handbook. **703**: 126-131.
- Ross, C. W., Prihodko, L., Anchang, J., Kumar, S., Ji, W. and Hanan, N.P. 2018. HYSOGs250m, global gridded hydrologic soil groups for curve-number-based runoff modeling. *Scientific Data* **5**. 180091. <https://doi.org/10.1038/sdata.2018.91>
- Sarangi, A., Bhattacharya, A. K., Singh, A. K. and Sambaiha, A. 2005. Performance of Geomorphologic Instantaneous Unit Hydrograph (GIUH) model for estimation of surface runoff. **In**: International conference on recent advances in water resources development and management. IIT, Roorkee, Uttaranchal, India. pp 569–581.
- Sarma, P. K., Sarmah, K., Chetri, P. K. and Sarkar, A. 2013. Geospatial study on morphometric characterization of Umtrew River basin of Meghalaya, India. *International Journal of Water Resources and Environmental Engineering*. **5**(8): 489-498.
- Saxena, R. K., Verma, K. S., Chary, G. R., Srivastava, R. and Barthwal, A. K. 2000. IRS-1C data application in watershed characterization and management. *International Journal of Remote Sensing*. **21**(17): 3197-3208. DOI: [10.1080/014311600750019822](https://doi.org/10.1080/014311600750019822)

- Schumm, S. A. 1956. The evolution of drainage system and slopes in Badlands at Perth Amboy, New Jersey. *Bulletin of the Geological Society of America*. **67**:214–236.
- Sheikh, A. H., Palria, S. and Alam, A. 2011. Integration of GIS and Universal Soil Loss Equation (USLE) for soil loss estimation in a Himalayan watershed. *Recent Research in Science and Technology*. **3**(3): 51-57.
- Shi, Z. H., Chen, L. D., Fang, N. F., Qin, D. F. and Cai, C. F. 2009. Research on the SCS-CN initial abstraction ratio using rainfall-runoff event analysis in the Three Gorges Area, China. *Catena*. **77**(1):1-7.
- Singh, G. and Panda, R. K. 2017. Grid-cell based assessment of soil erosion potential for identification of critical erosion prone areas using USLE, GIS and remote sensing: A case study in the Kapgari watershed, India. *International Soil and Water Conservation Research*. **5**(3): 202-211.
- Shrestha, R. K., Ahlers, R., Bakker, M. and Gupta, J. 2010. Institutional dysfunction and challenges in flood control: a case study of the Kosi flood 2008. *Economic and Political Weekly*. **14**(2):45–53.
- Soni, S. K., Tripathi, S. and Maurya, A. K. 2013. GIS based morphometric characterization of mini watershed - Rachhar Nala of Anuppur district, Madhya Pradesh. *International Journal of Advanced Technology and Engineering Research*. **3**(3): 32 – 38.
- Sreedevi, P. D., Subrahmanyam, K. and Ahmed, S. 2005. The significance of morphometric analysis for obtaining groundwater potential zones in a structurally controlled terrain. *Environmental Geology*. **47**(3):412–420.
- Strahler, A. N. 1952. Dynamic Basis of Geomorphology. *Bulletin of the Geological Society of America*. **63**: 923-938.
- Strahler, A. N. 1957. Quantitative analysis of watershed Geomorphology. *Transactions of the American Geophysical Union*. **38**:913–920.
- Strahler, A. N. 1958. Quantitative Geomorphology of Drainage Basins and Channel Networks. **In**: Handbook of Applied Hydrology (eds. V.T. Chow), McGraw Hill, New York, 439-476.

- Strahler, A. N. 1964. Quantitative Geomorphology of Basins and Channel Networks. **In:** Handbook of Applied Hydrology (eds. V.T. Chow). McGraw Hill Book Company, New York.
- Sukristiyanti, S., Maria, R. and Lestiana, H. 2018. Watershed-based Morphometric Analysis: A Review. **In:** Global Colloquium on Geosciences and Engineering - IOP Conference Series: Earth and Environmental Science. doi :10.1088/1755-1315/118/1/012028
- Thomas, J., Sabu, J. and Thirvikramaji, K. P. 2010. Morphometric aspects of a small tropical mountain river system, the southern Western Ghats, India. *International Journal of Digital Earth*. **3**(2): 135-156.
- Tian, Y. C., Zhou, Y. M., Wu, B. F. and Zhou, W. F. 2009. Risk assessment of water soil erosion in upper basin of Miyun Reservoir, Beijing, China. *Environmental Geology*. **57**: 937–942.
- Tirkey, A. S., Pandey, A. C. and Nathawat, M. S. 2013. Use of high-resolution satellite data, GIS and NRCS-CN technique for the estimation of rainfall-induced runoff in small catchment of Jharkhand, India. *GeocartoInternational*. **29** (7): 778–791.
- USDA. 1985. Soil conservation service: National Engineering Handbook, Sect 4 - Hydrology, Washington, DC.
- USDA. 1986. Urban hydrology for small watersheds, Technical Release-55, 2<sup>nd</sup> edition, United States Department of Agriculture.
- USDA. 2009. Natural Resources Conservation Service, National Engineering Handbook, United States Department of Agriculture, Washington DC.
- Verma, A. K. 2007. Rainwater harvesting techniques for increasing crop production in Nagaland. **In:** Composite Farming Practices and Economic Development (eds. A. Sharma, R. K. Singh). pp. 1-10.
- Verma, S., Singh, A., Mishra, S. K., Singh, P. K. and Verma, R. K. 2018. Efficacy of slope-adjusted Curve Number models with varying initial abstraction coefficient for runoff estimation. *International Journal of Hydrology, Science and Technology*. **8**(4): 317-338.
- Vincy, M. V., Rajan, B. and Pradeepkumar, A. P. 2012. Geographic Information System-based morphometric characterization of sub-watersheds of Meenachil river basin, Kottayam district, Kerala, India. *Geocarto International*. **27**(8): 661-684.

- Vinutha, D. N. and Janardhana, M. R. 2014. Morphometry of the Payaswini Watershed, Coorg District, Karnataka, India, Using Remote Sensing and GIS Techniques. *International Journal of Innovative Research in Science, Engineering and Technology*. **5**: 516-524.
- Vittala, S. S., Govindaiah, S. and Gowda, H. H. 2004. Morphometric analysis of sub-watersheds in the Pavagada area of Tumkur District, South India using remote sensing and GIS techniques. *Journal of the Indian Society of Remote Sensing*. **32**(4):351–362.
- Wakode, H. B., Dutta, D., Desai, V. R., Baier, K. and Azzam, R. 2013. Morphometric analysis of the upper catchment of Kosi River using GIS techniques. *Arabian Journal of Geosciences*. **6**(6):395–408.
- Walkey, A. and Black, I. A. 1934. Determination of organic matter in soil. *Soil Science*. **37**: 549-556.
- Wang, G., Wentz, S., Gertner, G. Z. and Anderson, A. 2002. Improvement in mapping vegetation cover factor for the Universal Soil Loss Equation by geostatistical methods with Landsat Thematic Mapper images. *International Journal of Remote Sensing*. **23**(18): 3649–3667.
- Wei, Y., Wu, X., Xia, J., Zeng, R., Cai, C. and Wang, T. 2019. Dynamic study of infiltration rate for soils with varying degrees of degradation by water erosion. *International Soil and Water Conservation Research*. **7**(2): 167-175.
- Wischmeier, W. H. and Mannering, J. V. 1969. Relation of soil properties to its erodibility. **In**: Proceedings of the Soil Science Society of America. **33**: 131-137.
- Wischmeier, W. H. and Smith, D. D. 1978. Predicting rainfall erosion losses. USDA Agricultural Research Services Handbook 537. USDA, Washington, DC. p 57.
- Withanage, S. N., Dayawansa, K. D. N. and De Silva, P. R. 2014. Morphometric analysis of the Gal Oya River Basin using spatial data derived from GIS. *Tropical Agricultural Research*. **26**(1):175–188.
- Woodward, D.E., Hawkins, R.H., Jiang, R., Hjelmfelt, A.T. Jr., Van Mullem, J.A. and Quan, Q.D. 2003. Runoff curve number method: Examination of the initial abstraction ratio. **In**: WorldWater & Environment Resources, Congress 2003 and Related Symposia, EWRI, ASCE, Philadelphia, Pennsylvania, USA.

- Yadav, S. K., Dubey, A., Szilard, S. and Singh, S. K. 2016. Prioritization of sub-watersheds based on Earth Observation Data of agricultural dominated Northern River Basin of India. *Geocarto International*. **33**(4): 339-356.
- Yangchan, J., Jain, A. K., Tiwari, A. K. and Sood, A. 2015. Morphometric Analysis of Drainage Basin through GIS: A Case study of Sukhna Lake Watershed in Lower Shiwalik, India. *International Journal of Scientific and Engineering Research*. **6**(2):1015-1023.
- Yousuf, A., Ara, S., Ahmed, S., Prasad, A. and Thakur, B. R. 2020. Remote Sensing and GIS based Morphometric Analysis of a Microwatershed. Urban Environment: Issues and Challenges. Publisher: RK Books New Delhi.
- Yue-Qing, X., Xiao-Mei, S., Xiang-Bin, K., Jian, P. and Yun-Long, C. 2008. Adapting the RUSLE and GIS to model soil erosion risk in a mountains karst watershed, Guizhou Province, China. *Environmental Monitoring and Assessment*. **141**: 275–286.
- Zade, M. R., Ray, S. S., Dutta, S. and Panigrahy, S. 2005. Analysis of runoff pattern for all major basins of India derived using remote sensing data. *Current Science*. **88**(8): 1301- 1305.

## APPENDICES

### APPENDIX – A

Table 1: Rainfall data of Dzumah watershed from 1998 to 2020

Year/Month	1998	1999	2000	2001	2002	2003	2004	2005	2006	2007	2008	2009	2010
January	13.0	1.4	12.0	9.4	11.8	29.3	0.0	11.6	0.0	2.6	30.1	0.0	0.0
February	19.6	0.0	3.8	55.1	10.6	17.6	8.9	47.9	6.2	78.9	14.2	5.1	9.8
March	68.7	6.1	46.0	21.7	43.5	43.5	16.0	122.4	20.9	29.1	74.0	24.0	29.1
April	120.3	27.4	87.4	93.3	221.5	175.1	155.7	48.6	94.9	120.2	45.0	31.6	73.5
May	74.8	247.8	208.6	117.8	149.0	147.5	94.7	182.0	267.0	143.7	189.3	130.8	200.9
June	67.8	80.0	263.1	289.5	202.0	236.1	222.0	220.1	327.2	355.6	297.9	116.7	285.3
July	167.2	222.3	401.3	267.9	346.6	193.1	490.5	159.3	259.3	322.7	223.8	219.0	366.0
August	148.6	357.9	429.5	286.3	340.6	242.6	213.7	396.5	95.0	500.3	207.6	169.8	376.9
September	163.1	225.2	282.1	230.2	182.0	226.5	325.9	238.5	248.4	214.0	286.6	188.7	206.8
October	97.8	178.6	92.9	224.2	11.1	230.7	151.9	118.8	85.2	198.9	171.3	74.9	97.8
November	113.0	31.1	0.0	25.0	90.5	11.9	22.7	0.0	21.5	76.0	0.0	7.5	0.4
December	0.0	2.0	0.0	0.0	16.0	20.4	0.0	16.6	9.1	14.5	6.5	0.0	10.8
Total Rainfall (mm)	1053.9	1379.8	1826.7	1620.4	1625.2	1574.3	1702.0	1562.3	1434.7	2056.5	1546.3	968.1	1657.3

Year/Month	2011	2012	2013	2014	2015	2016	2017	2018	2019	2020
January	12.1	25.3	0.0	0.0	24.2	30.5	0.7	23.0	0.0	18.5
February	3.0	14.4	7.8	26.0	26.3	8.3	0.7	6.7	27.6	9.7
March	77.6	14.6	66.1	33.9	32.0	34.0	127.9	31.8	79.2	22.5
April	91.8	112.6	106.9	41.2	178.2	108.5	226.0	71.4	73.3	153.9
May	195.5	44.1	316.2	137.6	89.4	214.8	111.7	135.5	185.8	134.2
June	474.2	240.2	198.0	114.5	188.8	203.0	278.7	354.7	195.0	266.2
July	259.8	366.6	249.5	311.5	322.9	264.2	485.6	240.0	271.3	199.9
August	287.6	197.0	476.7	269.9	177.9	398.9	492.5	302.8	274.5	80.3
September	223.4	183.9	119.6	149.5	232.8	283.7	235.9	115.7	173.4	157.6
October	54.8	109.3	143.9	89.4	61.3	33.6	130.0	64.0	244.8	175.7
November	0.0	19.1	0.0	0.0	20.7	130.7	16.4	13.3	52.9	35.2
December	0.0	0.0	0.0	4.8	9.6	5.8	31.8	50.0	0.9	0.0
Total Rainfall (mm)	1679.8	1327.1	1684.7	1178.3	1364.1	1716.0	2137.9	1408.9	1578.7	1253.7

APPENDIX – B

Table-1: AMC and runoff calculation of Dzumah watershed for the year 2019

Date	Rainfall(mm)	Sum of previous 5 days rainfall	AMC	CN	S(mm)	Q(mm)
01-Jun-19	9.7	59.4	3	96.52	9.15	5.02
02-Jun-19	0.0	69.1	3	96.52	9.15	0.00
03-Jun-19	42.2	48.7	2	92.22	21.43	28.50
04-Jun-19	3.8	54.9	3	96.52	9.15	1.00
05-Jun-19	2.6	58.7	3	96.52	9.15	0.46
06-Jun-19	0.8	58.3	3	96.52	9.15	0.01
07-Jun-19	0.0	49.4	2	92.22	21.43	0.00
08-Jun-19	4.1	49.4	2	92.22	21.43	0.43
09-Jun-19	1.2	11.3	1	83.86	48.88	0.00
10-Jun-19	3.4	8.7	1	83.86	48.88	0.02
11-Jun-19	0.0	9.5	1	83.86	48.88	0.00
12-Jun-19	0.0	8.7	1	83.86	48.88	0.00
13-Jun-19	16.0	8.7	1	83.86	48.88	3.34
14-Jun-19	1.2	20.6	1	83.86	48.88	0.00
15-Jun-19	23.3	20.6	1	83.86	48.88	6.97
16-Jun-19	0.5	40.5	2	92.22	21.43	0.00
17-Jun-19	0.0	41.0	2	92.22	21.43	0.00
18-Jun-19	0.0	41.0	2	92.22	21.43	0.00
19-Jun-19	5.4	25.0	1	83.86	48.88	0.20
20-Jun-19	2.2	29.2	1	83.86	48.88	0.00
21-Jun-19	19.2	8.1	1	83.86	48.88	4.82
22-Jun-19	29.0	26.8	1	83.86	48.88	10.36
23-Jun-19	10.2	55.8	3	96.52	9.15	5.42
24-Jun-19	0.0	66.0	3	96.52	9.15	0.00
25-Jun-19	0.4	60.6	3	96.52	9.15	0.00
26-Jun-19	0.4	58.8	3	96.52	9.15	0.00
27-Jun-19	9.6	40.0	2	92.22	21.43	2.72
28-Jun-19	4.1	20.6	1	83.86	48.88	0.06
29-Jun-19	0.1	14.5	1	83.86	48.88	0.00
30-Jun-19	5.6	14.6	1	83.86	48.88	0.22



Date	Rainfall(mm)	Sum of previous 5 days rainfall	AMC	CN	S(mm)	Q(mm)
01-Jul-19	0.8	19.8	1	83.86	48.88	0.00
02-Jul-19	28.5	20.2	1	83.86	48.88	10.04
03-Jul-19	22.5	39.1	2	92.22	21.43	11.58
04-Jul-19	0.0	57.5	3	96.52	9.15	0.00
05-Jul-19	5.1	57.4	3	96.52	9.15	1.74
06-Jul-19	0.3	56.9	3	96.52	9.15	0.00
07-Jul-19	4.4	56.4	3	96.52	9.15	1.33
08-Jul-19	2.9	32.3	1	83.86	48.88	0.00
09-Jul-19	0.0	12.7	1	83.86	48.88	0.00
10-Jul-19	0.7	12.7	1	83.86	48.88	0.00
11-Jul-19	26.6	8.3	1	83.86	48.88	8.88
12-Jul-19	2.6	34.6	1	83.86	48.88	0.00
13-Jul-19	1.9	32.8	1	83.86	48.88	0.00
14-Jul-19	0.0	31.8	1	83.86	48.88	0.00
15-Jul-19	2.3	31.8	1	83.86	48.88	0.00
16-Jul-19	0.2	33.4	1	83.86	48.88	0.00
17-Jul-19	0.0	7.0	1	83.86	48.88	0.00
18-Jul-19	0.0	4.4	1	83.86	48.88	0.00
19-Jul-19	0.0	2.5	1	83.86	48.88	0.00
20-Jul-19	56.0	2.5	1	83.86	48.88	30.16
21-Jul-19	1.2	56.2	3	96.52	9.15	0.06
22-Jul-19	0.0	57.2	3	96.52	9.15	0.00
23-Jul-19	0.0	57.2	3	96.52	9.15	0.00
24-Jul-19	10.2	57.2	3	96.52	9.15	5.42
25-Jul-19	3.8	67.4	3	96.52	9.15	1.00
26-Jul-19	4.5	15.2	1	83.86	48.88	0.10
27-Jul-19	10.4	18.5	1	83.86	48.88	1.28
28-Jul-19	81.4	28.9	1	83.86	48.88	51.73
29-Jul-19	1.2	110.3	3	96.52	9.15	0.06
30-Jul-19	0.0	101.3	3	96.52	9.15	0.00
31-Jul-19	3.8	97.5	3	96.52	9.15	1.00

Date	Rainfall(mm)	Sum of previous 5 days rainfall	AMC	CN	S(mm)	Q(mm)
01-Aug-19	1.1	96.8	3	96.52	9.15	0.05
02-Aug-19	7.8	87.5	3	96.52	9.15	3.57
03-Aug-19	11.2	13.9	1	83.86	48.88	1.52
04-Aug-19	5.2	23.9	1	83.86	48.88	0.17
05-Aug-19	0.0	29.1	1	83.86	48.88	0.00
06-Aug-19	1.0	25.3	1	83.86	48.88	0.00
07-Aug-19	6.4	25.2	1	83.86	48.88	0.34
08-Aug-19	0.5	23.8	1	83.86	48.88	0.00
09-Aug-19	24.2	13.1	1	83.86	48.88	7.48
10-Aug-19	10.4	32.1	1	83.86	48.88	1.28
11-Aug-19	0.0	42.5	2	92.22	21.43	0.00
12-Aug-19	0.0	41.5	2	92.22	21.43	0.00
13-Aug-19	40.2	35.1	1	83.86	48.88	17.98
14-Aug-19	4.9	74.8	3	96.52	9.15	1.62
15-Aug-19	2.2	55.5	3	96.52	9.15	0.32
16-Aug-19	0.8	47.3	2	92.22	21.43	0.00
17-Aug-19	15.4	48.1	2	92.22	21.43	6.31
18-Aug-19	56.0	63.5	3	96.52	9.15	48.72
19-Aug-19	2.1	79.3	3	96.52	9.15	0.29
20-Aug-19	0.0	76.5	3	96.52	9.15	0.00
21-Aug-19	0.1	74.3	3	96.52	9.15	0.00
22-Aug-19	12.2	73.6	3	96.52	9.15	7.06
23-Aug-19	0.5	70.4	3	96.52	9.15	0.00
24-Aug-19	8.9	14.9	1	83.86	48.88	0.87
25-Aug-19	0.0	21.7	1	83.86	48.88	0.00
26-Aug-19	2.8	21.7	1	83.86	48.88	0.00
27-Aug-19	12.2	24.4	1	83.86	48.88	1.86
28-Aug-19	43.7	24.4	1	83.86	48.88	20.56
29-Aug-19	1.8	67.6	3	96.52	9.15	0.20
30-Aug-19	2.9	60.5	3	96.52	9.15	0.58
31-Aug-19	0.0	63.4	3	96.52	9.15	0.00

Date	Rainfall(mm)	Sum of previous 5 days rainfall	AMC	CN	S(mm)	Q(mm)
01-Sep-19	3.6	60.6	3	96.52	9.15	0.90
02-Sep-19	0.4	52.0	2	92.22	21.43	0.00
03-Sep-19	1.2	8.7	1	83.86	48.88	0.00
04-Sep-19	4.8	8.1	1	83.86	48.88	0.13
05-Sep-19	12.6	10.0	1	83.86	48.88	2.00
06-Sep-19	0.8	22.6	1	83.86	48.88	0.00
07-Sep-19	0.0	19.8	1	83.86	48.88	0.00
08-Sep-19	0.0	19.4	1	83.86	48.88	0.00
09-Sep-19	1.8	18.2	1	83.86	48.88	0.00
10-Sep-19	0.0	15.2	1	83.86	48.88	0.00
11-Sep-19	0.4	2.6	1	83.86	48.88	0.00
12-Sep-19	9.2	2.2	1	83.86	48.88	0.94
13-Sep-19	3.7	11.4	1	83.86	48.88	0.04
14-Sep-19	1.5	15.1	1	83.86	48.88	0.00
15-Sep-19	0.0	14.8	1	83.86	48.88	0.00
16-Sep-19	1.5	14.8	1	83.86	48.88	0.00
17-Sep-19	5.4	15.9	1	83.86	48.88	0.20
18-Sep-19	0.6	12.1	1	83.86	48.88	0.00
19-Sep-19	1.8	9.0	1	83.86	48.88	0.00
20-Sep-19	0.0	9.3	1	83.86	48.88	0.00
21-Sep-19	0.0	9.3	1	83.86	48.88	0.00
22-Sep-19	9.5	7.8	1	83.86	48.88	1.02
23-Sep-19	20.0	11.9	1	83.86	48.88	5.21
24-Sep-19	9.0	31.3	1	83.86	48.88	0.89
25-Sep-19	7.0	38.5	2	92.22	21.43	1.46
26-Sep-19	1.6	45.5	2	92.22	21.43	0.01
27-Sep-19	2.3	47.1	2	92.22	21.43	0.08
28-Sep-19	0.0	39.9	2	92.22	21.43	0.00
29-Sep-19	1.3	19.9	1	83.86	48.88	0.00
30-Sep-19	73.4	12.2	1	83.86	48.88	44.75

Date	Rainfall(mm)	Sum of previous 5 days rainfall	AMC	CN	S(mm)	Q(mm)
01-Oct-19	7.5	78.6	3	96.52	9.15	3.35
02-Oct-19	0.1	84.5	3	96.52	9.15	0.00
03-Oct-19	0.0	82.3	3	96.52	9.15	0.00
04-Oct-19	2.4	82.3	3	96.52	9.15	0.39
05-Oct-19	0.0	83.4	3	96.52	9.15	0.00
06-Oct-19	0.0	10.0	1	83.86	48.88	0.00
07-Oct-19	12.1	2.5	1	83.86	48.88	1.82
08-Oct-19	9.0	14.5	1	83.86	48.88	0.89
09-Oct-19	8.4	23.5	1	83.86	48.88	0.75
10-Oct-19	7.6	29.5	1	83.86	48.88	0.57
11-Oct-19	25.8	37.1	2	92.22	21.43	14.24
12-Oct-19	0.0	62.9	3	96.52	9.15	0.00
13-Oct-19	0.0	50.8	2	92.22	21.43	0.00
14-Oct-19	0.0	41.8	2	92.22	21.43	0.00
15-Oct-19	0.0	33.4	1	83.86	48.88	0.00
16-Oct-19	15.4	25.8	1	83.86	48.88	3.08
17-Oct-19	2.9	15.4	1	83.86	48.88	0.00
18-Oct-19	0.0	18.3	1	83.86	48.88	0.00
19-Oct-19	0.0	18.3	1	83.86	48.88	0.00
20-Oct-19	0.0	18.3	1	83.86	48.88	0.00
21-Oct-19	0.7	18.3	1	83.86	48.88	0.00
22-Oct-19	0.0	3.6	1	83.86	48.88	0.00
23-Oct-19	0.0	0.7	1	83.86	48.88	0.00
24-Oct-19	1.9	0.7	1	83.86	48.88	0.00
25-Oct-19	31.2	2.6	1	83.86	48.88	11.76
26-Oct-19	22.6	33.8	1	83.86	48.88	6.58
27-Oct-19	97.2	55.7	3	96.52	9.15	89.54
28-Oct-19	0.0	152.9	3	96.52	9.15	0.00
29-Oct-19	0.0	152.9	3	96.52	9.15	0.00
30-Oct-19	0.0	151.0	3	96.52	9.15	0.00
31-Oct-19	0.0	119.8	3	96.52	9.15	0.00

Table-2: AMC and runoff calculation of Dzumah watershed for the year 2020

Date	Rainfall(mm)	Sum of previous 5 days rainfall	AMC	CN	S(mm)	Q(mm)
01-Jun-20	13.0	56.9	3	96.52	9.15	7.74
02-Jun-20	4.1	25.1	1	83.86	48.88	0.06
03-Jun-20	1.0	27.5	1	83.86	48.88	0.00
04-Jun-20	0.0	18.4	1	83.86	48.88	0.00
05-Jun-20	0.0	18.1	1	83.86	48.88	0.00
06-Jun-20	1.8	18.1	1	83.86	48.88	0.00
07-Jun-20	10.3	6.9	1	83.86	48.88	1.25
08-Jun-20	3.4	13.1	1	83.86	48.88	0.02
09-Jun-20	0.0	15.5	1	83.86	48.88	0.00
10-Jun-20	0.4	15.5	1	83.86	48.88	0.00
11-Jun-20	0.7	15.9	1	83.86	48.88	0.00
12-Jun-20	8.1	14.8	1	83.86	48.88	0.68
13-Jun-20	4.9	12.6	1	83.86	48.88	0.14
14-Jun-20	11.4	14.1	1	83.86	48.88	1.59
15-Jun-20	0.0	25.5	1	83.86	48.88	0.00
16-Jun-20	41.6	25.1	1	83.86	48.88	19.00
17-Jun-20	34.3	66.0	3	96.52	9.15	27.52
18-Jun-20	15.4	92.2	3	96.52	9.15	9.83
19-Jun-20	4.6	102.7	3	96.52	9.15	1.44
20-Jun-20	30.4	95.9	3	96.52	9.15	23.77
21-Jun-20	21.4	126.3	3	96.52	9.15	15.27
22-Jun-20	5.2	106.1	3	96.52	9.15	1.80
23-Jun-20	0.6	77.0	3	96.52	9.15	0.00
24-Jun-20	1.3	62.2	3	96.52	9.15	0.08
25-Jun-20	2.5	58.9	3	96.52	9.15	0.42
26-Jun-20	2.0	31.0	1	83.86	48.88	0.00
27-Jun-20	0.6	11.6	1	83.86	48.88	0.00
28-Jun-20	23.0	7.0	1	83.86	48.88	6.80
29-Jun-20	0.0	29.4	1	83.86	48.88	0.00
30-Jun-20	24.2	28.1	1	83.86	48.88	7.48

Date	Rainfall(mm)	Sum of previous 5 days rainfall	AMC	CN	S(mm)	Q(mm)
01-Jul-20	0.0	49.8	2	92.22	21.43	0.00
02-Jul-20	15.6	47.8	2	92.22	21.43	6.45
03-Jul-20	4.2	62.8	3	96.52	9.15	1.22
04-Jul-20	0.0	44.0	2	92.22	21.43	0.00
05-Jul-20	25.7	44.0	2	92.22	21.43	14.16
06-Jul-20	24.9	45.5	2	92.22	21.43	13.51
07-Jul-20	9.1	70.4	3	96.52	9.15	4.55
08-Jul-20	5.2	63.9	3	96.52	9.15	1.80
09-Jul-20	1.0	64.9	3	96.52	9.15	0.04
10-Jul-20	12.8	65.9	3	96.52	9.15	7.57
11-Jul-20	9.0	53.0	2	92.22	21.43	2.40
12-Jul-20	1.0	37.1	2	92.22	21.43	0.00
13-Jul-20	0.0	29.0	1	83.86	48.88	0.00
14-Jul-20	0.7	23.8	1	83.86	48.88	0.00
15-Jul-20	6.5	23.5	1	83.86	48.88	0.36
16-Jul-20	6.6	17.2	1	83.86	48.88	0.38
17-Jul-20	0.0	14.8	1	83.86	48.88	0.00
18-Jul-20	0.5	13.8	1	83.86	48.88	0.00
19-Jul-20	0.0	14.3	1	83.86	48.88	0.00
20-Jul-20	3.0	13.6	1	83.86	48.88	0.01
21-Jul-20	1.9	10.1	1	83.86	48.88	0.00
22-Jul-20	8.2	5.4	1	83.86	48.88	0.70
23-Jul-20	11.8	13.6	1	83.86	48.88	1.72
24-Jul-20	18.9	24.9	1	83.86	48.88	4.67
25-Jul-20	1.8	43.8	2	92.22	21.43	0.03
26-Jul-20	8.9	42.6	2	92.22	21.43	2.35
27-Jul-20	5.6	49.6	2	92.22	21.43	0.90
28-Jul-20	16.2	47.0	2	92.22	21.43	6.86
29-Jul-20	0.8	51.4	2	92.22	21.43	0.00
30-Jul-20	0.0	33.3	1	83.86	48.88	0.00
31-Jul-20	0.0	31.5	1	83.86	48.88	0.00

Date	Rainfall(mm)	Sum of previous 5 days rainfall	AMC	CN	S(mm)	Q(mm)
01-Aug-20	2.4	22.6	1	83.86	48.88	0.00
02-Aug-20	0.0	19.4	1	83.86	48.88	0.00
03-Aug-20	0.0	3.2	1	83.86	48.88	0.00
04-Aug-20	0.3	2.4	1	83.86	48.88	0.00
05-Aug-20	2.6	2.7	1	83.86	48.88	0.00
06-Aug-20	0.0	5.3	1	83.86	48.88	0.00
07-Aug-20	5.3	2.9	1	83.86	48.88	0.18
08-Aug-20	2.9	8.2	1	83.86	48.88	0.00
09-Aug-20	0.0	11.1	1	83.86	48.88	0.00
10-Aug-20	0.0	10.8	1	83.86	48.88	0.00
11-Aug-20	0.0	8.2	1	83.86	48.88	0.00
12-Aug-20	0.0	8.2	1	83.86	48.88	0.00
13-Aug-20	0.0	2.9	1	83.86	48.88	0.00
14-Aug-20	0.0	0.0	1	83.86	48.88	0.00
15-Aug-20	6.5	0.0	1	83.86	48.88	0.36
16-Aug-20	1.6	6.5	1	83.86	48.88	0.00
17-Aug-20	23.3	8.1	1	83.86	48.88	6.97
18-Aug-20	0.0	31.4	1	83.86	48.88	0.00
19-Aug-20	8.7	31.4	1	83.86	48.88	0.82
20-Aug-20	2.4	40.1	2	92.22	21.43	0.09
21-Aug-20	2.4	36.0	2	92.22	21.43	0.09
22-Aug-20	14.0	36.8	2	92.22	21.43	5.37
23-Aug-20	0.0	27.5	1	83.86	48.88	0.00
24-Aug-20	0.6	27.5	1	83.86	48.88	0.00
25-Aug-20	4.2	19.4	1	83.86	48.88	0.07
26-Aug-20	0.0	21.2	1	83.86	48.88	0.00
27-Aug-20	0.0	18.8	1	83.86	48.88	0.00
28-Aug-20	3.1	4.8	1	83.86	48.88	0.01
29-Aug-20	0.0	7.9	1	83.86	48.88	0.00
30-Aug-20	0.0	7.3	1	83.86	48.88	0.00
31-Aug-20	0.0	3.1	1	83.86	48.88	0.00

Date	Rainfall(mm)	Sum of previous 5 days rainfall	AMC	CN	S(mm)	Q(mm)
01-Sep-20	39.8	3.1	1	83.86	48.88	17.69
02-Sep-20	0.0	42.9	2	92.22	21.43	0.00
03-Sep-20	0.0	39.8	2	92.22	21.43	0.00
04-Sep-20	8.4	39.8	2	92.22	21.43	2.10
05-Sep-20	0.0	48.2	2	92.22	21.43	0.00
06-Sep-20	0.0	48.2	2	92.22	21.43	0.00
07-Sep-20	2.3	8.4	1	83.86	48.88	0.00
08-Sep-20	0.0	10.7	1	83.86	48.88	0.00
09-Sep-20	0.0	10.7	1	83.86	48.88	0.00
10-Sep-20	50.6	2.3	1	83.86	48.88	25.85
11-Sep-20	0.0	52.9	2	92.22	21.43	0.00
12-Sep-20	1.4	52.9	2	92.22	21.43	0.01
13-Sep-20	2.4	52.0	2	92.22	21.43	0.09
14-Sep-20	2.4	54.4	3	96.52	9.15	0.39
15-Sep-20	1.7	56.8	3	96.52	9.15	0.17
16-Sep-20	0.0	7.9	1	83.86	48.88	0.00
17-Sep-20	5.7	7.9	1	83.86	48.88	0.24
18-Sep-20	0.0	12.2	1	83.86	48.88	0.00
19-Sep-20	0.0	9.8	1	83.86	48.88	0.00
20-Sep-20	0.0	7.4	1	83.86	48.88	0.00
21-Sep-20	0.0	5.7	1	83.86	48.88	0.00
22-Sep-20	11.6	5.7	1	83.86	48.88	1.65
23-Sep-20	15.6	11.6	1	83.86	48.88	3.16
24-Sep-20	5.3	27.2	1	83.86	48.88	0.18
25-Sep-20	2.0	32.5	1	83.86	48.88	0.00
26-Sep-20	4.7	34.5	1	83.86	48.88	0.12
27-Sep-20	3.2	39.2	2	92.22	21.43	0.22
28-Sep-20	0.0	30.8	1	83.86	48.88	0.00
29-Sep-20	0.5	15.2	1	83.86	48.88	0.00
30-Sep-20	0.0	10.4	1	83.86	48.88	0.00



Date	Rainfall(mm)	Sum of previous 5 days rainfall	AMC	CN	S(mm)	Q(mm)
01-Oct-20	0.0	8.4	1	83.86	48.88	0.00
02-Oct-20	51.0	3.7	1	83.86	48.88	26.17
03-Oct-20	17.3	51.5	2	92.22	21.43	7.65
04-Oct-20	0.4	68.8	3	96.52	9.15	0.00
05-Oct-20	20.6	68.7	3	96.52	9.15	14.53
06-Oct-20	14.6	89.3	3	96.52	9.15	9.12
07-Oct-20	0.2	103.9	3	96.52	9.15	0.00
08-Oct-20	1.1	53.1	3	96.52	9.15	0.05
09-Oct-20	0.0	36.9	2	92.22	21.43	0.00
10-Oct-20	0.0	36.5	2	92.22	21.43	0.00
11-Oct-20	1.2	15.9	1	83.86	48.88	0.00
12-Oct-20	0.0	2.5	1	83.86	48.88	0.00
13-Oct-20	0.0	2.3	1	83.86	48.88	0.00
14-Oct-20	0.0	1.2	1	83.86	48.88	0.00
15-Oct-20	0.0	1.2	1	83.86	48.88	0.00
16-Oct-20	0.0	1.2	1	83.86	48.88	0.00
17-Oct-20	0.0	0.0	1	83.86	48.88	0.00
18-Oct-20	0.0	0.0	1	83.86	48.88	0.00
19-Oct-20	0.8	0.0	1	83.86	48.88	0.00
20-Oct-20	0.3	0.8	1	83.86	48.88	0.00
21-Oct-20	4.2	1.1	1	83.86	48.88	0.07
22-Oct-20	18.0	5.3	1	83.86	48.88	4.24
23-Oct-20	19.1	23.3	1	83.86	48.88	4.77
24-Oct-20	25.3	42.4	2	92.22	21.43	13.83
25-Oct-20	1.6	66.9	3	96.52	9.15	0.15
26-Oct-20	0.0	68.2	3	96.52	9.15	0.00
27-Oct-20	0.0	64.0	3	96.52	9.15	0.00
28-Oct-20	0.0	46.0	2	92.22	21.43	0.00
29-Oct-20	0.0	26.9	1	83.86	48.88	0.00
30-Oct-20	0.0	1.6	1	83.86	48.88	0.00
31-Oct-20	0.0	0.0	1	83.86	48.88	0.00